CANADIAN THESES ON MICROFICHE

I.S.B.N.

THESES CANADIENNES SUR MICROFICHE

National Library of Canada
Collections Development Branch

Canadian Theses on
Microfiche Service

Ottawa, Canada
K1A 0N4

Bibliothèque nationale du Canada
Direction du développement des collections

Service des thèses canadiennes
sur microfiche

NOTICE

The quality of this microfiche is heavily dependent upon the quality of the original thesis submitted for microfilming. Every effort has been made to ensure the highest quality of reproduction possible.

If pages are missing, contact the university which granted the degree.

Some pages may have indistinct print especially if the original pages were typed with a poor typewriter ribbon or if the university sent us a poor photocopy.

Previously copyrighted materials (journal articles, published tests, etc.) are not filmed.

Reproduction in full or in part of this film is governed by the Canadian Copyright Act, R.S.C. 1970, c. C-30. Please read the authorization forms which accompany this thesis.

AVIS

La qualité de cette microfiche dépend grandement de la qualité de la thèse soumise au microfilmage. Nous avons tout fait pour assurer une qualité supérieure de reproduction.

S'il manque des pages, veuillez communiquer avec l'université qui a conféré le grade.

La qualité d'impression de certaines pages peut laisser à désirer, surtout si les pages originales ont été dactylographiées à l'aide d'un ruban usé ou si l'université nous a fait parvenir une photocopie de mauvaise qualité.

Les documents qui font déjà l'objet d'un droit d'auteur (articles de revue, examens publiés, etc.) ne sont pas microfilmés.

La reproduction, même partielle, de ce microfilm est soumise à la Loi canadienne sur le droit d'auteur, SRC 1970, c. C-30. Veuillez prendre connaissance des formules d'autorisation qui accompagnent cette thèse.

THIS DISSERTATION
HAS BEEN MICROFILMED
EXACTLY AS RECEIVED

LA THÈSE A ÉTÉ
MICROFILMÉE TELLE QUE
NOUS L'AVONS REÇUE

NL-339 (r. 82/08)

Canada

National Library of Canada | Bibliothèque nationale du Canada

Canadian Theses Division | Division des thèses canadiennes

Ottawa, Canada
K1A 0N4

0-315-06105-7

54025

PERMISSION TO MICROFILM — AUTORISATION DE MICROFILMER

• Please print or type — Écrire en lettres moulées ou dactylographier

Full Name of Author — Nom complet de l'auteur

RUSSELL, SCOTT DANIEL

Date of Birth — Date de naissance	Country of Birth — Lieu de naissance
DEC. 08, 1952	U.S.A.

Permanent Address — Résidence fixe

Department of Botany & Microbiology
University of Oklahoma
Norman, Oklahoma 73019 USA

Title of Thesis — Titre de la thèse

Fertilization in Plumbago zeylanica: The structural basis of male cytoplasmic inheritance.

University — Université

University of Alberta

Degree for which thesis was presented — Grade pour lequel cette thèse fut présentée

Ph.D.

Year this degree conferred — Année d'obtention de ce grade	Name of Supervisor — Nom du directeur de thèse
1981	David D. Cass

Permission is hereby granted to the NATIONAL LIBRARY OF CANADA to microfilm this thesis and to lend or sell copies of the film.

The author reserves other publication rights, and neither the thesis nor extensive extracts from it may be printed or otherwise reproduced without the author's written permission.

L'autorisation est, par la présente, accordée à la BIBLIOTHÈQUE NATIONALE DU CANADA de microfilmer cette thèse et de prêter ou de vendre des exemplaires du film.

L'auteur se réserve les autres droits de publication; ni la thèse ni de longs extraits de celle-ci ne doivent être imprimés ou autrement reproduits sans l'autorisation écrite de l'auteur.

Date	Signature
October 9, 1981	Scott D. Russell

NL-91 (4/77)

THE UNIVERSITY OF ALBERTA

FERTILIZATION IN *PLUMBAGO ZEYLANICA*: THE STRUCTURAL BASIS OF MALE CYTOPLASMIC INHERITANCE

by

© SCOTT DANIEL RUSSELL

A THESIS

SUBMITTED TO THE FACULTY OF GRADUATE STUDIES AND RESEARCH

IN PARTIAL FULFILMENT OF THE REQUIREMENTS FOR THE DEGREE

OF DOCTOR OF PHILOSOPHY

IN

STRUCTURAL BOTANY

Department of Botany

EDMONTON, ALBERTA

Fall, 1981

THE UNIVERSITY OF ALBERTA

RELEASE FORM

NAME OF AUTHOR Scott Daniel Russell

TITLE OF THESIS Fertilization in *Plumbago zeylanica*: The Structural Basis of Male Cytoplasmic Inheritance

DEGREE FOR WHICH THESIS WAS PRESENTED Doctor of Philosophy

YEAR THIS DEGREE GRANTED Fall, 1981

Permission is hereby granted to THE UNIVERSITY OF ALBERTA LIBRARY to reproduce single copies of this thesis and to lend or sell such copies for private, scholarly or scientific research purposes only.

The author reserves other publication rights, and neither the thesis nor extensive extracts from it may be printed or otherwise reproduced without the author's written permission.

(SIGNED) Scott D. Russell

PERMANENT ADDRESS:

Department of Botany & Microbiology

University of Oklahoma

Norman, Oklahoma 73019 U S A

DATED October 9 1981

THE UNIVERSITY OF ALBERTA

FACULTY OF GRADUATE STUDIES AND RESEARCH

The undersigned certify that they have read, and recommend to the Faculty of Graduate Studies and Research, for acceptance, a thesis entitled Fertilization in *Plumbago zeylanica*: The Structural Basis of Male Cytoplasmic Inheritance submitted by Scott Daniel Russell in partial fulfilment of the requirements for the degree of Doctor of Philosophy in Structural Botany.

David D. Cass

Supervisor

John Hodkinson

Edwin A. Cossins

Curtis Strobeck

Ruth A. Stockey

William Ahgeson

External Examiner

Date October 7, 1981

Abstract

The megagametophyte of *Plumbago zeylanica* L. (Plumbaginaceae, Plumbaginoideae), lacking synergids, is among the most highly reduced in flowering plants. The female gametophyte consists of five cells: a large vacuolate egg with a micropylar filiform apparatus and chalazally-situated nucleus; a vacuolate central cell with fused polar nuclei directly opposite the egg nucleus, and three accessory cells (one chalazal cell and two lateral cells) which may degenerate prior to fertilization or persist into early embryogeny.

The microgametophyte is organized into three cells at floral anthesis: two connected spindle-shaped sperm cells, and a vegetative cell with a large polymorphic, lobed nucleus. A projection of one of the sperm cells wraps around the vegetative nucleus, lying in indentations on its surface and providing the structural basis of an association between the sperm and vegetative nucleus which is observed throughout pollen tube growth. Absolute counts of organelle content are given for eleven pairs of sperm cells. The associated sperm possesses the majority of the mitochondria and rarely contains plastids, whereas the other sperm cell has numerous plastids. The basis for this asymmetrical distribution of heritable organelles is apparently established prior to generative cell division.

Pollen tube growth is initiated within 15 minutes of pollination. After penetrating the stigmatic surface, the tube grows exclusively between the thick-walled cells of the transmitting tissue in the lower stigma and style. The tube enters the ovule through a micropyle formed by the inner integument, displaces several nucellar cells, and penetrates the megagametophyte through the egg's filiform apparatus. It continues to grow between the egg and central cell until reaching an area of strong curvature in the egg wall, 70-80 um deep in the megagametophyte, approximately 8.5 hr. following pollination, where a terminal aperture forms and the two sperm cells, vegetative nucleus and a limited amount of pollen cytoplasm are released. Components of the egg cell wall are disrupted near the tube aperture, and the disappearance of the inner and outer vegetative cell membrane and the sperm cell wall results in the plasma membrane of the

sperm becoming tightly appressed to that of the egg and central cells.

Gamete fusion is apparently initiated at one location in each of the sperm resulting in transmission of sperm nuclei into the egg and central cells. Membrane fusion events appear to be completed at additional sites as well as evidenced by the transient presence of identifiable sperm membranes within cells of the female gametophyte. Following gamete fusion, remnant sperm membranes in the egg and central cell rapidly vesiculate and may not be detected after several minutes have elapsed. Transmitted heritable sperm organelles may be identified in the egg and central cells. Morphological differences in plastid structure allow the identification of male plastids in the egg directly, and statistically significant size differences between sperm mitochondria and those of other cells in the male and female gametophyte permit sperm mitochondria in the central cell to be differentiated on a populational basis soon after gamete fusion. The timing of these observations relative to gamete fusion, the distance of sperm nuclei from their respective target nuclei, and the location of mitochondria and plastids flanking the sperm nuclei, corroborate the interpretation concerning paternal origin of these organelles. Organelles within unfused cytoplasmic bodies observed between the egg and central cell are similar to those in the sperm and presumably represent segments of the sperm cell which become separated from the main sperm cell body near gamete discharge. The process of nuclear fusion, initiated approximately 8.7 hr. after pollination, is similar to that in other angiosperm taxa described to date.

In terms of structure and function, the egg of *P. zeylanica* may be regarded as a single-celled egg apparatus, with numerous synergid structures and functions transferred to the egg. Unlike the typical synergid, however, the egg does not directly receive the pollen tube or undergo degenerative changes as a result of pollen tube arrival, and functions as a gamete in the establishment of the embryo. The implications of asymmetrical distribution of heritable organelles in the sperm are not yet fully explored, but suggest the possiblity of gametic recognition with conservation of sperm plastids within the embryo.

TABLE OF CONTENTS

CHAPTER		PAGE
I.	Introduction	1
	A. Studies in the family Plumbaginaceae	4
	B. Subfamily Staticoideae	5
	C. Subfamily Plumbaginoideae	7
II.	Materials and Methods	10
	A. Chemical fixation	10
	B. Physical fixation	11
	C. Specimen preparation	11
	D. Observation of isolated living sperm cells	12
	E. Serial reconstruction and quantitative cytology of sperm cells	12
	F. Statistical treatment of mitochondrial dimensions	13
III.	Sperm Ultrastructure: General Cytology and Association with Vegetative Nucleus	14
	A. Introduction	14
	B. Observations	16
	Ultrastructure within the mature pollen grain	16
	Structural interrelationships of sperms and vegetative nucleus	25
	Sperm cell modifications during pollen tube growth	32
	C. Discussion	32
	Sperm cell structure	32
	Structural associations involving sperm cells	38
IV.	Sperm Ultrastructure: Quantitative Cytology and Symmetry of Organelle Inheritance	41
	A. Introduction	41
	B. Results and Discussion	42
V.	Fertilization: Entry and Discharge of the Pollen Tube in the Embryo Sac	48
	A. Introduction	48
	B. Observations	48

Initiation and growth of the pollen tube into the ovule 48

Organization of the mature embryo sac before pollen tube arrival 52

Entry and discharge of the pollen tube in the megagametophyte 55

Pollen tube and egg cell walls following discharge of the pollen tube 58

Identification and fate of the vegetative nucleus in the megagametophyte 62

C. Discussion 71

VI. Fertilization: Gamete Fusion and Fate of the Male Cytoplasm 75

A. Introduction 75

B. Observations 76

Sperm cells in the megagametophyte before gamete fusion 76

Male gametes within egg and central cell subsequent to gamete fusion 82

Sperm membranes following gamete fusion; modifications of egg-central cell wall 82

Morphological evidence regarding male cytoplasmic transmission 88

Statistical evidence of male cytoplasmic transmission 91

Presence and identification of unfused cytoplasmic bodies between the egg and central cell 96

C. Discussion 101

VII. Summary and Conclusions 113

Literature Cited 116

Appendix 1. Morphometry of Sperm Cells 123

LIST OF TABLES

TABLE		PAGE
1.	Embryological studies in the subfamily Staticoideae	6
2.	Embryological studies in the subfamily Plumbaginoideae	8
3.	Descriptive statistics comparing the numerical content of mitochondria, plastids, and microbodies in sperms	43
4.	Scatter diagram of plastids vs. mitochondria in two groups of sperms	44
5.	Paired t test comparing numerical content of mitochondria, plastids, and microbodies in two groups of sperms	45
6.	Chronology of fertilization events in *Plumbago zeylanica* based on maximal growth rates following artificial pollination	49
7.	Descriptive statistics comparing mitochondrial widths in six cell types	92
8.	Student's t comparison of population means and variance in mitochondrial widths in six different cell types	93
9.	Student's t comparison of population means and variance in mitochondrial widths between mitochondria of known and unknown origin	96
10.	Program for calculating the number of organelles or other subcellular objects within a spindle shaped sperm cell	127

LIST OF FIGURES

FIGURE		PAGE
1.	Electron micrograph of two chemically-fixed sperm cells in longisection	17
2.	Electron micrograph of junction between two chemically-fixed sperm cells	17
3.	Electron micrograph of a chemically-fixed sperm cell	20
4.	Electron micrograph of sperm plastids in the pollen grain	20
5.	Electron micrograph of chemically-fixed sperm cell in longisection	20
6.	Electron micrograph of physically-fixed pollen grain	23
7.	Electron micrograph of physically-fixed sperm cell and vegetative nucleus	23
8.	Electron micrograph of junction between physically-fixed sperm cells, stained for polysaccharides	23
9.	Electron micrograph of physically-fixed pollen grain, stained for polysaccharides	23
10.	Electron micrograph of physically-fixed pollen grain, stained without periodic acid oxidation	23
11.	Schematic representation of the association between one sperm and the vegetative nucleus	25
12.	Electron micrograph of the structural association of sperm cell and vegetative nucleus	27
13.	Nomarski interference contrast micrograph of isolated sperm cells	27
14.	Nomarski interference contrast micrograph of isolated sperm cells	27
15.	Nomarski interference contrast micrograph of isolated sperm cells	27
16.	Nomarski interference contrast micrograph of isolated sperm cells	27
17.	Nomarski interference contrast micrograph of isolated sperm cells	27
18.	Nomarski differential interference micrograph of apical portion of pollen tube during rapid elongation phase	30
19.	Electron micrograph of pollen tube during rapid elongation phase	30
20.	Electron micrograph of vegetative nucleus apex during rapid elongation phase	30
21.	Electron micrograph of vegetative nucleus adjacent to sperm projection during rapid pollen tube elongation	30
22.	Electron micrograph of vegetative nucleus adjacent to sperm projection during rapid pollen tube elongation	30

23. Phase contrast micrograph of pollen tube during slow growth phase 33

24. Electron micrograph of a sperm plastid during late pollen tube growth 33

25. Electron micrograph of the pollen tube nearing the ovule 33

26. Electron micrograph of sperm mitochondrion during late pollen tube growth 33

27. Electron micrograph of two chemically-fixed sperm during late pollen tube growth 33

28. Electron micrograph of generative cell in immature pollen 46

29. Reconstruction of a mature embryo sac 50

30. Electron micrograph of median longitudinal section of egg and central cell nuclei in an unfertilized embryo sac 53

31. Electron micrograph of a pollen tube within the filiform apparatus at the base of the egg in cross section 53

32. Higher magnification electron micrograph of filiform apparatus in base of the egg near pollen tube 53

33. Electron micrograph of pollen tube apex in physical contact with nucellar cells 56

34. Electron micrograph of pollen tube penetrating the egg wall 56

35. Electron micrograph of filiform apparatus stained by the PA-TCH-SP reaction 56

36. Electron micrograph of longitudinal section of pollen tube within the base of the embryo sac 59

37. Electron micrograph of vesicles and related tubular membranous elements in the middle layer of a pollen tube 59

38. Electron micrograph of longitudinal section of pollen tube at the base of the embryo sac 59

39. Electron micrograph of pollen tube aperture in longitudinal section shortly after discharge 63

40. Electron micrograph of a pollen tube within the embryo sac stained by the PA-TCH-SP reaction 63

41. Electron micrograph of discharged vegetative nucleus between egg and central cell 65

42. Electron micrograph of pollen tube aperture one day after fertilization 65

43. Nomarski differential interference contrast micrograph of median section of the base of a freeze-substituted ovule 67

44. Nomarski differential interference contrast micrograph of median section of a freeze-substituted ovule 67

45. Reconstruction of pollen tube arrival, tube discharge and subsequent fertilization 69

46. Nomarski interference contrast micrograph of an unfused sperm cell between the egg and central cell 77

47. Nomarski interference contrast micrograph of unfused sperm cell between the egg and central cell 77

48. Electron micrograph of unfused sperm cell between the egg and central cell 77

49. Electron micrograph of unfused sperm cell between the egg and central cell 80

50. Electron micrograph of junction between unfused sperm cell and central cell 80

51. Electron micrograph of unfused sperm, associated pollen cytoplasm, and pollen tube 80

52. Low magnification electron micrograph of an embryo sac soon after gamete fusion showing egg nucleus and sperm nucleus within the egg 83

53. Electron micrograph of an unfused sperm nucleus in the egg flanked by two plastids of paternal origin. 83

54. Electron micrograph of unfused sperm nucleus within the central cell 85

55. Electron micrograph of unfused sperm nucleus within the central cell stained by the PA-TCH-SP reaction 85

56. Electron micrograph of pollen tube aperture and unfused sperm nucleus within the central cell 85

57. Electron micrograph of unfused sperm nucleus and associated cytoplasm in the egg 89

58. Electron micrograph of plastids in sperm cell within growing pollen tube 89

59. Electron micrograph of a typical plastid observed within a mature, unfertilized egg cell. 89

60. Electron micrograph of plastids flanking the sperm nucleus stained by the TCH-SP reaction 89

61. Electron micrograph of plastids near the egg nucleus stained by the TCH-SP reaction 89

62. Electron micrograph of unfused segment of sperm cytoplasm 97

63. Electron micrograph of unfused cytoplasmic body after gamete fusion. 97

64. Electron micrograph of unfused cytoplasmic body adjacent to an eight-celled embryo. 97

65. Nomarski interference contrast micrograph of sperm and egg nuclei during fusion. 97

66. Nomarski interference contrast micrograph of pollen tube aperture and wall modifications within the newly-formed zygote. 97

67. Nomarski interference contrast micrograph of sperm and central cell nuclear fusion and vegetative nucleus. 97

68. Reconstruction of gamete fusion 105

Acknowledgments

Over the past four years, the form and substance of this work has been been influenced by many people who each bear a mark in the final production of this thesis; not all of whom are mentioned, but to all, I am grateful.

The following people deserve special mention: Prof. David D. Cass, who provided generous support of my work in both time and resources, and who helped to see this project to a successful completion. Dr. Ruth A. Stockey and Dr. Daniel J. Peteya, who each helped to guide this study in separate but unique ways. Dr. A. Randall Olson, Dr. Bruce L. Robertson, and Michael W. Folsom, who helped to shape the environment of my work and lifestyle of the time.

I wish to thank the following people for their direct aid or influence in regard to specific parts of my work: Prof. H. Lloyd Mogensen, for instructing me in the art of re-embedding thick plastic sections for ultramicrotomy (Chapters 3 and 6), and serial ultrathin sectioning used extensively in Chapter 4. His unselfish generosity with his time, expertise, and laboratory facilities in the summers of 1978 and 1980 are deeply appreciated. Dr. Jan A. P. Janssens deserves much credit for his generous help in all aspects of computer work which entered into producing this thesis. Anabella Opazo cheerfully provided me with prints of over 2500 electron micrographs made possible the analyses of organelle content in Chapter 4. Thanks also to Prof. Donald B. Fisher for discussions which played an important role in formulating my thoughts about embryo sac function.

Special thanks to Dr. William A. Jensen, for aggreeing to serve as external examiner for this dissertation, and to the members of my committee for their careful consideration of this thesis.

I thank the Biological Sciences Electron Microscope unit and Natural Science and Engineering Research Council of Canada grant A-6103 to Dr. D. Cass for support of this study.

I. Introduction

In her *Systematic Embryology of the Angiosperms*, Davis (1966) refers to some 5,500 separate studies in summarizing the state of our knowledge concerning the structure and variability of the gametophyte in flowering plants. Undoubtedly, there were numerous publications which she could have cited but did not, and many more publications have appeared since. Among these published works, far fewer studies concern problems dealing with the basic biology and nature of sexual reproduction in angiosperms (as separated from taxonomic embryology). As more careful recent work has indicated, only during the last twenty years has the process of sexual reproduction in angiosperms been understood more clearly. To a large degree, the development of our knowledge has remained closely linked to the development of new techniques.

Early workers in the field of embryology were hampered by severe technical problems, including those problems inherent in using cleared ovules to visualize cells and nuclei involved in sexual reproduction. Near the turn of the century, techniques improved and with the advent of paraffin microtomy the embryological literature burgeoned. Biologists turned to improved methods of fixation, but in retrospect the types of image that proved aesthetically pleasing usually involved the use of coagulative fixatives which resulted in only the nucleus being well-preserved in the "acid" fixation image and only the "chondriome" and cytoplasm being well-preserved in the "basic" fixation image. The rest of the material was typically coagulated or often lost in solutions. Fixatives that have later proved to be important: osmium, glutaraldehyde and a variety of others, were rejected because the tissue proved too dense for effective observation after paraffin microtomy. In reality the material was often too well preserved by these fixatives, rendering material too dense for easy observation. This limitation was particularly important when the embryological convention of sectioning megagametophytic material at 12 to 30 um was followed. Johansen (1940) admonished researchers who used sections as thin as 5 um in studies on megagametogenesis because it led to problems in interpreting the embryo sac.

Adherence to the use of the early paraffin technology was not without impact. However, despite primitive techiques, several early ideas concerning the role of the "synergidae" included that they may "receive the pollen-tube and act as carriers of its influence to the pollen tube" (Ward, 1880). Further information from paraffin histology suggested the occurrence of at least four alternative pathways for the arrival of the pollen tube (Maheshwari, 1950) and on the basis of electron microscopy, it has been possible to confirm that two of these pathways occur *in vivo* in flowering plants. Recent electron microscopic work has revealed only a single pathway in angiosperms with normal egg apparati.

The careful light microscopic works of Finn and Wylie, among others, advanced embryological knowledge of the male gamete's role in fertilization during the first half of the twentieth century, but a number of dogmatic misconceptions have accumulated despite their work. The cellular nature of the sperm cell has represented such a source of controversy. The apparent origin of this conception was in a paper published by Nawashin (1909) soon after his discovery of double fertilization. His claim that the sperm existed as free nuclei, not as cells has remained dogma; his claim that differences in the size of the two sperm nuclei were the basis for gametic recognition (i.e., that the individual male gamete which will fuse with the egg can be identified before gamete fusion) has remained ignored. Finn, who collaborated on one of Nawashin's papers on the nature of the sperm (Nawashin and Finn, 1913), later reexamined the nature of the male gamete in some of the same taxa he had studied previously, and concluded by contradicting his early findings. He reported (Finn, 1925, 1935) that sperm are not only formed as cells from the inception of the generative cell during microspore division, but that the male gamete remains cellular even after discharge of the pollen tube into the embryo sac. This latter result has been corroborated on numerous occasions using electron microscopy (see Russell and Cass, 1981a for a review).

Predictably, the fate of the inconspicuous male cytoplasm during subsequent fertilization is also controversial. Possibly the earliest account on male cytoplasmic transmission was one by Strasburger (1884) which stated that male

cytoplasm was not involved in the process of fertilization. The careful work of Wylie (1923, 1941) was among the first accounts to report the transmission of sperm cytoplasm into the egg and central cell. Although often cited, his conclusion that male cytoplasmic transmission occurs has not gained wide acceptance among embryologists. Electron microscopic studies have tended to support the contention that most if not all male cytoplasm is shed prior to gamete fusion (Jensen and Fisher, 1968a; Went, 1970; Wilms, 1981), but only Jensen and Fisher have provided convincing electron micrographs to substantiate the concept that male cytoplasm is not transmitted into the embryo and endosperm (Jensen and Fisher, 1967, 1968a; Fisher and Jensen, 1969). Preliminary work with *Plumbago zeylanica* has provided evidence which would support the occurrence of male cytoplasmic transmission during gamete fusion (Russell, 1980).

In recent studies, the use of electron microscopy coordinated with the use of analytical light microscopy has provided important information which has extended our knowledge of the behavior and function of the physically inaccessible cells of the female gametophyte. In fact, our knowledge concerning the sexual function of the normal, female gametophyte *in vivo*, which typically occurs deep within the ovular tissues, has depended on the use of such techniques. Data which these anatomical studies provide has often been inferential, but when the series of detailed developmental stages constituting our knowledge of sexual reproduction are viewed analytically, considerable data is provided about processes that cannot presently be directly observed. The possiblities of extending one's knowledge of these processes depended on developing and applying a number of techniques to each problem, comparing similar sexual or gametophytic strategies in diverse plants, and thoroughly understanding reproduction in the selected plant.

The present study concerns sexual reproduction and fertilization in the flowering plant, *Plumbago zeylanica*, a plant which has been extensively studied with respect to embryo sac organization at the light microscopic level and organization of the egg at the electron microscopic level. The primary

contributions of the present study to our understanding of the reproductive biology of *P. zeylanica* relate to the cellular organization and behavior of the male gametophyte, arrival and entry of the pollen tube into the embryo sac, and the processes of gamete fusion and double fertilization. In order to reduce possibilities of misinterpretation and the selection of abnormally functioning embryo sacs, a detailed chronology of reproduction was constructed on the basis of artificial pollination of plants under controlled conditions. This chronology permitted the repetition of various stages of reproduction for experimental manipulation.

A. Studies in the family Plumbaginaceae

The family Plumbaginaceae Juss. to which *P. zeylanica* is allied, has been the subject of numerous systematic and embryological studies over the years. The family is considered "advanced" in recent systematic treatments of the angiosperms (Stebbins, 1974; Takhtajan, 1980) and this conclusion is supported by embryological data. Members of the family have pentamerous sympetalous flowers with connate calices and staminate filaments adnate to the corolla. The gynoecium is organized into a five-lobed stigma, fusing proximally to form the style, and an uniloculate ovary with a single ovule.

The mode of development and orientation of the ovule is consistent within the family, and is unique except for its occurrence in the Cactaceae. During the inception of the integuments, the ovule is directed upwards, but later unequal growth in the funiculus results in a 360° rotation in the orientation of the ovule; it becomes oriented upright again only near the end of its development. This type of development is described as being "circintropous" (Haupt, 1934) and results in the ovule being wrapped once around by the long funiculus which partially occludes the micropyle. The late encroachment of transmitting tissue into the locule results in the formation of an obturator which presses transmitting tissue into the ovule near the micropyle. The gynoecium tissues are organized into a closed style with a contiguous tract of specialized transmitting tissue extending from the stigmatic lobes to the summit of the ovary.

The female gametophyte is tetrasporic in origin, lacking in the formation of discrete cellular megaspores. The male gametophyte is usually trinucleate at anthesis with sperm cells formed prior to pollination and pollen tube growth.

The floral and anatomical characteristics mentioned herein are widely regarded as derived character states within the angiosperms. The presence of a dimorphic floral incompatibility system in some taxa of the family is a derived genetic feature. The two subfamilies of the Plumbaginaceae, namely the Staticoideae and the Plumbaginoideae, are distinguished largely on pollen morphological features, as well as differences in vegetative and floral morphology, and are also separated by differences in the organization of the female gametophyte.

B. Subfamily Staticoideae

The subfamily Staticoideae is by far the better represented subfamily, containing over 300 species in 12 genera. It is separated embryologically from the Plumbaginoideae mainly by the presence of dimorphic pollen grains and the presence of unreduced or only slightly reduced female gametophytes with conventional egg apparati, consisting of two synergids and the egg. In the male gametophyte, pollen grains originating from "pin" plants, where the style is exerted further than the anthers, tend to have an exine surface which is somewhat rugose, whereas those originating from "thrum" plants, which have flowers where the anthers are exerted farther than the stigmas, tend to have a smoother exine surface. The differing morphologies of stigmatic cells in pin and thrum plants appear to result in preferential adherence of compatible pollen grains on their respective stigmas (Dulberger, 1975). The occurrence of pin and thrum plants in the Plumbaginaceae is believed to represent a morphological adaptation to conserve pollen in a genetically-based self-incompatibility system (Baker, 1948).

Embryo sac ontogeny in the Staticoideae, despite much study (Table 1), is still controversial. Members of this subfamily often may have a minor reduction of the embryo sac, particularly "strike", or non-division, of the antipodal nuclei

Table 1: A summary of embryological work in the subfamily Staticoideae, family Plumbaginaceae.

Taxon	Embryo Sac Ontogeny Type	Author
Acantholimon glumaceum Boiss.	*"Lilium"*	Dahlgren, 1916
Armeria alpina Willd.	*"Lilium"*	Dahlgren, 1916
A. bupleuroides (?)	*Fritillaria*	Fagerlind, 1938b
A. plantaginea Willd.	*"Lilium"*	Dahlgren, 1916
A. vulgaris Willd.	*"Lilium"*	Dahlgren, 1916
A. vulgaris Willd. var. *maritima* (Miller) Willd.	97% *Fritillaria* 3% *Adoxa*	D'Amato, 1940b
Statice bahusiensis Fr.	*"Lilium"*	Dahlgren, 1916
S. bonduelli	*Fritillaria*	Fagerlind, 1939
S. eulimonium	*Penaea*	Fagerlind, 1939
S. japonica	*Fritillaria*	Ya-E, 1941
S. limonium L.	*Fritillaria*	D'Amato, 1940b
S. oleafolia Scop. var. *confusa* Godr.	20% *Adoxa*[1]	D'Amato, 1940a, 1949
S. sinuata	*Penaea*	Fagerlind, 1938b
S. sinuata var. *rosea*	*Fritillaria*	Fagerlind, 1939
S. suworowi	*Fritillaria*	Fagerlind, 1939

[1]The remaining 80% were apomictic, belonging to the *Ixeris dentata*-type of development.

during late megagametogenesis. In all, four different types of embryo sac ontogeny have been reported in the Staticoideae, and up to two different types have been reported in the same taxon (Table 1).

C. Subfamily Plumbaginoideae

The subfamily Plumbaginoideae is a cosmopolitan family of warm, dry regions and contains at least 24 species in four genera. It is separated from the Staticoideae by the presence of monomorphic pollen grains and highly reduced female gametophytes. Pollen grains of taxa in the Plumbaginoideae are believed to be monomorphic in structure, regardless of floral morphology, but in *Dyerophytum indicum* differences are visible at the electron microscope level (Erdtmann, 1970) and may be present in other taxa of the Plumbaginoideae, as well. The presence of pin and thrum flowers has been reported in three of the four genera of the Plumbaginoideae: *Plumbago* L., *Ceratostigma* Bunge, and *Dyerophytum* Kuntze (=*Vogelia* Lam.).

The embryo sac is constituted by two different developmental patterns in the Plumbaginoideae (Table 2) which differ slightly in their ontogeny, but presumably function identically during fertilization. In *Ceratostigma*, *Dyerophytum*, and *Plumbago*, the meiocyte nucleus divides into four megaspore nuclei which become aligned in a cruciate fashion and divide to form eight nuclei and five cells. Four polar nuclei occupy the center of the embryo sac. The remaining nuclei become incorporated into cells which retain a cruciate distribution within the embryo sac. The cell located at the micropyle becomes the egg; the remaining cells constitute the so-called lateral and antipodal cells (Haupt, 1934; Dahlgren, 1937). The four nuclei in the central cell fuse prior to embryo sac maturity to form a 4N "secondary nucleus."

Plumbagella Spach., a monotypic genus, differs slightly with respect to embryo sac ontogeny. After the four cruciate megaspore nuclei are formed, three of the nuclei fuse. The single 1N and 3N nuclei divide once again with subsequent cytokinesis resulting in the formation of an egg with a 1N nucleus at the micropylar end of the ovule and a single antipodal cell with a 3N nucleus at

Table 2: A summary of embryological work in the subfamily Plumbaginoideae, family Plumbaginaceae.

Taxon	Embryo Sac Ontogeny Type	Author
Ceratostigma plumbaginoides Bunge	*Plumbago*	Dahlgren, 1916, 1937 Boyes, 1939b D'Amato, 1943
C. willmottianum Stapf.		Boyes, 1939b Boyes and Battaglia, 1951
Dyerophytum indicum (Lamk.) Kuntze	*Plumbago*	Mathur, 1940 Mathur and Khan, 1941
Plumbago capensis Thunb.	*Plumbago*	Dahlgren, 1916 Haupt, 1934 Fagerlind, 1938a Boyes, 1939b D'Amato, 1940b Cass, 1972
P. coccinea Salisb.	*Plumbago*	Boyes, 1939b Boyes and Battaglia, 1951
P. europea L.	*Plumbago*	D'Amato, 1943 Veillet-Bartoszewska, 1958
P. pulchella Boiss.	*Plumbago*	Dahlgren, 1916
P. scandens L.	*Plumbago*	Boyes, 1939b Boyes and Battaglia, 1951
P. zeylanica L.	*Plumbago*	Dahlgren, 1916, 1937 Fagerlind, 1938a, 1938b Cass and Karas, 1974 Russell, 1980 Russell and Cass, 1981a, 1981b
Plumbagella micrantha (Ledeb.) Spach.	*Plumbagella*	Dahlgren, 1916 Fagerlind, 1938a Boyes, 1939a, 1939b, 1959

the opposite end of the ovule; the two remaining free nuclei fuse to form a 4N central cell nucleus prior to embryo sac maturity (Dahlgren, 1916; Fagerlind, 1938a; Boyes, 1939b).

II. Materials and Methods

Plants of *Plumbago zeylanica* L. have been maintained under long-day conditions in University of Alberta greenhouses since 1972 and are the same plants and clones of those used by Cass and Karas (1974). Unlike many other members of the Plumbaginoideae (Baker, 1948), *P. zeylanica* lacks a self-incompatibility response and produces seed a large proportion of the time (over 97% seed set). Under these conditions, the plants have thrived and produced large numbers of flowers throughout the year.

A. Chemical fixation

Chemically prepared tissue was routinely fixed 6-12 hr in 3% glutaraldehyde-M/15 phosphate buffer (pH 6.8) at 4°C, rinsed briefly in buffer, and postfixed in cold 2% buffered osmium tetroxide. Material was then dehydrated in a graded ethanol series followed by propylene oxide and embedded in low viscosity resin (Spurr, 1969).

In order to compare the effect of different chemical fixatives on sperm cell wall preservation, the following procedures were employed, in addition, on pollen grains collected at anthesis: i) 1-1/2 hr fixation in 3% glutaraldehyde with diaminobenzidine (2 mg/5 ml buffer) in 0.05 M propandiol buffer (pH 9.0) (Frederick and Newcomb, 1969), rinsed briefly in buffer, and fixed in osmium tetroxide as described above; ii) 3 hr fixation in 3% glutaraldehyde-3% paraformaldehyde (Karnovsky, 1965) in phosphate buffer (pH 6.8), rinsed, and fixed in osmium tetroxide as described above. iii) 2 hr fixation in unbuffered potassium permanganate. All materials were then dehydrated and embedded according to procedures outlined above. Among the chemical fixatives used, sperms fixed in standard glutaraldehyde and osmium appeared the least altered by preparation. Except as noted, all chemically fixed material illustrated in this study was prepared according to the first procedure.

B. Physical fixation

Material for physical fixation was immersed in an isopentane–12% methylcyclohexane solution cooled in a bath of liquid nitrogen, transferred to methanol at dry ice temperatures, and dehydrated in several changes of absolute methanol at −50°C (Jensen, 1962). After several days, the material was slowly warmed, transferred to propylene oxide at room temperature, and embedded in low viscosity resin.

C. Specimen preparation

Ultrathin sections were routinely cut using a Reichert OM U2 ultramicrotome and collected on uncoated nickel or gold grids. Selected stages in pollen tube growth and gamete deposition were first thick-sectioned, photographed using Nomarski interference optics, and then reembedded for ultrathin sectioning according to the technique described by Mogensen (1971). Sections were stained using 2% uranyl acetate in 45% ethanol followed by 0.2% lead citrate (Venable and Coggeshall, 1965), or by subjecting material mounted on gold grids to the periodic acid–thiocarbohydrazide–silver proteinate (PA–TCH–SP) reaction (Thiery, 1967), with 30 min oxidation in 1% periodic acid, 6 h in 0.2% thiocarbohydrazide in 20% acetic acid, and 30 min in 1% silver proteinate solution.

Sections for light microscopic examination were sectioned at 0.5 to 2.5 um using glass knives, dried on autoradiography slides (Jensen, 1962) and mounted in glycerine with 2% phenol. Selected sections were stained using the Periodic acid–Schiff's reaction (PAS) for insoluble carbohydrates (Jensen, 1962), aniline blue–black (ABB) for proteins (Fisher, 1968), and the Feulgen reaction for nucleic acids (Jensen, 1962). Sections were observed with a Zeiss Photomicroscope I using brightfield, phase contrast, and Nomarski interference contrast microscopy.

D. Observation of isolated, living sperm cells

Isolated, living sperm cells were examined by releasing the contents of mature pollen grains in a pollen tube growth medium and observing them in Nomarski interference optics. The sucrose content of the medium was adjusted so that sperm cell volume remained constant throughout the 30 min observation period (Cass, 1973). Sperm cells which displayed cytoplasmic activity were photographed with a Zeiss Photomicroscope I at 2 to 5 min intervals during the observation period.

E. Serial reconstruction and quantitative cytology of sperm cells

Serial ultrathin sections of chemically-fixed pollen grains were collected using naked slot grids, transferred on the surface of a drop of water, and mounted on Formvar-coated slot grids (Galey and Nilsson, 1966). Serial sections containing sperm cells were numbered consecutively, photographed in the electron microscope, and printed at the same magnification. Each specimen block sectioned contained at least 10 pollen grains; the specimen block used for the majority of the organelle counts contained over fifty pollen grains which were sectioned simultaneously. The quantitative content of organelles was determined by counting only the single median section of each organelle. When a single section or maximum of two sections were unavailable, surrounding sections were scanned in order to determine whether any median sections of organelles were lost; series in which three or more consecutive sections were not available were not used. Mitochondria were the smallest organelles, measuring typically 0.25 to 0.30 um. The average section thickness (0.06 to 0.10 um) provided that each organelle was represented in at least three sections.

In order to determine the length of the sperm projection, a two-dimensional line was plotted over the center of the sperm projection using a plastic overlay. At bends in the line, points were plotted and the section number containing the center of the sperm projection at that point was recorded. Average section thickness was determined by measuring the diameter of the sperm nucleolus (assumed to be spherical) and dividing by the number of

sections in which the nucleolus penetrated the section. The distance and height between two adjacent points on the line was converted into micrometers and recorded. The total length of the sperm projection was then calculated as the sum of the distances between adjacent points, using the Pythagorean theorem.

F. Statistical treatment of mitochondrial dimensions

Mitochondrial dimensions as observed on printed electron micrographs with a minimum final magnification of X 5800 were measured using a caliper measuring device accurate to 0.05 mm. The greatest mitochondrial width, as measured in near-median sections of mitochondria, was selected as the most reliably measured dimensional parameter since it was less likely to be influenced by organelle orientation and was easily reproducible. Only mitochondria whose membranes were clearly seen in cross section were measured, since these represent organelles which are in near-median section. At least five cells were used for each population of mitochondria; no mitochondrion was measured more than once. Mitochondria were measured in six cells of origin: within sperm cells within inactive pollen grains and growing tubes near the ovule, in the pollen grain and growing pollen tube, in the egg and in the central cell. Two additional classes were constructed for mitochondria of unknown origin, including mitochondria located within 0.5 um of the sperm nucleus soon after gamete fusion and in cytoplasmic bodies located between the egg and central cell after gamete fusion. Descriptive statistics, an analysis of variance, and Student's t comparison of the means and populational variances were conducted between all of the populations measured.

III. Sperm Ultrastructure: General Cytology and Association with Vegetative Nucleus[1]

A. Introduction

In flowering plants, small nonmotile male gametes fulfill the essential and highly specialized roles of fertilization and endosperm initiation. Apparently passive cells, the sperms are structurally simple; yet their nuclear content determines half of the hereditary makeup of the embryo and their cytoplasmic content often plays a significant part in cytoplasmic inheritance in the embryo. Determination of patterns of cytoplasmic inheritance are clearly influenced by sorting patterns and competition between organelles during generative cell formation (Hagemann, 1976) and maturation (Clauhs and Grun, 1977), yet few reports specifically concern the descendent sperm cells which actually participate in double fertilization. As knowledge of male cytoplasmic inheritance in angiosperms expands, it has become evident that a greater understanding of sperm cytology is necessary on both genetic and embryological grounds.

The earliest and most striking evidence for the occurrence of male cytoplasmic inheritance in angiosperms were independent reports in 1909 that plastids, in particular, may follow non-Mendelian patterns of inheritance in *Mirabilis* and *Pelargonium*. In the former plant, Correns (1909) reported exclusively maternal patterns of plastid inheritance; in the latter, Baur (1909) reported biparental patterns of plastid inheritance resulting in variegated patterns during leaf development (see reviews by Grun, 1976; Gillham, 1978). The complementary information provided by the work of Correns and Baur established the basis for extensive research using plastid mutants to follow lines of male inheritance (Hagemann, 1976). Although no genetic evidence exists for any zygotic "restriction mechanism" in angiosperms which would systematically eliminate a given class of male (or female) cytoplasmic organelles (Hagemann, 1976), to the

---

[1]This chapter originally appeared in Protoplasma entitled "Ultrastructure of the Sperms of *Plumbago zeylanica*. 1. Cytology and Association with the Vegetative Nucleus," ©1981 by Springer-Verlag, Vienna. This chapter is reproduced herein by permission of Springer-Verlag and may not be reproduced elsewhere without their permission.

best of my knowledge this has been directly examined only in the case of plastid inheritance in *Oenothera erythrosepala* (Meyer and Stubbe, 1974). Direct observations of sperm organelle structure in pollen grains and during tube growth may provide information on whether specific organelles or classes of organelles undergo alterations in ultrastructure which could affect their viability. It is expected that knowledge of the types and relative proportion of organelles within sperms of *Plumbago zeylanica* may aid in predicting their transmissibility into the zygote and the possibility of their inheritance in the next generation.

Certain embryological adaptations which may facilitate the passage of sperms within the pollen tube and their subsequent transmission into the embryo and endosperm have remained virtually unstudied, as have the specific structural changes required for gametic transmission. The prevalent assumption that sperms within pollen tubes travel independently of the sperms and vegetative nucleus (Maheshwari, 1949) does not appear to apply in *P. zeylanica*. In this plant, the association of the sperms and vegetative nucleus may represent an adaptation to promote the passage of the sperms from the stigma to the embryo sac. One published work has reported detailed observations of sperm ultrastructure during pollen tube passage (Jensen and Fisher, 1968b). The specific structural changes, if any, required for sperms to fuse with the egg and central cell have been postulated, but are yet to be described from direct ultrastructural observation. Additional embryological issues which may influence the transmission of male cytoplasm, including differences between paired sperm cells and the possible non-transmission of some sperm cytoplasm, are the subjects of continuing research. Contrary to published literature (Maheshwari, 1949; Jensen and Fisher, 1968b; Cass, 1973), the two sperms of *Plumbago* appear to differ in cell volume; however, the biological significance of this observation remains unknown.

The present study describes sperm cytology and structural relationships in pollen grains and tubes of *P. zeylanica* using light and electron microscopy of chemically and physically fixed tissues, and Nomarski interference microscopy of isolated, living sperm cells. The genus *Plumbago* was originally selected for study because of the structural simplicity of its embryo sac, reported previously in

Cass and Karas (1974) and Russell and Cass (1981b). The embryo sac of this plant functions without synergids and instead the pollen tube releases male gametes directly between the egg and central cells (Russell, 1980). For this reason, *Plumbago* is particularly suitable for studying the structural basis of male cytoplasmic inheritance in angiosperms and determining the fate of the male cytoplasm during the process of double fertilization. The present study represents the first part undertaken in such an investigation.

B. Observations

Ultrastructure within the mature pollen grain

Sperm cell organization

Mature pollen grains of *P. zeylanica* each contain two roughly spindle-shaped male gametes which are delimited by the sperm plasma membrane, a rudimentary cell wall, and enclosed together within an internal pollen plasma membrane. These sperms are derived from the same generative cell and share a common transverse cell wall, but differ significantly with respect to their morphology. The male gamete immediately adjacent to the vegetative nucleus has a long, slender (usually <1 um wide) projection which wraps around the periphery and occupies embayments of the vegetative nucleus; the other male gamete has a short free end projecting into vegetative cytoplasm. In one sperm cell, reconstructed from serial ultrathin sections, this projection reached a length of 30 um (Fig. 11), while the other sperm cell (not shown) was only 8 um long.

Both sperm cells contain a normal complement of organelles, the majority of which are clustered near the nucleus in the widest part of the cell (Fig. 1, 4, 5, 12). The sperm cells observed contain numerous mitochondria, plastids, endoplasmic reticulum (ER), dictyosomes, vesicles, and small vacuoles. Nuclei are elongate (about 3 by 6 um) with numerous pores in the nuclear envelope (Fig. 5). A nucleolus is typically present in the nucleus and although small (approx. 1 um), it is readily identifiable in light microscopic preparations (Fig. 15, 18). Nuclear chromatin is only slightly condensed (Fig. 12).

Figs. 1-2: Electron micrographs of chemically fixed mature pollen grains.

Fig. 1: Electron micrograph of two chemically-fixed sperm cells in longisection. Lobes of the vegetative nucleus (*VN*) ensheath part of the sperm cell (*S*) at a number of locations (black arrowheads). Endoplasmic reticulum is found near the outer surface of the sperm (white arrowheads). X 14,600.

Fig. 2: Electron micrograph of junction between two chemically-fixed sperm cells formed by the presence of a common vesiculate cell wall (*cw*) and plasmodesmata (arrowheads). Mitochondrion (*m*) is located in pollen cytoplasm. X 53,100.

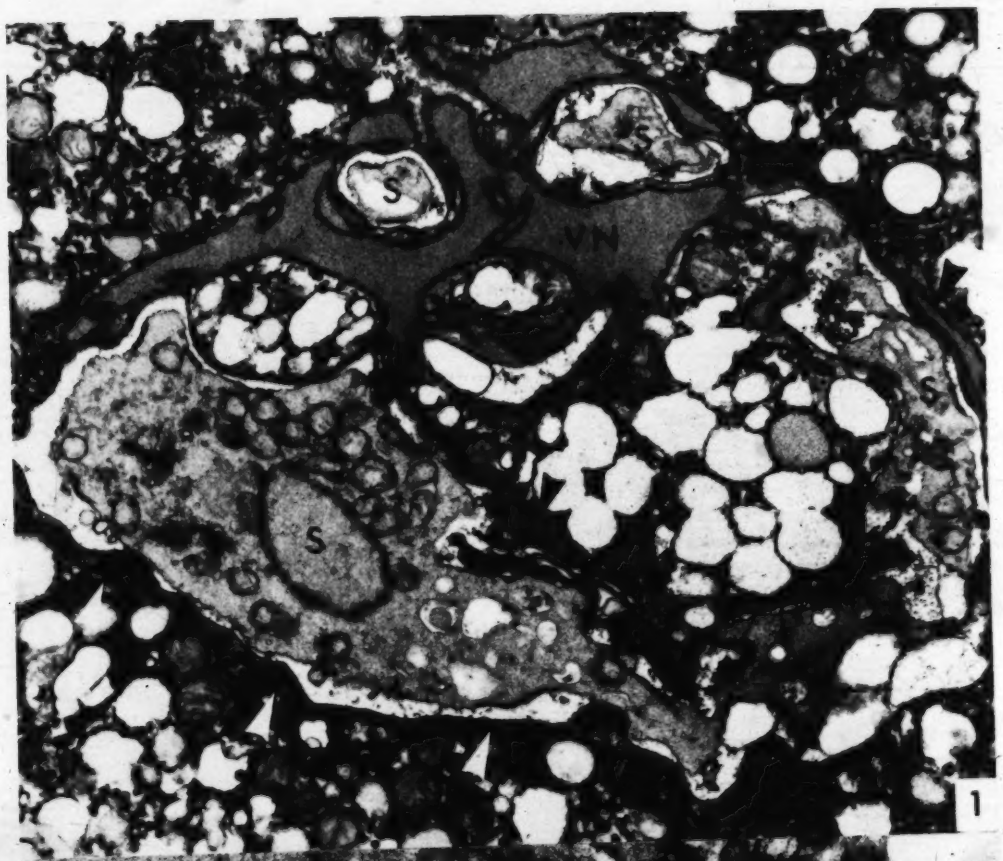
S
VW
S
1

CW
m
2

Sperm mitochondria are usually smaller than those in vegetative cytoplasm and are spheroidal to ellipsoidal in shape, possessing narrow but well-developed cristae (Fig. 5). Plastids (Fig. 3, 4) are larger than mitochondria, and their stromata are electron dense in uranium and lead stained material. Plastids contain a number of rudimentary lamellae, internal vesicles, ribosomes, and occasionally, paracrystalline structures in their stromata (Fig. 4 and inset). Paracrystalline structures like these have been found within immature and senescent plastids in somatic tissues and are believed to be composed of accumulated enzymes or ferritin (Toyama, 1980). Mitochondria and plastids are often found in clusters composed almost exclusively of either mitochondria (Fig. 5) or plastids (Fig. 4), and the two are rarely seen together in a given thin section of sperm cell. (An exception can be seen in Fig. 3.) An as yet unidentified class of single-membrane bound organelles was occasionally seen in association with plastids (Fig. 3, 4; unlabeled arrows). These bodies could represent either electron-dense vesicles or microbodies. Microbodies, although rare in angiosperm gametophytes, have been reported in the female gametophyte of *P. zeylanica* (Cass and Karas, 1974).

Sperm cell dictyosomes are abundant, well-developed, and possess numerous cisternae, with clear vesicles present near the maturing face of the dictyosome. Occasionally, an apparently anastomosing network of tubular ER is seen near dictyosomes (Fig. 5). Lamellar cisternae of ER occur as isolated segments at the periphery of the cell but are rarely well developed (Fig. 5, 11). In freeze-substituted material (Fig. 8-10), dictyosomes, some vesicles, ER, and the sperm cell wall are all stained by the PA-TCH-SP reaction.

A rudimentary cell wall appears to surround the sperms in chemically (Fig. 2) and physically fixed pollen grains (Fig. 6, 7; unlabelled arrows). In chemically fixed tissues, the cell wall varies from 0.1 to 0.2 um in thickness and contains numerous vesicles. Polysaccharides were poorly stained by the PA-TCH-SP reaction in chemically fixed tissues (Fig. 3; compare with Fig. 2, prepared without PA). In contrast, freeze-substituted sperms have narrower cell walls, 0.05 to 0.1 um wide, with vesicles restricted to the segment of wall shared by the two

Figs. 3-5: Electron micrographs of chemically fixed mature pollen grains.

Fig. 3: Electron micrograph of a chemically-fixed sperm cell. Transection of a sperm cell containing mitochondria (*m*), plastids (*p*), and an unidentified single membrane-bound organelle (arrows). X 20,500.

Fig. 4: Electron micrograph of sperm plastids in the pollen grain. An aggregation of sperm plastids (*p*) some containing paracrystalline structures (arrowheads). Unidentified single membrane-bound organelles (arrows) are associated with plastids. N=nucleus. (Fixed with glutaraldehyde-diaminobenzidine and osmium tetroxide.) X 13,800 inset= X 77,500.

Fig. 5: Electron micrograph of chemically-fixed sperm cell in longisection containing a nucleus (*N*) with numerous nuclear pores (small arrows), mitochondria (*m*), dictyosomes (*d*), and tubular endoplasmic reticulum (*ter*). *er* = endoplasmic reticulum (vegetative cell); *VN* = vegetative nucleus. X 28,100.

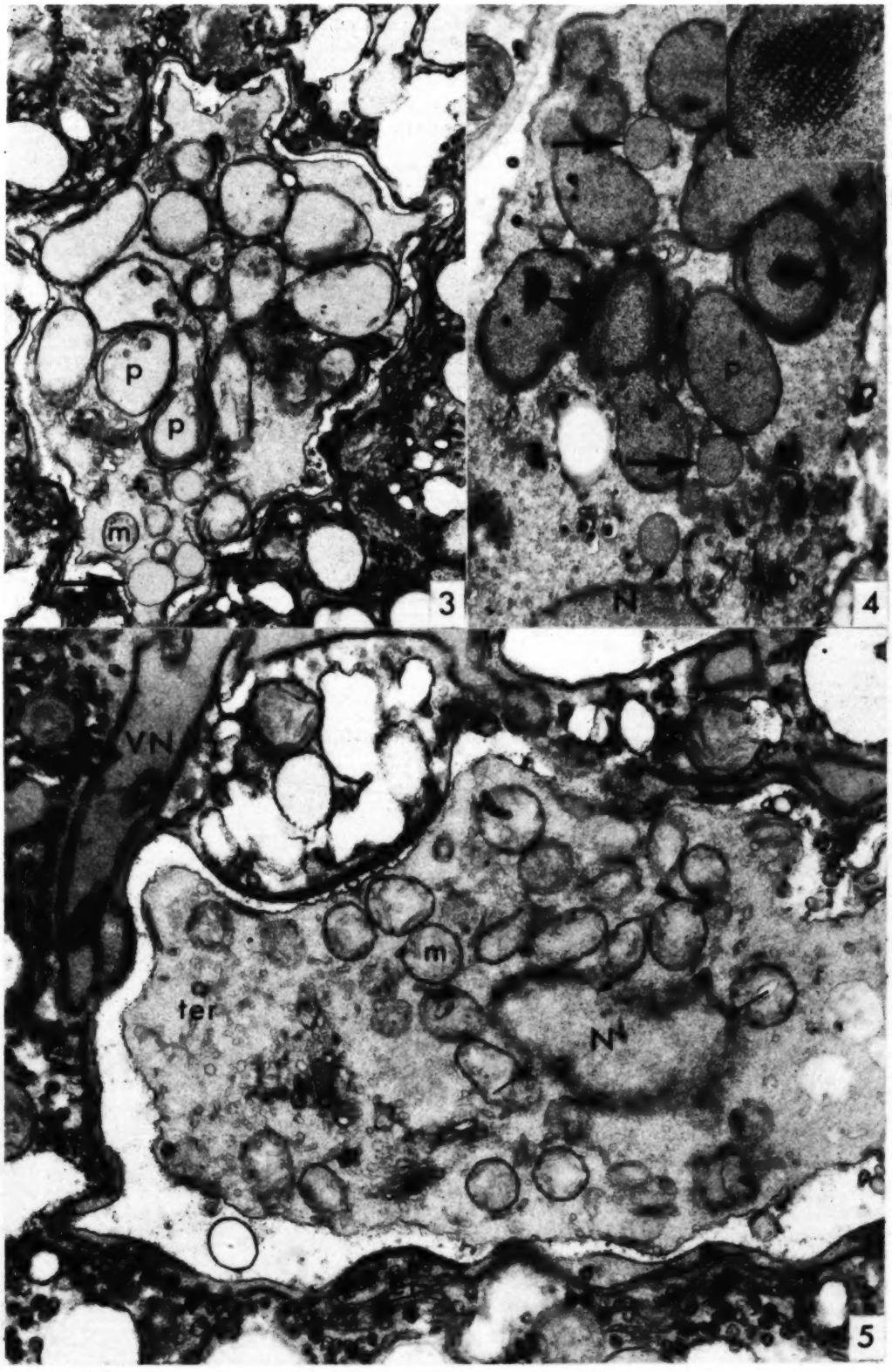
P
P
m
3
P
N
4
VN
m
ter
N
5

sperms. Physically-fixed cell walls stain intensely after the PA-TCH-SP reaction (Fig. 8-10). Comparing the speed of fixation, the uniformity of wall thickness, and the density of PA-TCH-SP staining after freeze-substitution, it appears that physically fixed sperm cell walls are less altered by preparation than those fixed by chemical means.

Microtubules were not observed in sperm cells during the course of this study, although identical techniques reveal numerous microtubules in generative cells of *P. zeylanica* (Chapter 4). At anthesis and throughout pollen tube growth, microtubules are rare or possibly absent. Probable microfilaments were seen in *P. zeylanica* (Fig. 24, unlabeled arrow), but difficulties in preserving microfilaments may exist since they were observed infrequently.

Vegetative cell organization

The vegetative cell contains a large polymorphic nucleus, many mitochondria, plastids, occasional starch grains, ER, ribosomes, and numerous dictyosomes and polysaccharide vesicles. The nucleus, up to 13 um long, is a highly lobed, irregular structure with deep embayments (Fig. 1, 6, 11, 12) and numerous nuclear pores (Fig. 1, 5). Within embayments of the nuclear envelope and immediately surrounding the nucleus, rough endoplasmic reticulum often forms intricate membrane arrays (Fig. 11, 12). Elsewhere, lamellar ER is often found adjacent to sperm cells becoming especially pronounced on the surface opposite to the vegetative nucleus (Fig. 1, 5, 11, 12). In freeze-substituted preparations, the perinuclear cytoplasm contains few vesicles or other organelles and sometimes appears to surround cellular projections of the sperm (Fig. 6, 7).

The vegetative pollen cytoplasm contains numerous, small vesicles with PA-TCH-SP stained polysaccharides (Fig. 8, 9, 10). These vesicles can be divided into two classes on the basis of size and staining characteristics, and can be identified in both chemically and physically fixed tissues. Following periodic acid oxidation the smallest vesicles, 0.05 to 0.1 um in size, stained densely with the PA-TCH-SP reaction (Fig. 8, 9; compare Fig. 10 without PA oxidation). The remaining vesicles, from 0.3 to 0.6 um in median section, have an electron-dense PA-TCH-SP reactive perimeter and less densely stained

Figs. 6-10. Frozen-substituted pollen grains stained with uranium and lead (Fig. 6, 7) and by PA-TCH-SP reaction (Fig. 8, 9, 10).

Fig. 6: Electron micrograph of physically-fixed pollen grain. Near-median section of vegetative nucleus (*VN*) showing a sperm cell (*S*) inserted within uniformly gray perinuclear cytoplasm. Two aggregations of rough endoplasmic reticulum (*er*) are present near sperm projection (labeled arrowhead). Region enclosed in box is shown in Fig. 7. X 9,200.

Fig. 7: Electron micrograph of physically-fixed sperm cell and vegetative nucleus. Sperm cell (*S*), cell wall (small arrows) and vegetative nucleus (*VN*) are visible. Unlabeled arrowheads indicate nuclear envelope. X 43,900.

Fig. 8: Electron micrograph of junction between physically-fixed sperm cells, stained for polysaccharides. Junction between two sperm cells (*S*) with an extensive segment of shared cell wall (arrows). *d* = dictyosome; *pv* = polysaccharide vesicle. X 17,100.

Fig. 9: Electron micrograph of physically-fixed pollen grain, stained for polysaccharides. Sperm cells (*S*) delimited by PA-TCH-SP reactive cell walls (small arrowheads). Possible plasmodesma at the sperm cell junction is indicated by an arrow. *ter* = tubular endoplasmic reticulum; *v* = vesicle. X 38,200.

Fig. 10: Electron micrograph of physically-fixed pollen grain, stained without periodic acid oxidation. Sperm (*S*) and cell wall (arrows) after PA-TCH-SP reaction with periodic acid oxidation. (This figure was printed with the same contrast photographic paper as in Figs. 8 and 9, but exposed three times longer.) *pv* = polysaccharide vesicle. X 43,600.

6
7
S
v
ter
S
8
S
S
py
9
S
pv
10

contents (Fig. 8, 10). In freeze-substituted preparations of vegetative cytoplasm, PA-TCH-SP reaction products were also detected in dictyosomes, starch grains, and the pollen intine.

Structural interrelationships of sperms and vegetative nucleus

Associations within mature pollen grains

In mature pollen grains of *P. zeylanica*, the two sperm cells are directly linked; they share a transverse cell wall with plasmodesmata and are enclosed together by the inner vegetative cell plasma membrane (Fig. 2, 8, 9). One of these two sperms is also associated with the vegetative nucleus as a consistent feature of pollen grain organization (Fig. 1, 5, 6, 11, 12). The basis of this association appears to be a long, narrow projection of the sperm cell (averaging <1 um wide and about 30 um long; Fig. 11) which wraps around the periphery of the vegetative nucleus and occupies embayments of that nucleus. Analysis of

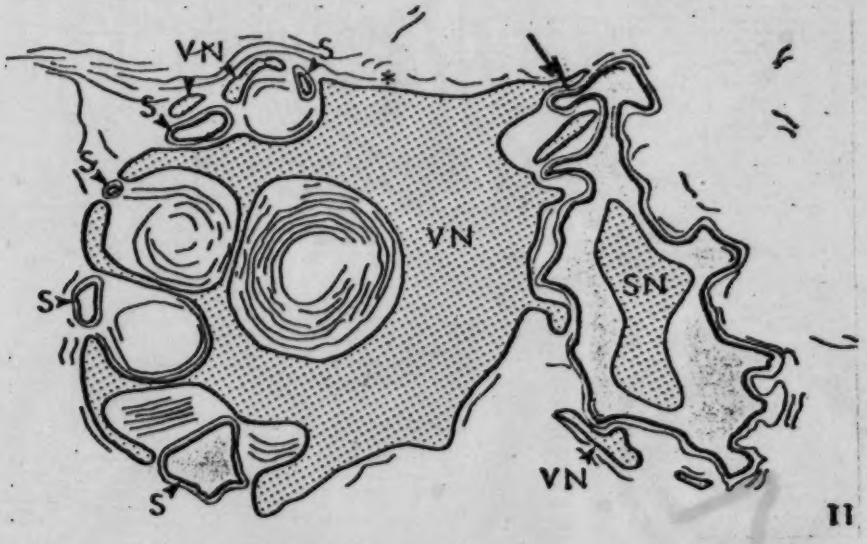

Fig. 11: Schematic representation of the association between one sperm and the vegetative nucleus in a pollen grain as traced from an electron micrograph. A reconstruction of this sperm prepared using serial sections revealed that this sperm's projection (labeled arrowheads) was about 30 um long, extending from the arrow, wrapping clockwise around the periphery of the vegetative nucleus, and terminating near the asterisk. Note aggregations of ER (represented by thin lines). Embayments and ensheathing lobes (labeled arrowheads) of the vegetative nucleus are evident. *S* = sperm cell; *SN* = sperm nucleus; *VN* = vegetative nucleus. X 10,400.

serial ultrathin sections also reveals that nearly 70% of the sperm projection and 10% or more of the main cell body may be ensheathed by lobes of the vegetative nucleus. While sperms never directly contact the vegetative nucleus, sometimes sperm projections are separated from the nuclear envelope by as little as 0.1 um; projections are typically embedded in a morphologically distinct perinuclear cytoplasm (Fig. 1, 6, 7, 11, 12). Although I looked specifically for cellular structures which might directly link one sperm or its surrounding membranes with the vegetative nucleus, I was unable to find any.

Associations of sperms and vegetative nucleus within isolated pollen grain contents

Reconstructing the sperm-vegetative nucleus association in the living state is simplified by releasing pollen grain contents into a medium designed for pollen tube growth and briefly observing them with Nomarski interference optics. Newly isolated sperm cells appear roughly spindle-shaped and are closely associated with the vegetative nucleus and with one another (Fig. 13, 16). While both sperms are similar in shape, the one adjacent to the vegetative nucleus has a longer projection and greater cellular volume than the other sperm. Part of this sperm appears to extend just within the edge of the vegetative nucleus membrane, presumably in embayments of the nuclear envelope (Fig. 14, 16).

Observation of living sperm cells in isolation also provides information on the regulation of sperm cell shape and the possibility of independent cell movement. Sperms remaining surrounded by their native pollen cytoplasm do not change greatly in cell shape or structural association over the observation interval (Fig. 16, 17). However, sperms which were separated from surrounding pollen cytoplasm appeared to undergo rapid degenerative changes in both cell shape and structural association within 10 minutes (Fig. 13-15). Cytoplasmic activity was observed in sperm cells throughout the observation period, but in none of the sperms observed were conformational changes reversed. Sperms did not appear to display directional movement or any shape changes that appeared related to possible motility.

Fig. 12: Electron micrograph of the structural association of sperm cell and vegetative nucleus in a mature pollen grain. Complementary surfaces formed by a projection of the sperm cell (*S*; black arrows) and ensheathing lobes of vegetative nucleus (*VN*; white arrows) are evident. The other sperm cell is visible in the upper right corner, immediately adjacent (arrowheads) to the first sperm cell. X 13,000.

Figs. 13-15. Sperm cells (*S*) and vegetative nucleus (*VN*) immediately after isolation in a pollen tube growth medium. Photographed with Nomarski differential interference optics at 5 minute intervals. Unlabeled arrowheads indicate a sperm cell projection in Fig. 14 and the internal pollen plasma membrane in Fig. 15. X 1,200.

Figs. 16 and 17. Same as Figs. 13-15, except isolated in pollen cytoplasm and photographed over a 20 minute interval. Arrowheads indicate a sperm cell projection in Fig. 16 and sperm-to-sperm junction in Fig. 17. X 1,880.

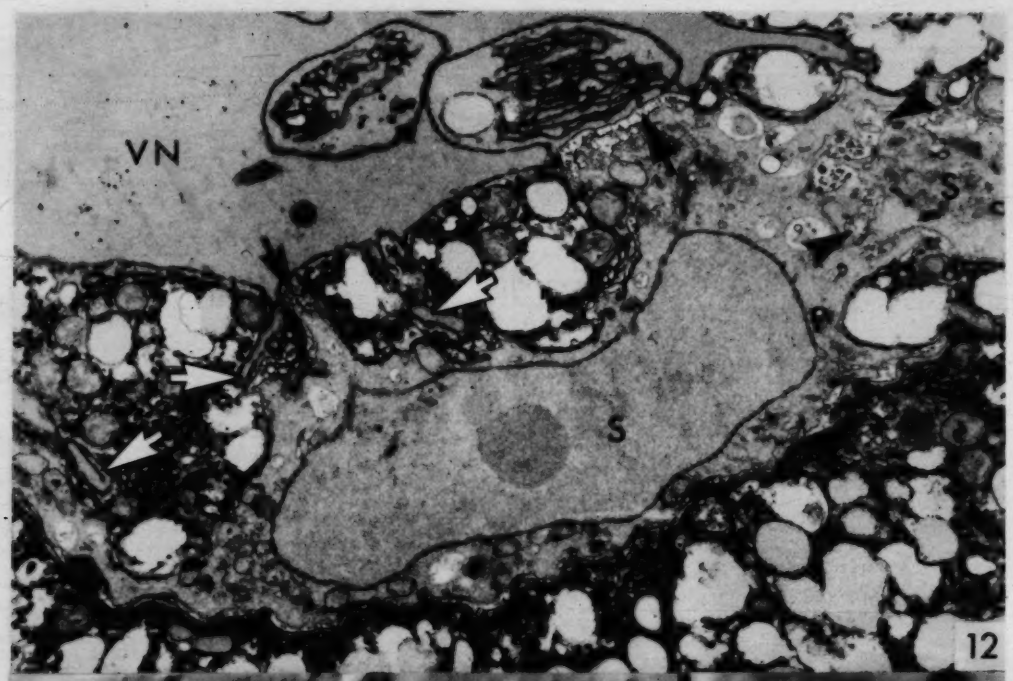

12

13

14

15

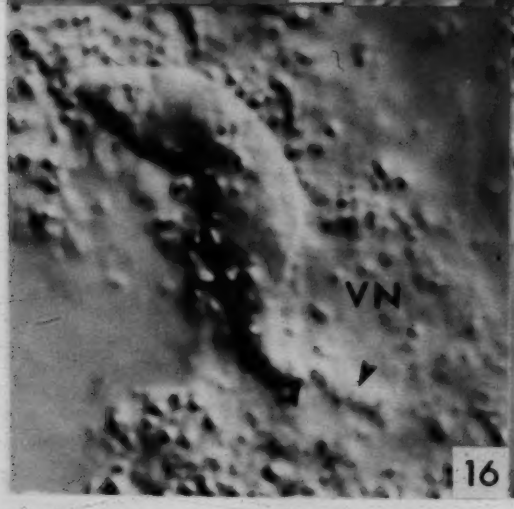

16

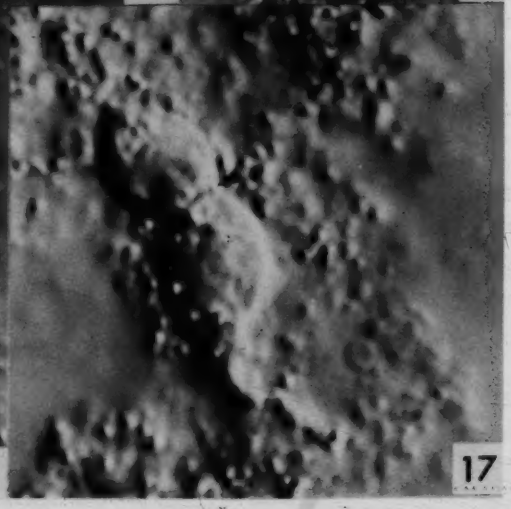

17

Associations of sperm and vegetative nucleus within the pollen tube

The nature of the sperm–vegetative nucleus association appears unchanged throughout pollen tube growth, but the distance between these two structures is greatly altered during rapid tube elongation. Early pollen tube growth is rapid (up to 5 mm/hr or more, *in vivo*) and pollen tube diameter is relatively narrow (usually <10 um wide). During this phase, the main body of the vegetative nucleus precedes the sperm cells by up to 50 um (Fig. 18, 19) and is nearly as wide as the bore of the tube. The vegetative nucleus is highly elongated, with numerous lobed extensions near its apex (Fig. 20, arrows). Sperm cells travel within the tube as a linked pair, and continue to share a common cell wall.

In light microscopy, a strand passing between the vegetative nucleus and the leading sperm cell can be distinguished (Fig. 18, 19). Electron microscopic examination reveals that this strand is composed of vegetative nucleus, internal pollen plasma membrane, and projections of the leading sperm cell (Figs. 19–22). Projections of sperm cytoplasm are relatively narrow and sometimes appear to be isolated within a thin layer of perinuclear cytoplasm (Fig. 21). The leading sperm cell is demonstrably contiguous for over 30 um from the center of the strand (Fig. 19, unlabeled arrow) to the sperm cell common wall; it may become more than 60 um long, since sperm cytoplasm can also be recognized near the main body of the vegetative nucleus (Fig. 19, unlabeled arrowheads). The vegetative nucleus, itself, stretches to >40 um at this stage (Fig. 19 and 22). The region of sperm–vegetative nucleus overlap may extend for a distance of >35 um (a length consistent with that of the sperm projection in pollen grains; see Fig. 11).

During a slower phase of pollen tube elongation (about 250 um/hr, *in vivo*) which occurs near the ovule, tube diameter increases until the two sperms can fit beside each other in the tube (Fig. 23). Sperms remain associated with the vegetative nucleus even after entering the micropyle (unpublished data), but more loosely than before as the sperms become more rounded (Fig. 24, 27). In these last two figures, sperm projections do not occur, but lobes of vegetative

Figs. 18-22: Chemically-fixed style with growing pollen tube.

Fig. 18: Nomarski differential interference micrograph of apical portion of pollen tube during rapid elongation phase in the upper style. The pollen tube apex is oriented toward the top of the page. The strand composed of vegetative nucleus (*VN* and sperm cell (*S*) linking these two bodies is labeled in an electron micrograph of this section in Fig. 19. X 2,400.

Fig. 19: Electron micrograph of pollen tube during rapid elongation phase obtained by reembedding and ultrathin-sectioning the section shown in Fig. 18. Unlabeled arrowheads indicate strands of sperm cell cytoplasm associated with elongate vegetative nucleus (*VN*). Two sperms (*S*) remain linked by a shared cell wall. X 2,800.

Fig. 20: Electron micrograph of vegetative nucleus apex during rapid elongation phase at higher magnification. The leading face of the vegetative nucleus displays numerous lobes in the nuclear envelope (small arrows). X 9,430.

Fig. 21: Electron micrograph of vegetative nucleus adjacent to sperm projection during rapid pollen tube elongation. Segments of sperm cell (*S*) are visible near the thin perinuclear cytoplasm at the trailing edge of the same vegetative nucleus. X 17,650.

Fig. 22: Electron micrograph of vegetative nucleus adjacent to sperm projection during rapid pollen tube elongation. The most proximal portion of vegetative nucleus (*VN*) is also associated with sperm cell. The same segment of vegetative nucleus is indicated by a labeled arrowhead in Fig. 19. X 12,350.

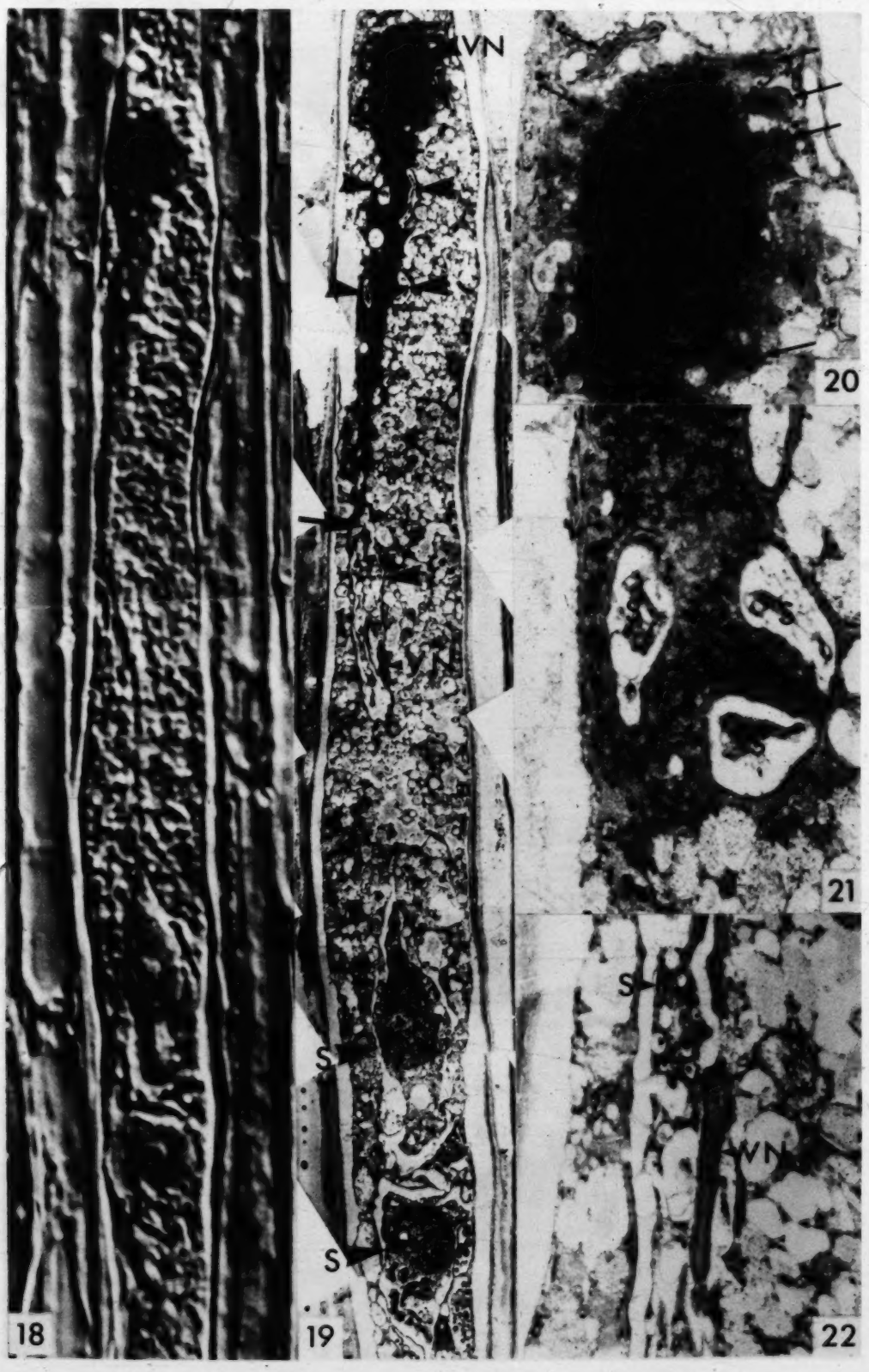
VN
VN
S
S
S
VN
18
19
20
21
22

nucleus are located as closely as 0.1 um from the leading sperm. Sperm cells appear to remain connected by plasmodesmata as the pollen tube nears the micropyle, (Fig. 27, arrow), and remain closely associated even after their discharge from the pollen tube within the embryo sac (Russell, 1980).

Sperm cell modifications during pollen tube growth

During the course of pollen tube growth, sperms become more rounded and less irregularly shaped in both chemically and physically fixed stylar tissues (Fig. 18, 23, 25). In freeze-substituted material, sperm cells become rounded and more regularly shaped, but not spherical. Sperms continue to possess a periodic acid-Schiff's (PAS) reactive cell wall, visible in unstained sections as a clear region (Fig. 23); however, the stainablity and extent of this wall decreases during pollen tube growth. Sperm cell projections are usually observed but are less extensive than in pollen grains.

Sperm organelles are not greatly modified during pollen tube growth, but changes in the condition of mitochondria appear noteworthy. Sperm mitochondria, which are round at anthesis and have narrow cristae (Fig. 5), elongate during pollen tube growth and their cristae expand considerably (Fig. 26). These alterations were also observed in the pollen tube but were not observed in surrounding stylar tissue (unpublished data). The sperm nucleus becomes more nearly spherical near the completion of tube growth, presumably as a result of changes in cell shape. Nuclear contents appear to become slightly more condensed (Fig. 23, 25). No significant changes were observed in the nucleolus or in plastids.

C. Discussion

Sperm cell structure

Sperm and generative cells examined to date share a number of common cytological features. These include the presence of a nucleus, free and bound ribosomes, endoplasmic reticulum, vesicles, dictyosomes, and mitochondria[2]. Additionally, generative and sperm cells are delimited by their own plasma

---

[2]In a single exception, *Epidendrum scutella*, the generative cell appears to lack mitochondria (Cocucci and Jensen, 1969a).

Fig. 23: Phase contrast micrograph of pollen tube during slow growth phase Frozen-substituted pollen tube fixed during the slow phase of tube growth near the ovule. Somewhat rounded sperm cells (*S*) remain surrounded by a clear zone (arrowheads) which represents cell wall. Vegetative nucleus (*VN*) remains closely associated with sperms. The pollen tube apex is shown in the upper right corner of this figure. X 2,500.

Figs. 24-27: Electron micrographs of chemically fixed pollen tubes in the style.

Fig. 24: Electron micrograph of a sperm plastid during late pollen tube growth near the ovule. An unlabeled arrow in the pollen cytoplasm indicates probable bundle of microfilaments. X 53,500.

Fig. 25: Electron micrograph of the pollen tube nearing the ovule showing the vegetative nucleus (*VN*) leading two rounded sperm cells (*S*). Pollen tube is just emerging from the stylar transmitting tissue (*TT*). The inner integument is shown nearby (*Int*). X 3,500.

Fig. 26: Electron micrograph of sperm mitochondrion during late pollen tube growth. Sperm mitochondria (*m*) become elongate, and cristae expand during late phases of pollen tube growth. X 50,000.

Fig. 27: Electron micrograph of two chemically-fixed sperm during late pollen tube growth. Two rounded sperm cells remain linked (arrow) as pollen tube approaches the ovule. *N* = nucleus; *p* = plastid. X 11,400.

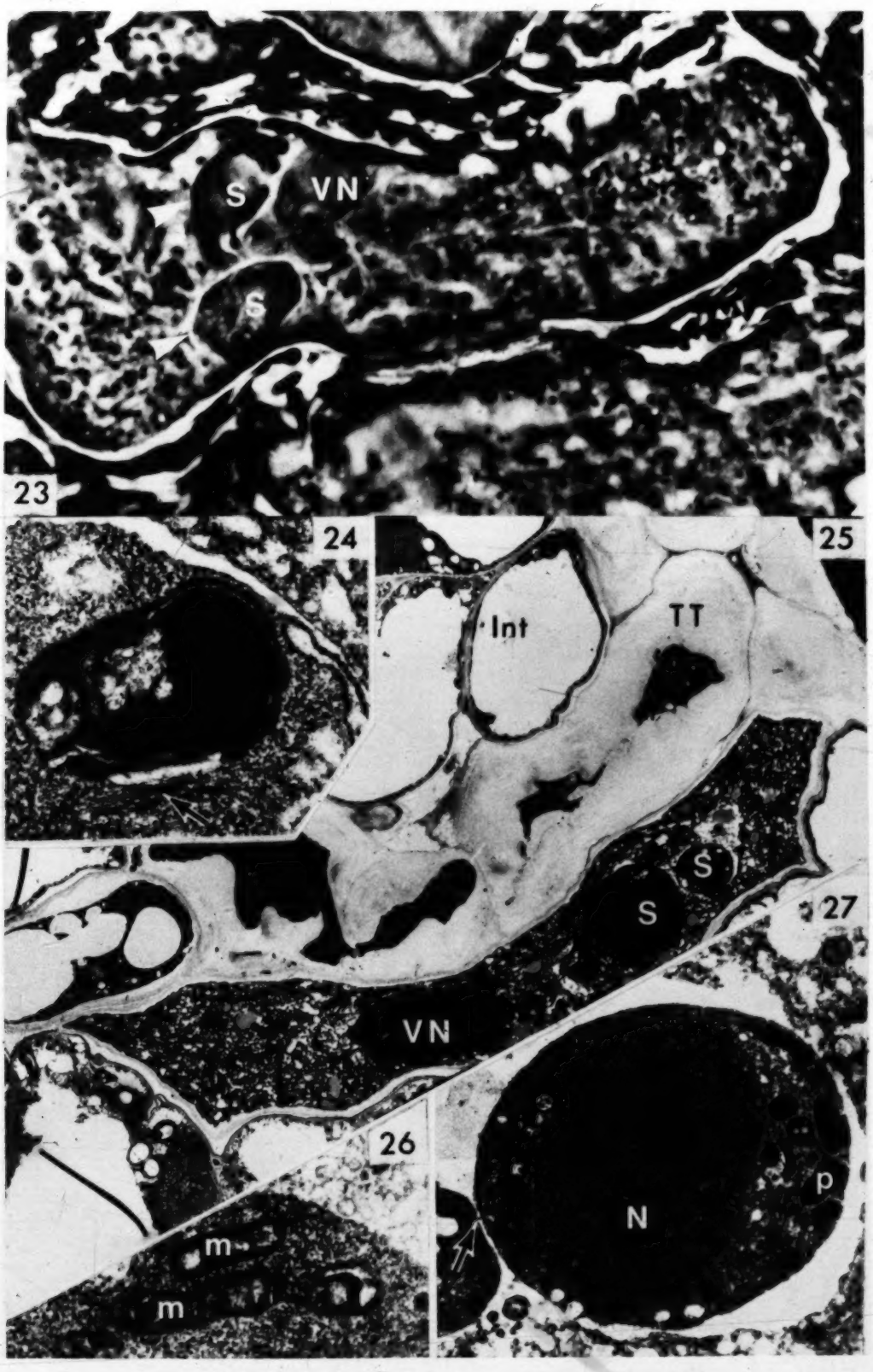
S
VN
S
23
24
25
Int
TT
S
S
27
VN
26
m
m
N
p

membrane and are surrounded by the inner vegetative cell membrane. However, the cytology of flowering plant sperms appears to vary with regard to the inclusion of plastids, microtubules, microfilaments, and the presence and extent of a surrounding cell wall (Cass, 1973; Cass and Karas, 1975; Cheng, Shiyi, Liyun, Xiuru, and Jiaheng, 1980; Hoefert, 1969; Jensen and Fisher, 1968b; Karas and Cass, 1976).

The presence of generative cell plastids appears to be a prerequisite for the transmission and inheritance of male plastome genes (Hagemann, 1976). Angiosperms which display uniparental (maternal) patterns of plastome inheritance, as do the majority of flowering plants (Gillham, 1978), typically exclude plastids during generative cell cytokinesis (Hagemann, 1976) or eliminate plastids by means of a "lethality factor" during generative cell maturation (Clauhs and Grun, 1977). However, the presence of plastids in the generative cell, while permitting transmission of paternal plastids into the sperm, does not necessitate their genetic expression in the embryo. In some varieties of *Oenothera*, a well-described but apparently little understood process of nucleocytoplasmic incompatibility appears to decrease the replication rate of male plastids, alters their genetic expression, and eventually may result in the elimination of paternal plastids within the mature plant (Grun, 1976; Gillham, 1978). A number of other possibilities in which generative cell plastids may be transmitted but uninherited include: i) spontaneous or nuclear-induced failure of sperm plastids to replicate or to express certain genetic characteristics; ii) differential plastid apportionment during generative cell division; iii) transmission of sperm plastids into a cell lineage which is unrepresented in the mature plant (e.g., the suspensor or basal cell); iv) failure of sperm cytoplasm to enter the egg during gamete fusion. Although cytological evidence contradicts the fourth alternative in *P. zeylanica* (Russell, 1980), an evaluation of the remaining options will require a thorough knowledge of plastome genetics and ultrastructure in this plant. In considering the transmission of other heritable structures in the generative or sperm cell cytoplasm, including mitochondria or virions, similar arguments may be made. Presuming that conditions of non-inheritance like those described above are not

in effect, one would expect, based on the present study of sperm cytology, that *P. zeylanica* will display biparental inheritance patterns of plastid and mitochondrial genes, and transmit other heritable structures present in male cytoplasm.

The nature of the cell walls surrounding male gametes may be expected to influence sperm cell physiology and gametic transmission, yet there is no clear, general understanding of their construction and extent. In *P. zeylanica*, plasmodesmata and vesicles are present in sperm cell walls regardless of preparative techniques used; fibrillar substructure is not visible. In four different chemical fixation regimes, variable distances were observed between sperm and vegetative cell membranes and attempts to stain the sperm cell wall with the PAS and PA-TCH-SP reactions produced negligible results. Thus, sperm cell walls which were chemically fixed appeared to be altered during preparation. Physically-fixed, freeze-substituted mature pollen grains produced a far more consistent image of sperm cell wall structure and thickness, staining intensely after PAS and PA-TCH-SP reaction. In these preparations, the sperm cell wall is 0.05 to 0.1 um wide and decreases after several hours of pollen tube growth to less than 0.03 um. Near the completion of pollen tube growth, the sperm boundary appears to consist of only a thin layer of polysaccharides rather than a conventional cell wall. Following discharge from the pollen tube, sperm cell wall appears to disperse almost completely (unpublished data), and therefore would not be expected to interfere with the completion of gamete fusion.

The regulation of mature sperm cell shape in *P. zeylanica* is an intriguing question in light of the structural relationships reported between sperms and the vegetative nucleus. In this regard, the presence and extent of microtubules and microfilaments should receive special consideration, as these two structures are generally believed to have major cytoskeletal roles. The establishment of the spindle shape typical of mature sperm cells occurs in the progenitor (generative) cell in *P. zeylanica*. At this stage the generative cell has numerous, longitudinally-oriented microtubules located adjacent to the plasma membrane. Presumably, these microtubules serve, at least in part, a cytoskeletal role and

may as in *Endymion* and *Haemanthus* generative cells aid in the transformation of the immature, ellipsoidal generative cell into its mature spindle shape (Burgess, 1970; Sanger and Jackson, 1971). Apparently, in *Endymion*, some cytoskeletal microtubules may become incorporated in forming the mitotic spindle during generative cell division (Burgess, 1970). In *P. zeylanica*, a similar phase of microtubular depletion seems to occur during sperm cell formation; however, in sperms of this plant, unlike sperms of other trinucleate pollen reported to date (*Beta*, Hoefert, 1969; *Hordeum*, Cass, 1973; Cass and Karas, 1975; *Secale*, Karas and Cass, 1976; *Triticum*, Cheng, et al., 1980), cytoskeletal microtubules apparently are not re-established after generative cell division. In *Plumbago* unlike the latter plants, cellular morphogenesis appears to precede sperm cell formation (unpublished data), whereas in *Hordeum*, *Secale*, and *Triticum*, the onset and completion of morphogenesis apparently follows sperm formation. *Beta* appears to represent an intermediate case, in which the onset of morphogenesis precedes generative cell division, but is not completed until after the two sperms are formed (Hoefert, 1969, 1971).

The presence of infrequently observed microfilaments may contribute to the regulation of sperm cell shape but the extent of their influence is unknown. Correlated light microscopic examination of living, isolated sperm cells reveals that immediately upon release from the pollen grain, local irregularities in sperm shape decrease and that sperms initially retain their spindle shape and structural associations. Sperms also display extensive cell plasticity *in vivo* during passage in normally growing pollen tubes (Fig. 18, 19). Such observations of sperm cytology and behavior suggest that the external environment of sperm cells plays an important role in maintaining cell shape. Observed shape changes *in vivo* may result largely from changing cytoplasmic conditions in the pollen grain and growing pollen tube. Based on the apparent absence of highly organized cellular components known to influence cell movement in other biological systems, and my own observations of living, isolated sperms, I feel that the possibility of directional motility in sperm cells of *P. zeylanica* is highly unlikely.

Structural associations involving sperm cells

The two sperms and the vegetative nucleus are consistently associated in pollen grains and tubes of *P. zeylanica* independent of the mode of fixation or other preparative procedures (see section 3.2). The two sperms are joined by a transverse cell wall with plasmodesmata (Fig. 2, arrowheads) and are surrounded by the inner vegetative cell membrane. The transverse cell wall probably originates during generative cell cytokinesis. One of the two sperm cells is consistently associated with the vegetative nucleus, sharing complex complementary boundaries over much of its surface. The basis of this association appears to be a long, narrow projection of the associated sperm cell which wraps around and occupies embayments of the vegetative nucleus; only a thin sheath of perinuclear cytoplasm appears to separate these two structures. Lobes of the vegetative nucleus, in turn, partially ensheath this associated sperm cell. Two important features of the sperm–vegetative nucleus association, namely: i) the extensive surface area shared by sperm and vegetative perinuclear cytoplasm, and ii) the elaborate morphological relationship between one sperm and the vegetative nucleus, suggest that the conformational relationship of these two structures may help stabilize their association. The only recent report which presents information comparable to the present study is that of Jensen and Fisher (1970), in which the sperms of cotton are apparently associated with the vegetative nucleus, but this association in cotton lacks the morphological complexity observed in *Plumbago*. Since it seems unlikely that two large structures like these could be stabilized exclusively by their conformation, I looked specifically for cellular structures which might directly link one sperm or its surrounding membranes with the vegetative nucleus. I was, however, unable to observe any such structures.

The occurrence of associations between sperm cells and the vegetative nucleus may facilitate the passage of sperms within the pollen tube and assure their nearly simultaneous delivery into the embryo sac. Rapid pollen tube growth, while being an obvious advantage in gametophytic competition, would be counterproductive if it resulted in the inadvertent exclusion of male gametes

from the growing pollen tube. Possibly, especially in light of rapid pollen tube elongation rates in *P. zeylanica* (which reach 5 mm/hr (>80 um/min) in artificially pollinated styles; unpublished observations), such a linkage may represent a competitive advantage in delivering both sperms to the lower style and ovule more effectively. As pollen tube growth slows, the sperms and vegetative nucleus approach the growing tip and seem less tightly associated: they share less surface area and the sperm projection becomes less conspicuous. Sperm-to-sperm connections are retained throughout pollen tube growth and may also aid in delivering both male gametes into the region between the egg and central cell where gamete fusion occurs (Russell, 1980; Russell and Cass, 1981b). Successful gamete transmission in the *Plumbago* system, as well as in the more common system in angiosperms where gamete transmission is mediated by a synergid, probably requires some form of gamete recognition with specific conditions of membrane receptivity. Since the conditions favorable for gamete fusion are likely to be transient following pollen tube discharge, the close association of sperm cells could promote their efficient co-transmission at a time when the receptivity of target cell membranes is being rapidly altered.

Sexual reproduction in *P. zeylanica*, and apparently all members of the tribe Plumbagineae (Russell, 1980), occurs in the absence of synergids, the cell type in angiosperm megagametophytes which normally receives the pollen tube and physically mediates sperm transmission. Using previous studies of male gamete structure as a basis for comparison (Cass, 1973; Cass and Karas, 1975; Cheng, et al., 1980; Hoefert, 1969; Jensen and Fisher, 1968b; and Karas and Cass, 1976), I have been unable to find any unique modifications in *P. zeylanica* sperm structure which may facilitate the process of gamete delivery in a synergidless angiosperm, with the possible exception of sperm-to-sperm connections and associations with the vegetative nucleus. Theoretically, simultaneous delivery of both male gametes should be favored in angiosperm reproductive systems where sperms must each be delivered to different female cells to effect double fertilization; however, the generality of the structural features described in *Plumbago* is yet unknown and may prove to be relatively

common as other flowering plant sperms are critically examined.

IV. Sperm Ultrastructure: Quantitative Cytology and Symmetry of Organelle Inheritance

A. Introduction

In the majority of angiosperm male gametophytes, the generative cell lacks plastids (Gillham, 1978) either as a consequence of unequal distribution of plastids during the formation of the generative cell (Hagemann, 1976) or as a result of degeneration of plastids during generative cell maturation (Clauhs and Grun, 1977). Those taxa which do contain generative cell plastids are divided into two groups: plants which regularly contain numerous generative cell plastids (Dexheimer, 1965; Diers, 1963; Knoth, 1975; Lombardo and Gerola, 1968) and those which inconsistently may possess few or single plastids (Hoefert, 1969). The consistency of these cytological results with the genetic data suggest the possibility that cytological study of generative cells may reliably allow prediction of whether paternal plastids are transmitted, or whether such transmission is impossible because of their absence.

The predictive value of cytological examination in cases of possible biparental inheritance, where paternal plastids are observed, rests on the assumption of symmetrical plastid inheritance during generative cell division and sperm cell formation, and that the numerical content of plastids remains constant (or nearly constant) throughout sperm maturation to gamete fusion. The numerical content of heritable organelles may also prove to be an important parameter in predicting the initial influx of male organelles and the possible extent of their influence during early embryogenesis.

The present study reports on the numerical content and spatial distribution of heritable organelles in paired sperm cells within the pollen grain at anthesis in *Plumbago zeylanica*.

B. Results and Discussion

The microgametophyte of *P. zeylanica* contains two spindle-shaped sperm cells and a vegetative nucelus. The two sperm cells consistently differ in morphology and may thereby be distinguished from one another: the single sperm cell which is most closely associated with the vegetative nucleus bears a long, slender cellular projection which wraps around the vegetative nucleus; the second sperm cell, is connected with the first by plasmodesmata and a common cell wall, but is not directly associated with the vegetative nucleus. Details concerning the nature and possible significance of this relationship are discussed in the preceding chapter.

Reconstruction of 11 pairs of sperm cells within the pollen grain reveal quantitative and qualitative differences in the number of heritable organelles present in each sperm cell after generative cell division (Table 3, 4). The sperm associated with the vegetative nucleus possessed most of the mitochondria (ave. 256.2) including numerous mitochondria within the cellular projection (ave. 80; Table 3). The other sperm (unassociated with the vegetative nucleus) possessed significantly fewer such mitochondria (ave. 39.82; $p < .0001$; Table 5, 6).

The distribution of plastids showed an even greater disparity between the two sperm cells. The sperm which is associated with the vegetative nucleus contained at most two plastids and typically none (ave. 0.45), whereas the other sperm cell had from eight to 46 plastids (ave. 24.2; Table 3). The dissimilarity of these two types of sperm is demonstrated in the scatter diagram in Table 4.

Observations of over 50 pollen grains indicated that the presence of numerous plastids in the sperm unassociated with the vegetative nucleus was consistent. In several cases where the sperm containing plastids appeared to be in direct contact with the vegetative nucleus, other sections of the same pollen grain were examined with particular care. In these sections, the second sperm was clearly visible and possessed a cellular projection tightly associated with the vegetative nucleus. The presence of plastids in the sperm associated with the vegetative nucleus was observed in three of the eleven sperm cells. In each, the plastids are consistently located within 0.5 um of the junction with the other

Table 3: Descriptive statistics comparing the numerical content of mitochondria, plastids, and microbodies in two groups of sperm cells differentiated on the basis of association with the vegetative nucleus; and within the sperm associated with the vegetative nucleus, two minor groups based on cellular location of organelles within the sperm cell body and cellular projection.

Group I: Sperms associated with the vegetative nucleus.
Group II: Sperms unassociated with the vegetative nucleus.

VARIABLE	N	MINIMUM	MAXIMUM	MEAN	STD DEV	.9500 CONFIDENCE INTERVAL
SPERM I TOTAL						
1.MITOCHONDRIA	11	154	319	256.18	59.75	(216.04,296.33)
2.PLASTIDS	11	0	2	0.45	0.82	(-.0962,1.0056)
3.MICROBODIES	11	0	2	0.40	.70	(-.10018,.90018)
SPERM II TOTAL						
1.MITOCHONDRIA	11	22	52	39.82	10.95	(32.460,47.176)
2.PLASTIDS	11	8	46	24.18	12.83	(15.564,32.800)
3.MICROBODIES	11	0	8	3.50	2.51	(1.7076,5.2924)
SPERM I PROJECTION						
1.MITOCHONDRIA	11	36	122	80.18	30.30	(59.825,100.54)
2.PLASTIDS	11	0	0			
3.MICROBODIES	11	0	1	0.09	0.30	(-.11165,.29347)
SPERM I BODY						
1.MITOCHONDRIA	11	107	257	176.00	46.43	(144.81,207.19)
2.PLASTIDS	11	0	2	0.45	0.82	(-.09647,1.0056)
3.MICROBODIES	11	0	1	0.30	0.48	(-.04556,.64555)

Table 4: Scatter diagram comparing the numerical content of mitochondria and plastids in two groups of sperm cells based on association with the vegetative nucleus. (Overlapping points are represented by a number which corresponds to the number of points which coincide.)

Group I: Sperms associated with the vegetative nucleus.
Group II: Sperms unassociated with the vegetative nucleus.

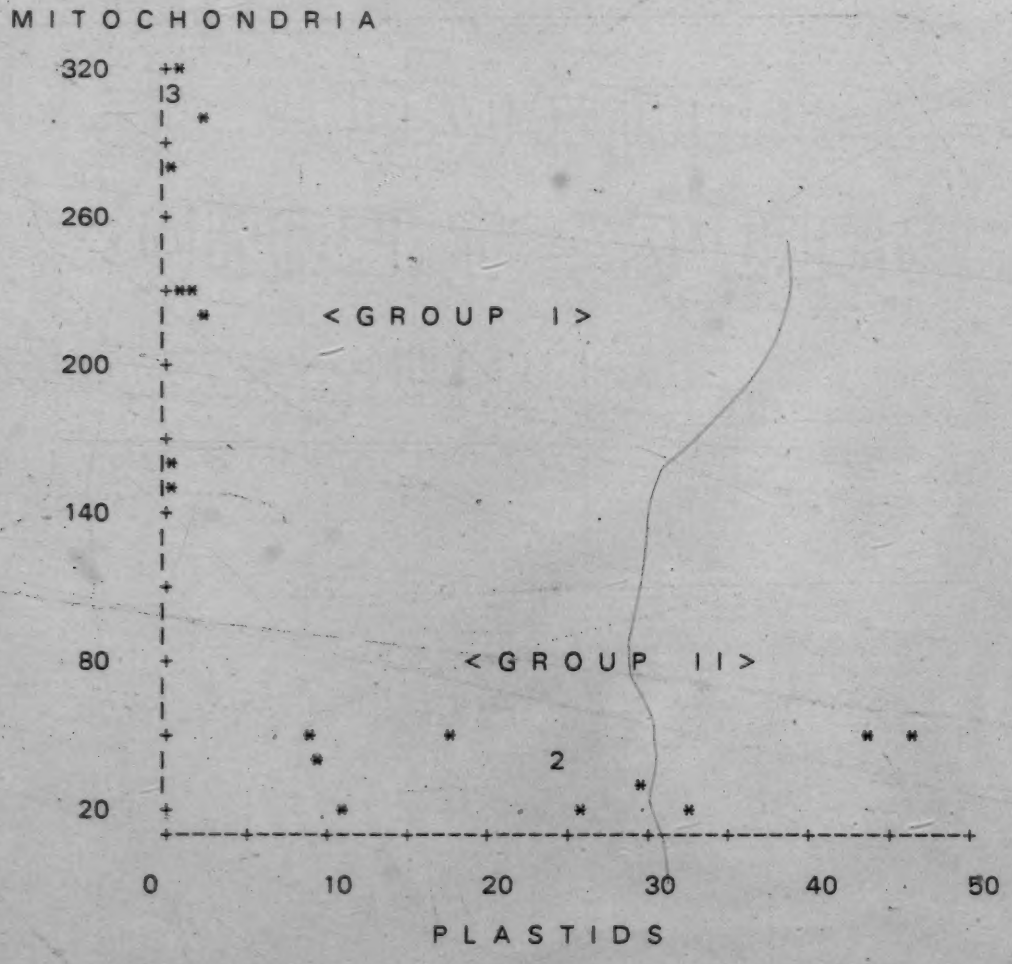

Table 5: Paired t test comparing the numerical content of mitochondria, plastids, and microbodies in two groups of sperm cells, organized with respect to organelle type.

Group I: Sperms associated with the vegetative nucleus.
Group II: Sperms unassociated with the vegetative nucleus.

VARIABLE	CELL	SPERM II	SPERM I	TEST STATISTIC	DF	SIGNIF
MITOCHONDRIA	MEAN	39.818	256.18	T=-11.812	11	.0000
PLASTIDS	MEAN	24.182	.45455	T= 6.1749	11	.0001
MICROBODIES	MEAN	3.1818	.36364	T= 3.7052	11	.0041

sperm cell.

The occurrence and distribution of single membrane-bound bodies with homogenous contents, resembling microbodies, were also recorded. The sperm which is associated with the vegetative nucleus contained significantly fewer microbodies (0-2; ave. 0.45) than did the other sperm (0-8 microbodies; ave. 3.5; $p = .0014$; Table 3, 5, 6).

Preliminary evidence strongly suggests that the apportionment of heritable organelles in the sperm is determined by the distribution of these organelles prior to generative cell division. At a late stage of generative cell maturation after the generative cell has become free from the intine and is becoming elongated (Fig. 28), plastids are found almost exclusively at one pole of the cell and most mitochondria are located at the other pole. The mechanism by which plastid and mitochondrial distribution patterns originate within the generative cell is unknown, but the polarization of the generative cell appears associated with the development of a cellular projection near the middle of generative cell maturation. Future patterns of organelle distribution are organized with respect to this polarity, with mainly mitochondria in the half of the generative cell associated with the vegetative nucleus. 91

Fig. 28: Electron micrograph of generative cell in immature pollen near the middle of generative cell maturation. Plastids (*P*) are located at one pole of the cell; mitochondria (*M*) are located at the opposite pole. Establishment of generative cell polarity has occurred by this stage as the cell begins to undergo elongation into a spindle shape. Longitudinally-oriented microtubules (unlabelled arrowheads) are numerous at the periphery of the cell next to the generative cell wall and are regarded as essential organelles in the establishment of generative and sperm shape, although absent in the mature sperm of *P. zeylanica*. (*N*) generative cell nucleus. UA-PbCit staining. X 22,000.

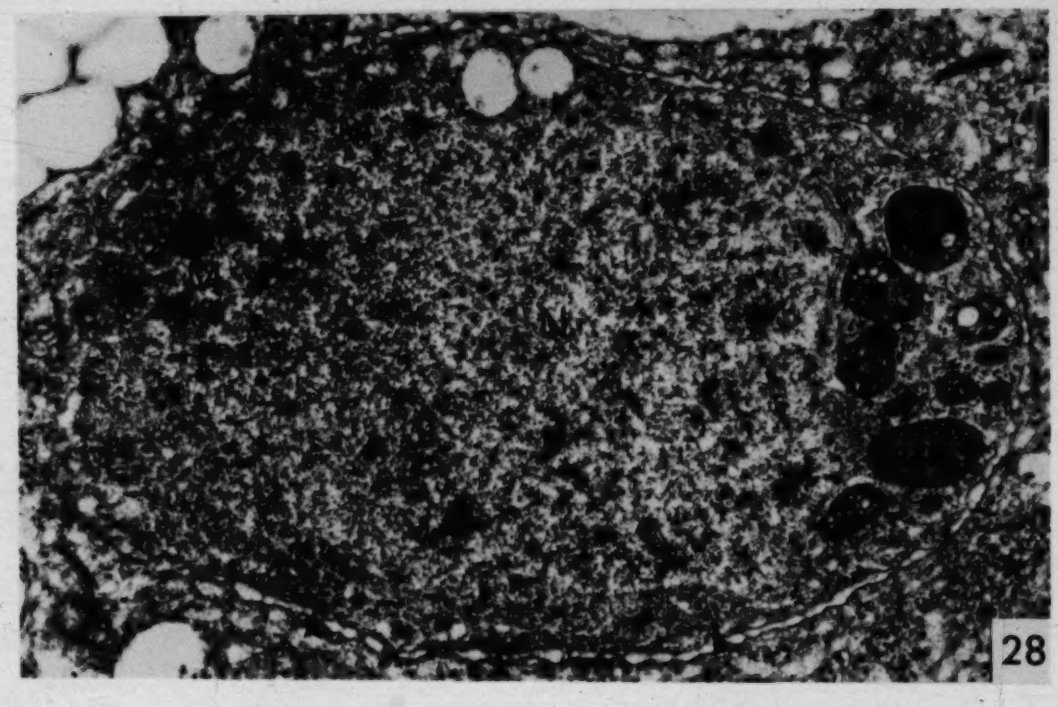

28

V. Fertilization: Entry and Discharge of the Pollen Tube in the Embryo Sac

A. Introduction

The course of the pollen tube in the *Plumbago* and *Plumbagella*-type embryo sacs is problematical in light of current concepts of angiosperm gamete transfer. Lacking synergids and identifiable antipodal cells, basic questions remain concerning the organization and behavior of these reduced embryo sacs during reproductive function. Cass and Karas (1974) examined the fine structure of the egg of *Plumbago*, concluding that in a number of ways it displays features more typical of synergids in the normal egg apparatus: evidence of greater physiological activity, presence of a filiform apparatus, and extreme micropylar position of the egg are among the more significant similarities.

In early accounts of fertilization and embryogenesis in the Plumbaginoideae, Dahlgren (1916, 1937) was unable to document the entry of the pollen tube and fusion of sperm nuclei, but contended that double fertilization probably occurs as it does in more typical megagametophytes. Only in recent years have these questions once again been addressed (Russell, 1980, Russell and Cass, 1981b) and in resolving these issues the study of *Plumbago zeylanica* has revealed an alternative pathway for pollen tube growth and confirmed the presence of double fertilization in the absence of synergids. The present study traces the course of final pollen tube growth and discharge within the embryo sac of *P. zeylanica* and introduces an examination of the fate of pollen tube nuclei which will be discussed more fully in the following chapter.

B. Observations

Initiation and growth of the pollen tube into the ovule

Initiation of pollen tube growth occurs within 15 minutes of pollination; the successful pollen tube penetrates over 20 mm of gynoecial tissue in the most rapidly developing pollen tubes and may arrive at the ovule within less than 8-1/2 hr (Table 6). The newly formed pollen tube penetrates between the top layers of cells at the stigmatic surface and within one cell layer enters the

Table 6: Chronology of fertilization events in *Plumbago zeylanica* based on maximal growth rates following artificial pollination of flowers emasculated prior to anthesis (in hours:minutes).

Initiation of pollen tube growth; penetration of stigma	0 - 0:15
Rapid pollen tube growth in lower style	0:15 - 4:30
Slower pollen tube growth in lower style	4:30 - 8:10
Arrival of pollen tube at ovule; penetration of micropyle	8:15 - 8:20
Penetration of nucellus and filiform apparatus; entry and discharge of the pollen tube into the embryo sac	8:25
Gamete fusion; transmission of sperm nuclei	8:30
Initiation of nuclear fusion; fertilization	8:40

Fig. 29: Reconstruction of a mature embryo sac of *P. zeylanica*. A large, vacuolate egg (*E*) with numerous cell wall ingrowths at its base (*FA* = filiform apparatus) occupies the micropylar end of the megagametophyte. It is partially surrounded within the embryo sac by a central cell (*CC*) with its nucleus opposite the nucleus of the egg cell. Three accessory cells of widely varying shapes and sizes are present within the mature embryo sac, but do not directly participate in the fertilization process and appear to be ephemeral structures. Degeneration may occur before fertilization, as in the case of the antipodal cell shown (*AC*), or during later embryogeny, as would be the case in the lateral cells (*LC*) shown. Approximately X 800.

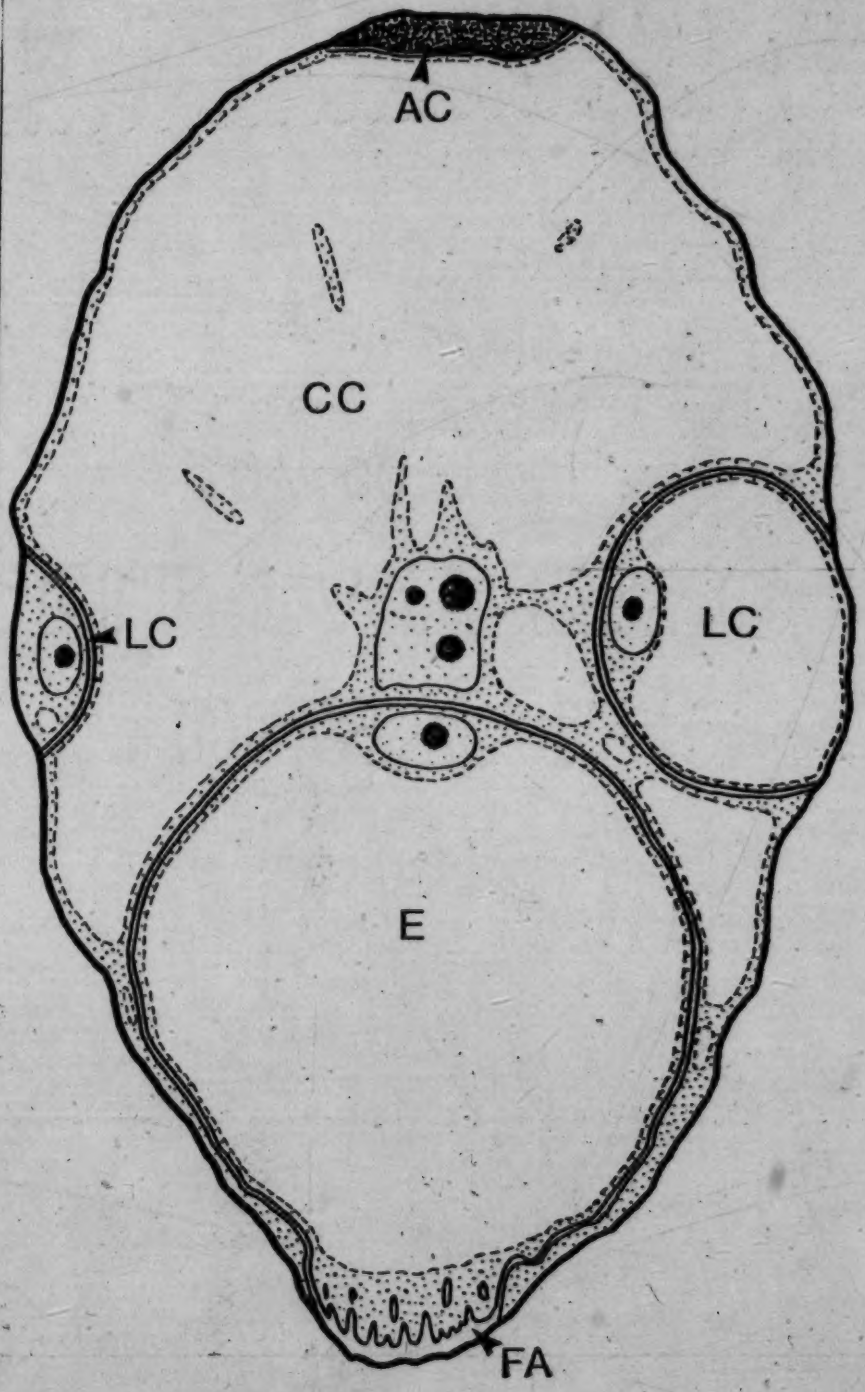

29

modified cell wall matrix of the closed transmitting tissue. Arms of transmitting tissue reaching into the stigmatic lobes fuse proximally to form a single, contiguous cylinder in the style; it ends abruptly at the summit of the ovary forming an obturator which is appressed to the single ovule in the uniloculate ovary. The pollen tube does not leave the cylinder of transmitting tissue during growth until arrival at the ovule, and during this time is not observed outside of the intercellular wall matrix formed by these cells. As the pollen tube reaches the base of the style, it emerges from the transmitting tissue, skirts the edge of the funiculus, which partially occludes the micropyle, and enters the ovule through a micropyle formed by the inner integument. Growth of the pollen tube is known to be relatively slow within this region (Chapter 3), but a narrowing of the diameter of the pollen tube at the micropyle may increase the rate of tip growth near the ovule. At the base of the nucellus (Fig. 33), pollen tube breadth increases significantly and a corresponding lag in the rate of elongation appears to occur.

The nucellar region through which the tube enters the megagametophyte does not undergo as many periclinal divisions during its ontogeny as do surrounding nucellar areas, but in other respects the morphological organization of this tissue appears unspecialized for ultimate pollen tube penetration. Upon pollen tube arrival, the middle lamellae of cell walls within this region appear to become disorganized (Fig. 33, arrows) and intercellular space between these cells becomes evident. The pollen tube apparently presses between these cells, displacing them, during its passage through the nucellus. The cytoplasm of surrounding nucellar cells does not appear to undergo recognizable morphological alteration prior to the arrival of the pollen tube, but soon afterwards may rapidly become electron-dense (Fig. 36, 38) as an apparent consequence of pollen tube passage.

Organization of the mature embryo sac before pollen tube arrival

The unfertilized megagametophyte of *P. zeylanica* consists of five cells: the egg, central cell, and three accessory cells: two lateral cells and one chalazal cell (Fig. 29). The mature egg is a highly polarized cell occupied by a prominent central vacuole. The nucleus, numerous mitochondria, and a majority of the

Fig. 30: Electron micrograph of median longitudinal section of egg and central cell nuclei in an unfertilized embryo sac. Cytoplasmic areas (arrowheads) within the central cell nucleus (*PN*) represent evidence for the prior fusion of polar nuclei. Numerous mitochondria and a majority of the plastids are located in the cytoplasm surrounding the central cell and egg nucleus (*N*). A continuous thin cell wall separates egg (*E*) and central cell (*CC*). UA-PbCit staining. X 5300.

Fig. 31: Electron micrograph of a pollen tube within the filiform apparatus at the base of the egg in cross section. The embryo sac wall at the base of the egg is composed of the cell walls of the egg and degenerate remains of nucellar cells crushed during embryo sac ontogeny. The stellate pattern of the base of the egg evident in cross section is the result of the encroachment of intact nucellar cells. *FA* filiform apparatus; *PT* pollen tube. UA-PbCit staining. X 3450.

Fig. 32: Higher magnification electron micrograph of filiform apparatus in base of the egg near pollen tube. Filiform projections contain aligned internal fibrils evident here in both cross (black arrowheads) and longitudinal section (white arrowheads). Electron-opaque areas within the filiform apparatus cell wall may represent areas of degenerate egg cell cytoplasm trapped during the development of the filiform apparatus. UA-PbCit. X 22,850.

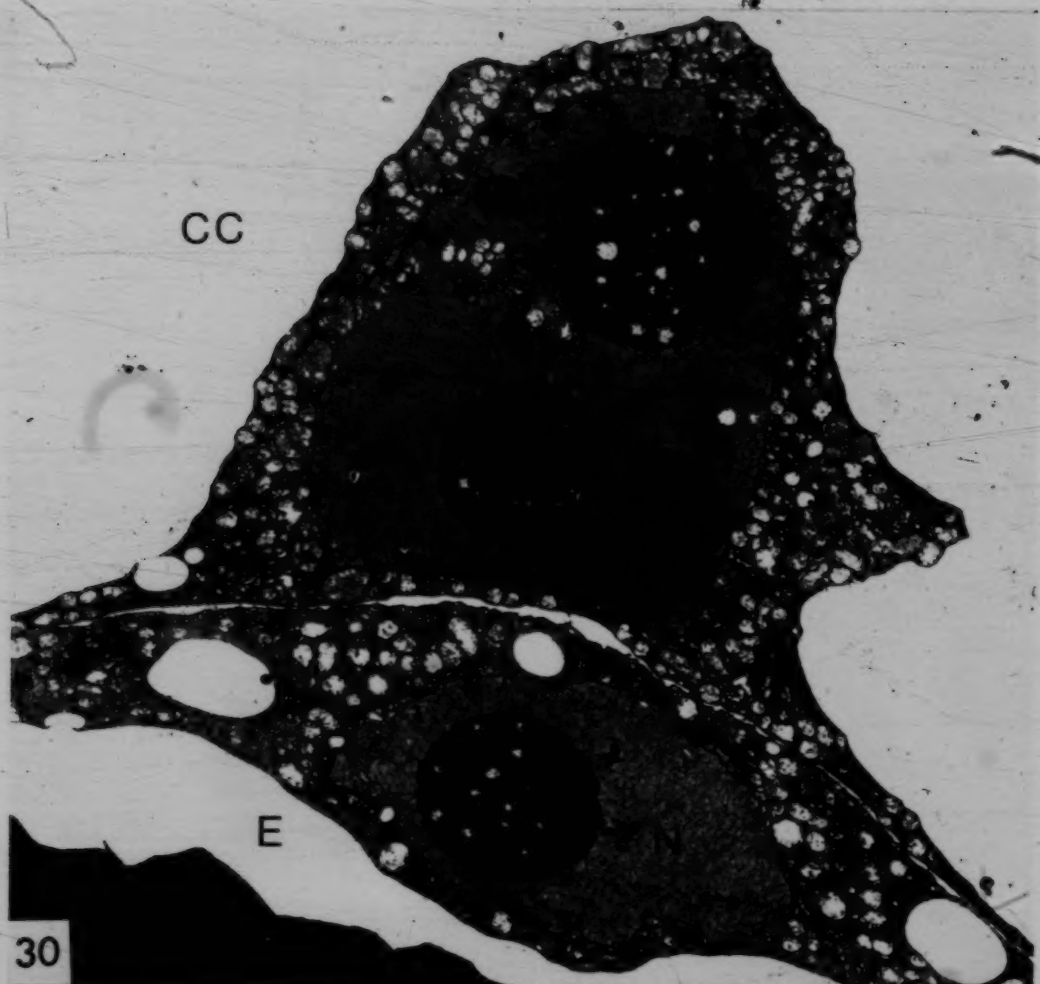

30

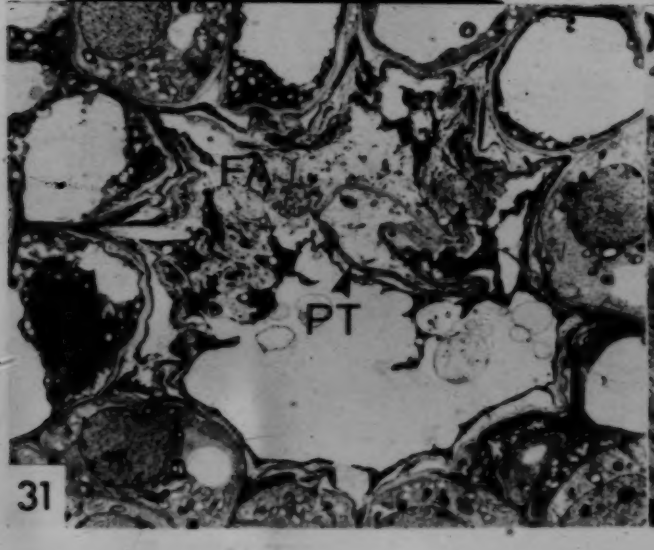

31

32

plastids are located at the chalazal end (Fig. 30), while the extreme micropylar end of the egg possesses mitochondria and numerous cell wall ingrowths forming the filiform apparatus (Fig. 31; Cass and Karas, 1974, Fig. 9, 10). Elements of the filiform apparatus are located at the base of the egg cell, largely near the junction between the egg and megagametophyte cell walls (Fig. 31) and consist of an electron-lucent wall matrix with numerous longitudinally-oriented fibrils (Fig. 32) of polysaccharidic content (Fig. 35). Fibrils subjected to the TCH-SP reaction were unstained without prior periodic acid oxidation. Fibrils of the same structure are also seen in the micropylar egg cell wall for 20 to 30 um above the junction with the megagametophyte wall; such fibrils are absent within the mid-lateral and chalazal egg cell wall (Fig. 30, 39, 40). Membranous inclusions within the filiform apparatus stain similarly to plasma membrane and may represent isolated segments of cytoplasm trapped in the cell wall during its formation (Fig. 32, 35).

The central cell nucleus is produced by the fusion of polar nuclei and is situated opposite the egg nucleus (Fig. 29, 30). Its cytoplasm is largely perinuclear and is linked by narrow strands to a thin layer of cytoplasm bordering the central cell (Fig. 29). Accessory cells are attached to the periphery of the embryo sac. Although these cells have no obvious function, they may persist for varible periods of time during embryogenesis without undergoing morphological alteration. Typically the antipodal cell degenerates prior to embryo sac maturity, while the degeneration of the lateral cells is temporally more variable (Fig. 29). Ultrastructure of the egg cell wall in the mid-lateral and chalazal part of the egg varies in granularity, with short segments of randomly-aligned fibrillar material commonly observed (Fig. 29, 39, 40; Cass and Karas, 1974).

Entry and discharge of the pollen tube in the megagametophyte

The pollen tube enters the megagametophyte by penetrating the embryo sac near the filiform apparatus at the base of the egg (Fig. 31, 43) and continues its growth between the egg and central cell, displacing egg cell wall material to either side of the pollen tube during its passage (Fig. 34, 36). The

Fig. 33: Electron micrograph of pollen tube apex in physical contact with nucellar cells near the micropyle. The nucellus (*Nc*) between the micropyle and egg (*E*) is structurally modified, consisting of two to three cells in thickness; surrounding regions of nucellus vary from three to over five cell layers in thickness. As the pollen tube (*PT*) approaches the embryo sac, the middle lamellae of intervening nucellar cells within this region appear to break down (unlabelled arrows). Starch grains (*s*) are frequently seen in the most micropylar nucellar cells. UA–PbCit. X 3080.

Fig. 34: Electron micrograph of pollen tube penetrating the egg wall in a newly fertilized embryo sac. Pollen tube (*PT*) located in and above the region of the filiform apparatus (*FA*) has been crushed as a consequence of probable osmotic changes encountered during chemical preparation (compare Fig. 29 prepared by freezing and the use of anhydrous solvents). Note fibrillar nature of the micropylar and lateral regions of egg wall (*EW*). Crystals are visible in the egg wall (arrows) near the the embryo sac wall and nucellus (*Nc*). UA–PbCit staining. X 11,750.

Fig. 35: Electron micrograph of filiform apparatus stained by the PA–TCH–SP reaction using PA–TCH–SP reaction. The filiform apparatus contains aligned structural fibrils (arrowheads), probably cellulosic in nature and unstained without prior PA oxidation). Filiform apparatus fibrils are oriently longitudinally with respect to the egg (*E*) and pollen tube (*PT*), and may provide structural support during tube passage. Numerous regions of electron–dense material probably represent degenerating segments of cytoplasm isolated during the development of the filiform apparatus. PA–TCH–SP reaction. X 18,700.

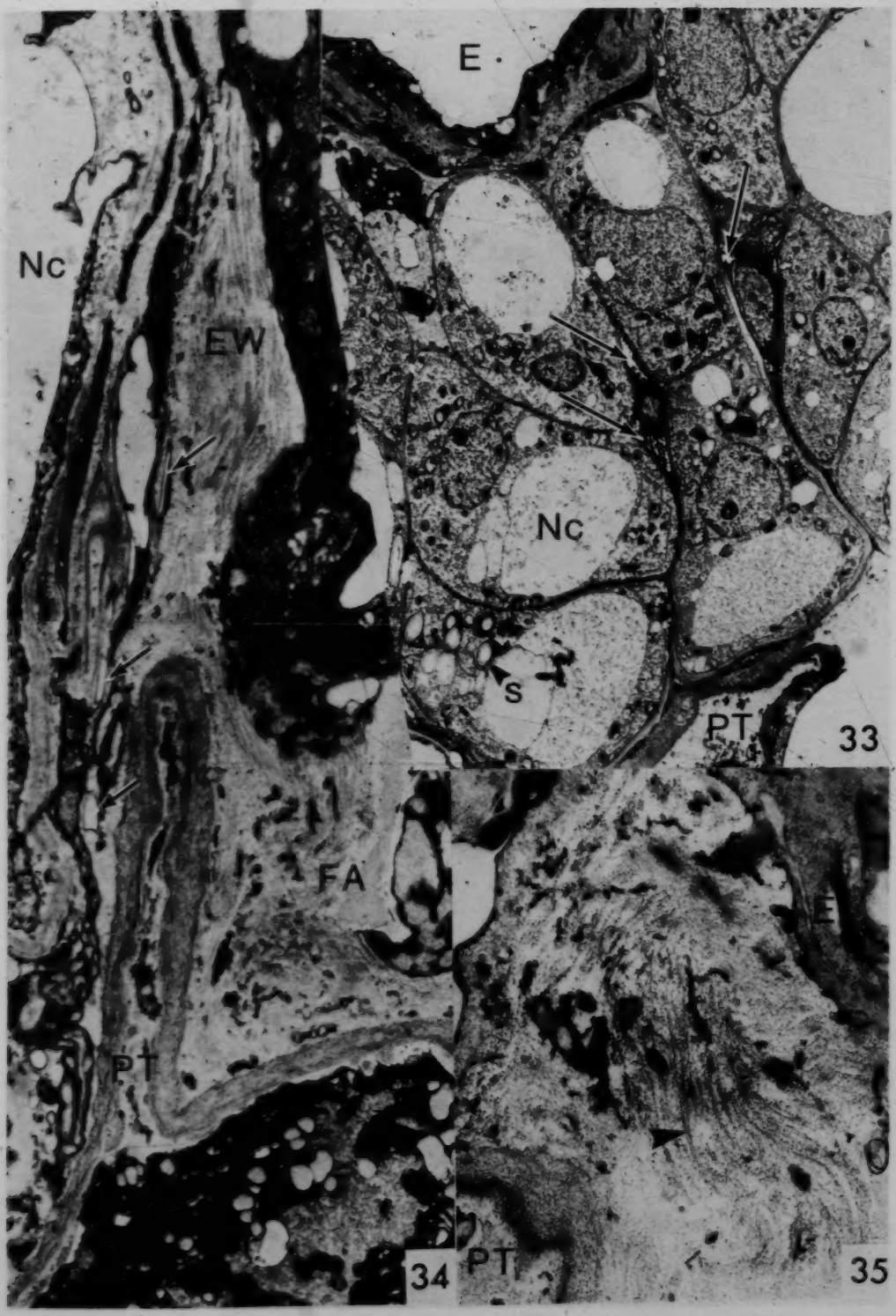
E
Nc
EW
Nc
S
PT
33
FA
PT
34
E
PT
35

course of the pollen tube above the base of the egg indicates that the tube apex is either deflected or redirected at the base of the embryo sac, and that the pollen tube commonly diverges from the previous plane of growth (Fig. 36, 38, 43). During continued growth, the pollen tube forms an arc which conforms to the contour of the egg cell for the remaining 60 to 70 um of pollen tube elongation. Growth ceases when the pollen tube arrives at a region of strong curvature near the chalazal end of the egg, a terminal aperture forms, and the release of pollen tube contents between the egg and central cell begins (Fig. 39, 42, 43). During pollen tube discharge, two sperms, a vegetative nucleus, and a limited amount of pollen cytoplasm are quickly released. Since the male gametes approach the tip of the pollen tube during late stages of pollen tube growth (Chapter 3), it is likely that the male gametes are released soon after pollen tube discharge is initiated and therefore relatively little pollen cytoplasm would have to be expelled in the process. The occurrence of a relatively small amount of pollen ejecta is confirmed by observations of freeze-substituted material (Fig. 43). In physically-fixed material apparently only the cytoplasm released from the pollen tube undergoes immediate degeneration; pollen cytoplasm within the tube proximal to the aperture does not appear to change in structure or staining characteristics soon after pollen tube discharge has occurred (Fig. 43, 44). Within minutes of aperture formation, the discharged pollen cytoplasm becomes electron dense to electron opaque (Fig. 39, 40). The ground substance becomes osmiophilic and is highly stained in the TCH-SP reaction. Although secretory vesicles do not themselves appear to degenerate, they may follow anomalous fusion patterns, fusing with themselves producing blocks of material lodging within the tube (Fig. 40) or with embryo wall (Fig. 42), or remain free within the tube or outside of it (Fig. 40). Mitochondrial cristae swell and material at the edge of the outer mitochondrial membranes becomes dense; mitochondria and organelles other than vesicles loose their integrity within hours of discharge from the pollen tube.

Pollen tube and egg cell walls following discharge of the pollen tube

In chemically-fixed materials, the discharged pollen tube appears flattened within the embryo sac and any cytoplasm trapped within distal parts of the tube

Fig. 36: Electron micrograph of longitudinal section of pollen tube within the base of the embryo sac near the time of fertilization. Entry of the pollen tube into the embryo sac results in several alterations in ovular and embryo sac structure; nucellar cells (*Nc*) separate at the middle lamella, become displaced to either side of the pollen tube (*PT*), and rapidly degenerate. (This section was fixed at about 8.8 hr. after pollination, within 20 minutes of expected pollen tube arrival.) The base of the egg (*E*) is pushed inward at the filiform apparatus (*FA*) by the intrusion of the pollen tube. The structure of the pollen tube, which is clearly bilamellate above the micropyle (see arrowheads), becomes trilamellate after pollen tube penetration has occurred. The middle layer of the pollen tube becomes evident after pollen tube arrival; it consists of more loosely organized fibrils than either of the inner or outer layers of the pollen tube and contains vesicles (*v*) with a related layer of aligned tubular membranous elements (seen in more detail in Fig. 37). This region eventually seals the pollen tube at the base of the egg and may be associated with the slower degeneration of pollen cytoplasm proximal to this point. UA–PbCit staining. X 5850.

Fig. 37: Electron micrograph of vesicles and related tubular membranous elements in the middle layer of a pollen tube. Note loosely organized fibrils within this layer of the pollen tube wall. The structure, location, and rapid formation of this region suggest that the middle layer of the pollen tube, formed only at the base of the egg cell, may serve to rapidly seal the base of the embryo sac and structurally reinforce this area. The vesicles (*v*) and related tubular membranes (arrowheads) presumably function in deposition of this wall. UA–PbCit staining. X 13,500.

Fig. 38: Electron micrograph of longitudinal section of pollen tube at the base of the embryo sac near the time of fertilization. Elements of the filiform apparatus (*FA*) are clearly evident within the egg cell (*E*) and contain a fibrillar component which is stained by the PA–TCH–SP reaction. Starch grains (*s*) and wall components were densely stained by this reaction when PA oxidation preceded thiocarbohydrazide and silver proteinate; staining in the plasma membrane was evident without prior PA oxidation but was enhanced by this treatment. PA–TCH–SP reaction. X 3600.

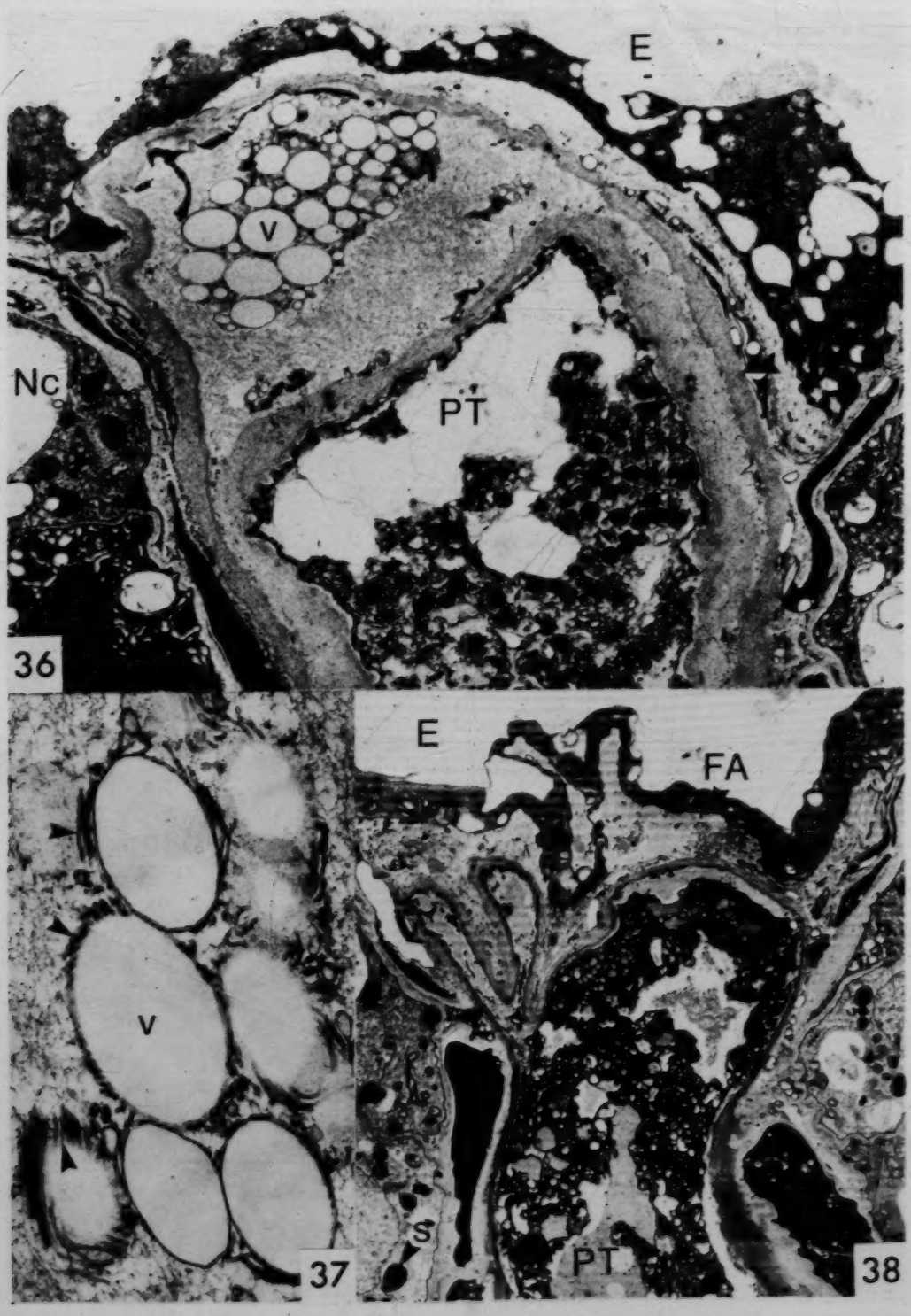
E
V
Nc
PT
36
E
FA
V
S
PT
37
38

(Fig. 34) appears highly degenerate, resembling the discharged pollen cytoplasm (Fig. 40, 42). Organelles, if recognizable, may appear degenerate in all regions of the pollen tube where the plasma membrane is disrupted. Where the plasma membrane is intact proximally in the tube pollen, cytoplasm may appear nearly unaltered (Fig. 36, 38), but likely undergoes subsequent degeneration during embryogeny. While it is likely that these changes all occur within a day of pollen tube discharge, observations of material prepared by freeze-substitution suggest that such degenerative changes occur much more slowly than the chemical preparations would indicate.

When preparations are frozen fixed at liquid nitrogen temperatures and material is dehydrated by cold, non-aqueous solvents, the pollen tube remains inflated between the egg and central cell, at least until the completion of fertilization (Fig. 44). The base of the pollen tube becomes folded at the level of the filiform apparatus near the base of the embryo sac (Fig. 43) and the free passage of materials between proximal and distal portions of the pollen tube is partially blocked. Pollen cytoplasm does not appear to degenerate within the tube at this stage, but discharged cytoplasm stains densely, appears less highly structured, and is probably highly degenerate, as, apparently, is the vegetative nucleus (Fig. 41).

Near the aperture, the pollen tube is constructed of a single layer which is relatively constant in its ultrastructural appearence. The pollen tube wall contains numerous, periodate-sensitive, aligned fibrils; these are most conspicuous proximal to the pollen tube aperture (Fig. 40, arrows), and somewhat less well-organized near the aperture (Fig. 39, 40). In more proximal regions, particularly near the base of the embryo sac, pollen tube ultrastructure becomes more complex following pollen tube discharge. In the micropyle and nucellus, the structure of the pollen tube is bilamellate, consisting of an outer, denser layer of fibrillar cell wall bounding an inner layer of slightly less dense material. It is possible that a significant proportion of this inner layer may be deposited soon after pollen tube discharge, when numeorus polysaccharide vesicles may be present, but before pollen cytoplasm degenerates. An intermediate layer which

forms between these two layers at the base of the egg contains loosely-packed fibrils within an electron-lucent matrix, numerous vesicles, and numerous tubular membrane systems associated with the vesicles (Fig. 36, 37). The ultrastructural appearance of this region is modified rapidly near the time of fertilization and may effectively seal this region from the distal part of the pollen tube soon after fertilization. The pollen tube wall becomes an integral part of the base of the embryo at later stages and may provide some structural strengthening of the micropylar nucellus. Remnants of the pollen tube in the micropyle within the outer wall of the massive suspensor have been observed with the light microscope throughout early embryogeny to the time of cotyledon initiation and do not appear to undergo extensive breakdown. The coalescence of pollen tube vesicles following pollen tube discharge is frequent, but apparently does not contribute to the formation of an organized, continuous cell wall (Fig. 42).

The chalazal egg cell wall contains periodate-sensitive, loosely-packed fibrils, with an electron-lucent background component, which differs in appearance from those walls of pollen tube origin (Fig. 39, 40). Near the region of the pollen tube aperture, egg cell wall components are often present as vesicles or clumps of material adhering to the plasma membranes of the egg and central cell (Fig. 39, 40, arrowheads). The region most likely to directly participate in transference of the sperm nuclei to the female cells, namely that region of the embryo sac nearest the pollen tube aperture, has few areas of intact cell wall (Fig. 39, 42, 44) and may therefore not be expected to interfere with processes of membrane recognition and fusion which may occur during subsequent gamete fusion.

Identification and fate of the vegetative nucleus in the megagametophyte

Following pollen tube discharge, a single body resembling an "X-body" (*sensu* Fisher and Jensen, 1969) is observed between the egg and central cell, at varying distances from the tip of the pollen tube. The body is highly electron-dense, containing numerous electron-opaque granules, and is not delimited by a membrane (VN, Fig. 41). The present interpretation, that this structure represents the highly degenerate remains of the vegetative nucleus is

Fig. 39: Electron micrograph of pollen tube aperture in longitudinal section shortly after discharge stained by the TCH-SP reaction without prior PA oxidation. Both halves of pollen tube wall (*PTW*) are visible; the pore is located on the left side of the figure and is distinguished by the continuity of degenerating pollen cytoplasm through the aperture (arrows). Material discharged from the pollen tube is located within the region between the plasma membranes of the egg (*E*) and central cell (*CC*). Degenerating pollen cytoplasm is osmiophilic (as observed in unstained material) and stains densely in the TCH-SP reaction regardless of prior PA oxidation. Remnant areas of egg cell wall are appressed to the plasma membranes of the egg and central cells (arrowheads). Regions of egg cell wall in the immediate vicinity of the pollen tube aperture are rare and appear disrupted, a probable result of the arrival and discharge of the pollen tube. Degenerating mitochondria (*M*) in this figure are located within pollen cytoplasm near the aperture and just beyond it. H_2O-TCH-SP reaction. X 36,400.

Fig. 40: Electron micrograph of a pollen tube within the embryo sac stained by the PA-TCH-SP reaction by use of the PA-TCH-SP reaction. Section is serial to that shown in Fig. 39, but several micrometers proximal to the pollen tube aperture. Fibrillar structure visible within proximal regions of the pollen tube (arrows) becomes random nearer the aperture (at the left side of the figure). Areas of egg cell wall (arrowheads) are visible adhering to the egg and central cell plasma membranes and are distinguished by their characteristically loosely-organized dense fibrils and their transparent surrounding material. PA-TCH-SP reaction. X 33,400.

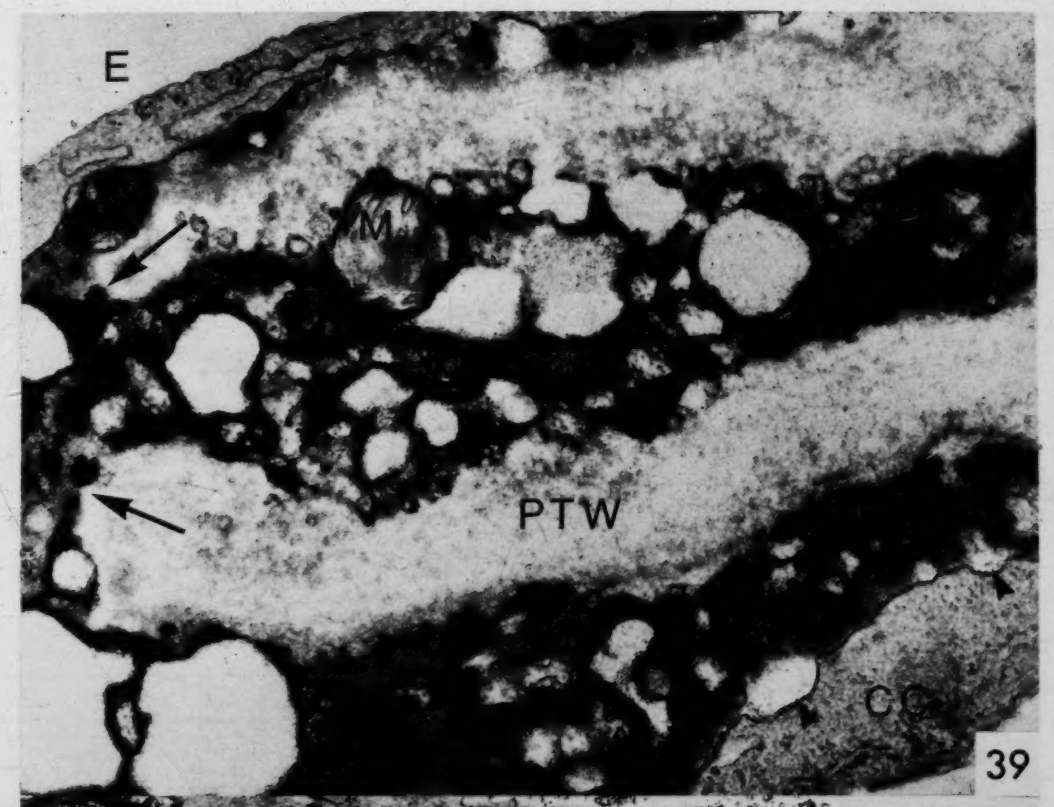

39

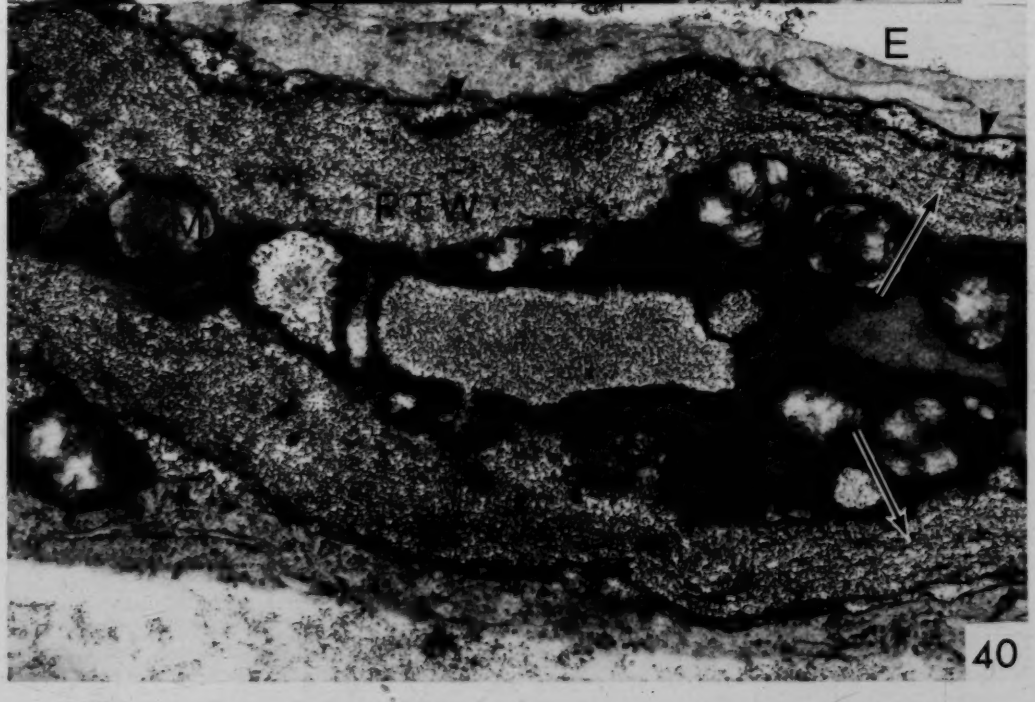

40

Fig. 41: Electron micrograph of discharged vegetative nucleus between egg and central cell near the time of pollen tube discharge. Vegetative nucleus (*VN*) rapidly degenerates following discharge and is surrounded by degenerating pollen cytoplasm (*dPC*). Compare this figure to Fig. 44, 65-67 for typical location of the vegetative nucleus relative to other cells within the embryo sac. UA-PbCit staining. X 10,400.

Fig. 42: Electron micrograph of pollen tube aperture one day after fertilization. The location of the pollen tube (*PT*), between the suspensor (*S*) and endosperm (*En*) is unchanged during later embryogeny. The coalescence of discharged secretory vesicles forms an irregular wall layer (arrow) beyond the aperture of the pollen tube (arrowheads). Eight-celled embryo stage. UA-PbCit staining. X 17,200.

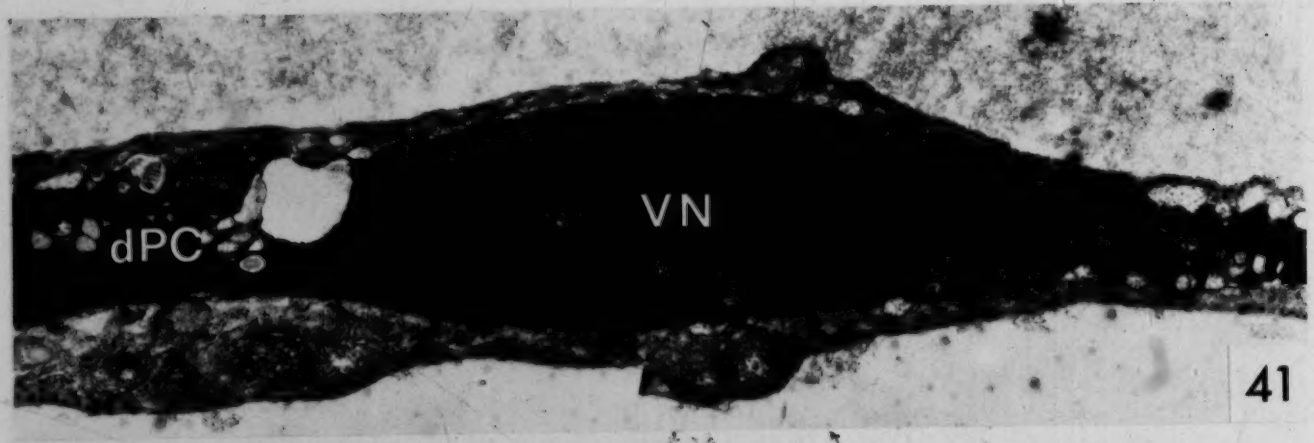

41

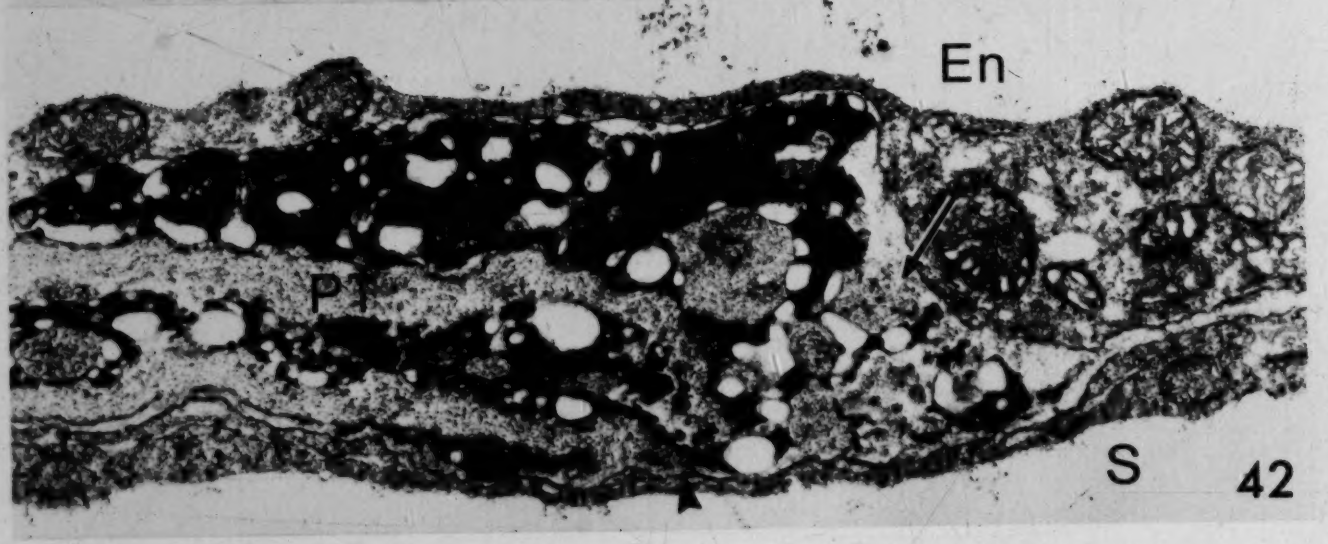

42

Figs. 43 and 44: Color photomicrographs of 2 um thick plastic sections of a freeze-substituted ovule stained with Periodic acid-Schiff's reaction (PAS) for insoluble carbohydrates (pinkish to red color), and aniline blue black for proteins (bluish colors). X 1600.

Fig. 43: Nomarski differential interference contrast micrograph of median section of the base of a freeze-substituted ovule near the time of nuclear fusion. Inflated portion of pollen tube (*PT*) in a thick section of the same ovule as displayed in Fig. 44, approx. 2 um away. Partial occlusion of the pollen tube at the base of the egg (*E*) is visible at the tip of the unlabeled arrowhead, near the egg cell wall projections forming the filiform apparatus (*FA*). *Nc* nucellus.

Fig. 44: Nomarski differential interference contrast micrograph of median section of a freeze-substituted ovule near the time of nuclear fusion. Remains of the sperm nuclei (unlabeled arrowheads) are visible after fusion with the central cell nucleus (*PN*) and near the time of fusion with the egg nucleus (*EN*). The membrane of the sperm nucleus fusing with that of the egg is visible in a different optical plane of this section (inset) and indicates that nuclear fusion has yet to be completed in the egg. Nuclear fusion appears to be initiated at the edge of the egg nucleus nearest the pollen tube aperture (unlabeled arrows) in the egg and, similarly, at the nearest face of the secondary nucleus in relation to the pollen tube within the central cell. This indicates that nuclei probably follow a direct route in approaching both of the female nuclei, unlike the proposed pathway in cotton, for which is proposed that a direct pathway is followed by the sperm nucleus prior to the formation of the primary endosperm nucleus, but a circumferential pattern of sperm nucleus movement in the egg cell (Jensen, 1973). The vegetative nucleus (*VN*) is visible between the egg (*E*) and endosperm (*En*) in this embryo sac, in its characteristic position, between the two female reproductive nuclei. Egg cell wall, which is continuous prior to arrival and discharge of the pollen tube, appears disrupted near the aperture of the pollen tube. (Pinkish tinge near the edge of the egg cytoplasm near the nucleus is an interference artifact and does not appear stained in PAS under brightfield microscopy).

Fig. 45: Reconstruction of pollen tube arrival, tube discharge, and subsequent fertilization in *P. zeylanica* based on chemically and physically fixed preparations. The pollen tube (*PT*) enters the ovule through a micropyle formed by the inner integument (*II*), passes between several nucellar cells (*Nc*), penetrates the embryo sac through the filiform apparatus at the base of the egg (*E*) and completes growth between the egg and the central cell (*CC*), forming a terminal aperture near a region of strong curvature in the side of the egg. Discharge of the pollen tube results in the release of two male gametes, vegetative nucleus, and a limited amount of pollen cytoplasm between these two cells. The sperm nuclei come to fuse with the central cell and egg nuclei, respectively, (arrowheads) and the vegetative nucleus (*VN*) remains lodged between the egg and central cell. Approximately X 800.

(Reconstruction was based on fertilization events documented in Figs. 43 and 44 for events of pollen tube–embryo sac interaction, and on embryo sac shown in Fig. 30 for morphology of female reproductive nuclei, nucleoli, and nucellar cell patterns.)

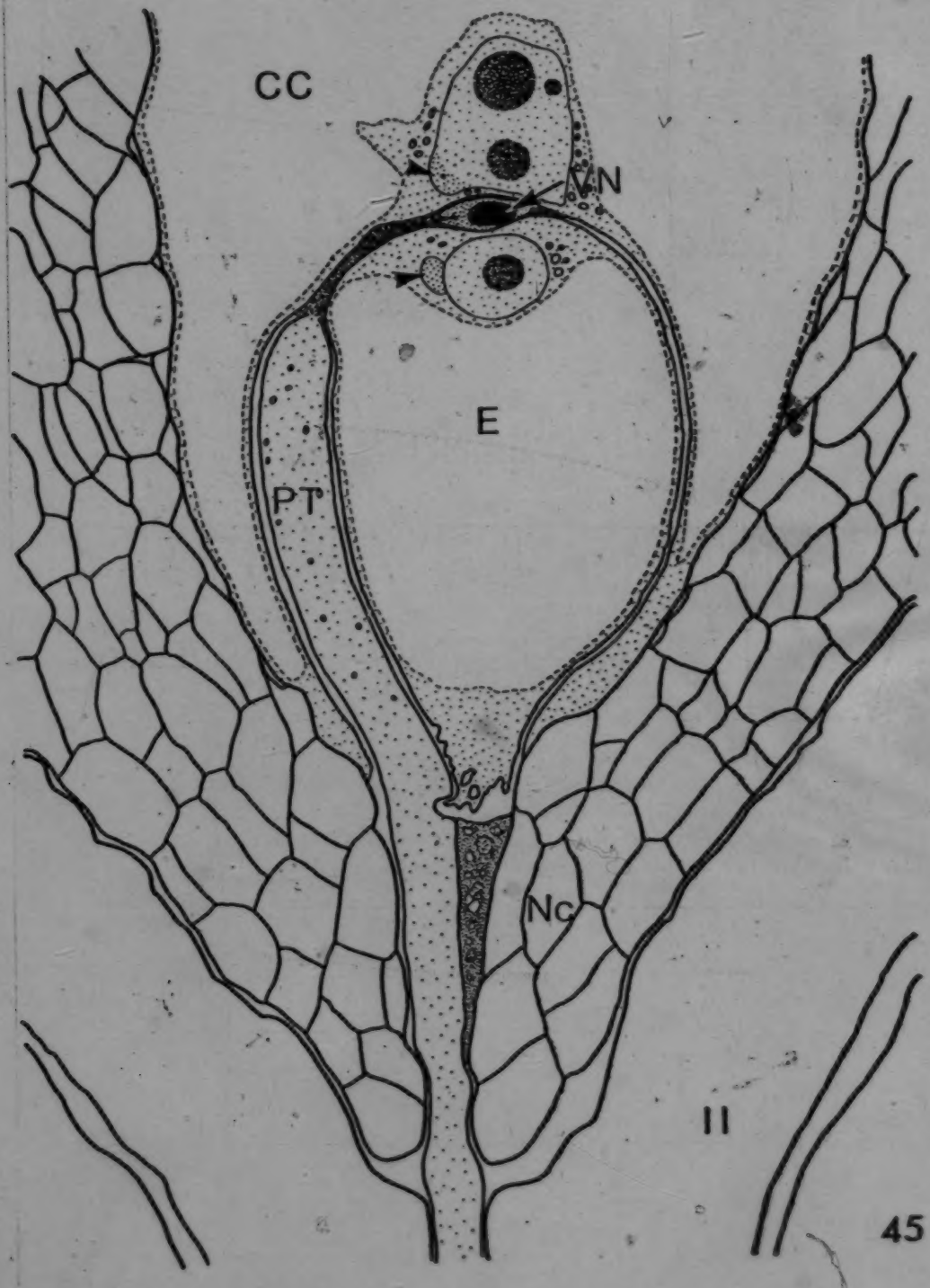

45

largely based on its affinity for aniline blue-black, its positive reaction to the Feulgen stain, and its size and location between the egg and central cell within the embryo sac. The presence of only one such body resembling the classically-described "X-bodies" is consistent with the absence of synergids, which in normal flowering plants, is considered to account for the origin of the second X-body (Fisher and Jensen, 1969).

C. Discussion

Electron microscopic studies have revealed a single, consistent pathway by which pollen tubes enter the embryo sac of angiosperms possessing synergids. The pollen tube penetrates a single synergid which begins to degenerate before, during, or soon after pollen tube arrival (Jensen, 1973; Mogensen, 1978). The embryo sac of *Plumbago*, lacking synergids, has revealed an alternative to this mode of pollen tube penetration. The pollen tube initially emerges from the thick-walled cells of the transmitting tissue, directly entering the ovule of *P. zeylanica* through a micropyle formed by the inner integument (Fig. 45). Displacing several intervening nucellar cells between the inside of the micropyle and the embryo sac, the pollen tube penetrates the embryo sac through egg cell wall ingrowths of the filiform apparatus at the most micropylar region of the egg. Pollen tube growth continues and is completed in the intercellular space between the egg and central cell, terminating near a region of sharp curvature of the egg, 70 to 80 um deep into the embryo sac. A terminal aperture is formed at this time, and the vegetative nucleus, two sperm cells and a limited amount of pollen cytoplasm are released between the egg and central cell plasma membranes. Degeneration of the discharged pollen cytoplasm and vegetative nucleus rapidly ensues and is initiated prior to gamete fusion (Chapter 6).

The entry of the pollen tube into the embryo sac is unassociated with the degeneration of any receptor cell within the female gametophyte; however, an extramural region of degeneration is clearly delimited by the egg and central cell plasma membranes. In freeze-substituted material, degeneration is initially limited to material ejected from the pollen tube - an observation which strongly suggests

that the stimulus for cytoplasmic degeneration originates in the embryo sac, and competence for response resides between the egg and central cell. No degenerate material apparently related to the fertilization process was observed within either of these two cells following gamete fusion. The discharged vegetative nucleus, which is initially located near the tip of the pollen tube, comes to lie near the summit of the egg, and may become lodged between the nuclei of both the egg and central cell. Its size, location (*ie.*, in discharged pollen cytoplasm between cells in the embryo sac), and protein content corroborate the identification of this structure shown in Fig. 41 as the discharged vegetative nucleus.

Following the completion of pollen tube discharge, the delivery of male gametes into the embryo sac, and possibly simultaneously with gametic transmission into cells of the female gametophyte, the base of the pollen tube is sealed by intensive wall synthesis at a location near the base of the embryo sac. The pollen tube, which is bilamellate prior to pollen tube arrival, develops a third, intermediate layer after pollen tube arrival, quickly generating numerous vesicles and a thick, loosely fibrillar cell wall. This layer appears to originate soon after pollen tube arrival and results in at least partial occlusion of the pollen tube within the time required for nuclear fusion to begin in both chemically and physically fixed preparations (see Table 6, for a timetable of fertilization events). In chemically fixed material of this developmental stage, the pollen tube often appeared collapsed, sealing the base of the embryo sac. This phenomenon, probably partially induced by a pressure surge from the embryo sac during chemical fixation and the hydration of the intermediate layer, was not as evident in tissues prepared by use of freeze substitution. At later stages, this region of cell wall completely occludes the pollen tube at the base of the egg, and forms a structure analagous (at least in function) to the "plug" described by Jensen and Fisher (1968a) and van Went (1970).

The embryo sac of *Plumbago zeylanica* should be regarded as exhibiting a highly specialized and reduced egg apparatus consisting of a single, modified egg cell. When compared to the typical egg apparatus (Jensen, 1973), the

ultrastructural organization of the egg of *P. zeylanica* bears a striking resemblance to that of a synergid (Cass and Karas, 1974). The presence of a filiform apparatus, the ultrastructural appearance of a physiologically active cell, and the extreme micropylar position of the egg are all bases for comparing the egg of *Plumbago* with a synergid (Cass, 1972; Cass and Karas, 1974). The course of pollen tube entry into the embryo sac through the filiform apparatus at the base of the egg and that the egg provides a specific location for pollen tube discharge and gamete fusion reinforce these similarities. Major differences between this egg and a synergid include: 1) the egg of *Plumbago* does not directly receive the pollen tube; 2) there is no visible alteration of egg cytoplasm required for pollen tube growth or discharge, or for passage of sperm nuclei; 3) the egg functions as a gamete and gives rise to a normal embryo. The important functions of an egg apparatus, namely receiving the pollen tube and serving as depositional site for two sperm cells, are relegated to an intercellular location in *P. zeylanica*. The absence of recognizable degenerative changes in the egg of *P. zeylanica* contrasts with the system reported in the majority of conventional embryo sacs where synergid degeneration precedes, accompanies, or follows pollen tube penetration into the embryo sac (Jensen, 1973).

The precise role, if any, of synergid degeneration in conventional embryo sacs is unknown, but in *P. zeylanica* degenerative changes in pollen cytoplasm appear to be restricted to that cytoplasm which is discharged between the egg and central cell in physically-prepared material. While numerous concepts concern the importance of synergid degeneration in determining the receptive synergid prior to pollen tube penetration (van der Pluijm, 1964; Jensen and Fisher, 1968a), it is by no means evident that cellular degeneration, *per se*, is required for successful pollen tube penetration. Cases where visible synergid degeneration does not occur (van Went, 1970) or where it is technique-dependent (Fisher and Jensen, 1969) would indicate that the important events relating to the identity of the receptive synergid are determined chemically and may not always be morphologically expressed until the arrival of the pollen tube. Cellular degeneration of female gametophyte cells does not appear to play an important

role in determining the course of ultimate pollen tube growth in *P. zeylanica*. The alternative possibility that cytoplasmic degeneration accompanying pollen tube discharge may serve a role in modification of the male gamete and the site of gametic transmission prior to gamete arrival (Mogensen, 1978), is supported by the present data, and suggests that synergid degeneration events may also provide an integral feature in preparing gametes and cells of the embryo sac for the presumably transient conditions of receptivity which may occur prior to successful gamete fusion in angiosperms.

VI. Fertilization: Gamete Fusion and Fate of the Male Cytoplasm

A. Introduction

In flowering plants, the concept that male gametes are deposited in the embryo sac through a single receptive synergid is implied by the presence of the pollen tube and its discharged cytoplasm within that synergid (Jensen, 1973). Although the transitory presence of the sperm cells in the synergid has been documented in several instances (Cass and Jensen, 1970; Cocucci and diFulvio, 1969; Wilms, 1981), ideas concerning the transmission of male cytoplasm – particularly the extent, symmetry, and mechanism of transmission – have remained largely controversial (Jensen and Fisher, 1967, 1968a; Fisher and Jensen, 1969; Wilms, 1981). The transmission of heritable cytoplasmic organelles by the male gametophyte was proposed in the early 1900's (Baur, 1909; Correns, 1909). In these and later studies, the evidence for male cytoplasmic transmission and the inheritance of characteristics of the male cytoplasm in subsequent generations has been convincing (Grun, 1976; Gillham, 1978), but these studies alone present insufficient evidence on which to establish whether incorporated organelles originate from the sperm, vegetative cell (pollen tube), or both. Morphological evidence, first attempted by light microscopy of paraffin-embedded sections (Wylie, 1941) and later by electron microscopy (Meyer and Stubbe, 1974), has been unable to resolve these basic questions to date. Since the presence of disorganized and densely-stained synergid cytoplasm has often interfered with such observations, it has recently been proposed that examination of these processes in flowering plants that lack synergids may play a role in resolving this controversy (Russell, 1980).

The mechanism by which gametic nuclei are transmitted to the egg and central cell is still largely unknown; however, if transmission occurs by cellular fusion, extra-nuclear components of the male gametes will be transmitted into cells of the female gametophyte and their detection should be possible soon after the arrival of sperm nuclei into the egg and central cell. The problems associated with visualizing the crucial stages and identifying morphological

differences between organelles of different cellular origin have been largely resolved in the present study of fertilization in *Plumbago zeylanica* and contribute structural information to the process of gamete fusion in flowering plants. The present study outlines the condition of the male gametes after their discharge into the embryo sac and proposes a sequence of events during gamete fusion which terminate in the transmission of heritable cytoplasmic organelles of the male gamete into the egg and central cell.

B. Observations

An aperture forms at the tip of the pollen tube soon after its arrival within the embryo sac and results in the discharge of the pollen tube and the release of the vegetative nucleus, some pollen tube cytoplasm, and the two male gametes (Chapter 5). Regardless of the preparative technique used, the discharged pollen cytoplasm appears to begin degradative changes soon after it is injected into the intercellular space between the egg and central cell. Released pollen tube organelles appear to degenerate rapidly. The vegetative nucleus is situated between the egg and central cell and gradually approaches the chalazal part of this region. Discharged pollen cytoplasm continues to degenerate following gamete fusion, but undergoes less rapid alteration after fertilization. Even as late as several days after the arrival of the pollen tube it may be possible to distinguish the pollen tube wall between the suspensor and the endosperm cells and the degenerating remains of the pollen cytoplasm and vegetative nucleus.

Sperm cells in the megagametophyte before gamete fusion

The transitory nature of developmental stages between gamete discharge and fusion is clearly suggested by the rarity of such reports in the literature (most recently, Cass and Jensen, 1970; Cocucci and diFulvio, 1969; Wilms, 1981); in the present study, one megagametophyte observed displayed these stages (Fig. 46–51; Table 6). In this series, it is evident that the two male gametes remain near the pollen tube aperture, and become tightly appressed against the egg and central cell plasma membranes, surrounded by discharged, degenerating pollen cytoplasm on their remaining faces (Fig. 46, 47). The two

Fig. 46: Nomarski interference contrast micrograph of an unfused sperm cell between the egg and central cell in transection of megagametophyte. Sperm cell with nucleus and nucleolus evident is indicated by unlabeled arrowheads. The more proximal sperm cell discharged into this embryo sac is shown in Fig. 47. *CC* central cell; *E* egg; *Nc* nucellus; *PT* pollen tube. (Electron micrographs of this sperm shown in Fig. 50, 51.) Unstained. X 2575.

Fig. 47: Nomarski interference contrast micrograph of unfused sperm cell between the egg and central cell in a section several micrometers proximal to Fig. 46. Pollen tube is curved at this level and has become crushed during chemical preparation. Differences in the shape of the region between egg and central cell are evident between this and the previous figure. (Electron micrographs of this sperm shown in Fig. 48, 49.) Unstained. X 2575.

Fig. 48: Electron micrograph of unfused sperm cell between the egg and central cell shown in Fig. 47. Sperm nucleus (*SN*), located centrally within the sperm cytoplasm, is visible. The cellular nature of the sperm is clearly evident in the unfused male gamete soon after pollen tube discharge, although gametes are delimited by a single membrane rather than two, as before pollen tube arrival. Discharged material (including the sperms, pollen tube, pollen cytoplasm, and vegetative nucleus) are restricted to the intercellular region between the egg and central cell; these objects are not seen within cells of the female gametophyte except when fusion has occurred and then only nuclei and cytoplasmic organelles originating in the sperm cells have been identified. UA–PbCit staining. X 4350.

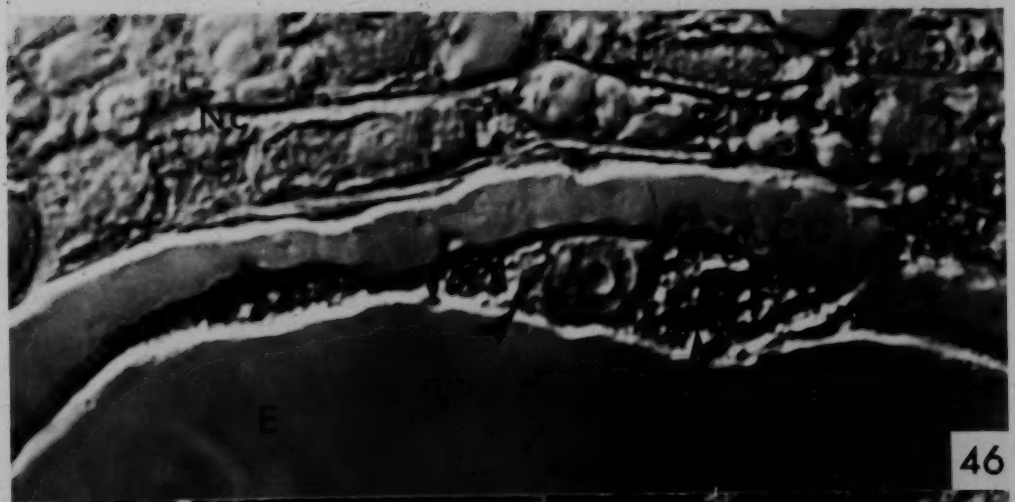

46

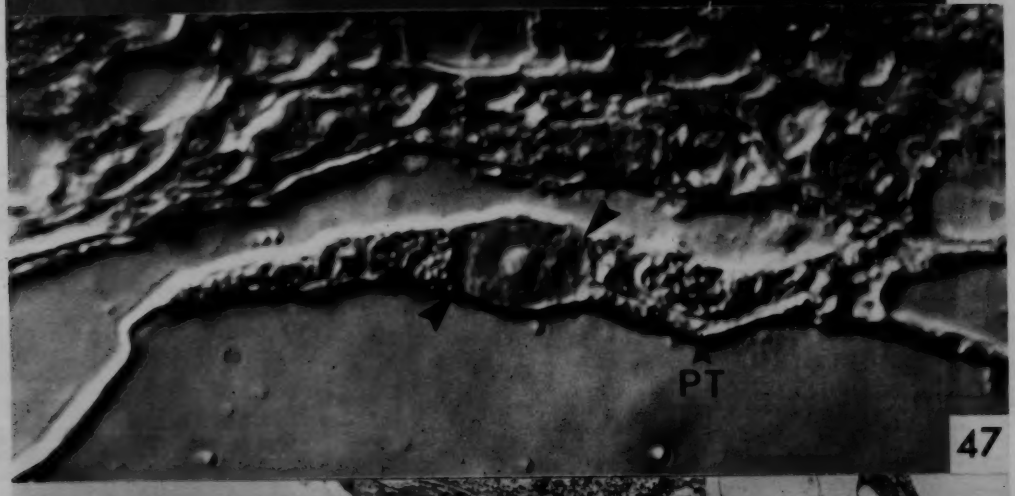

47

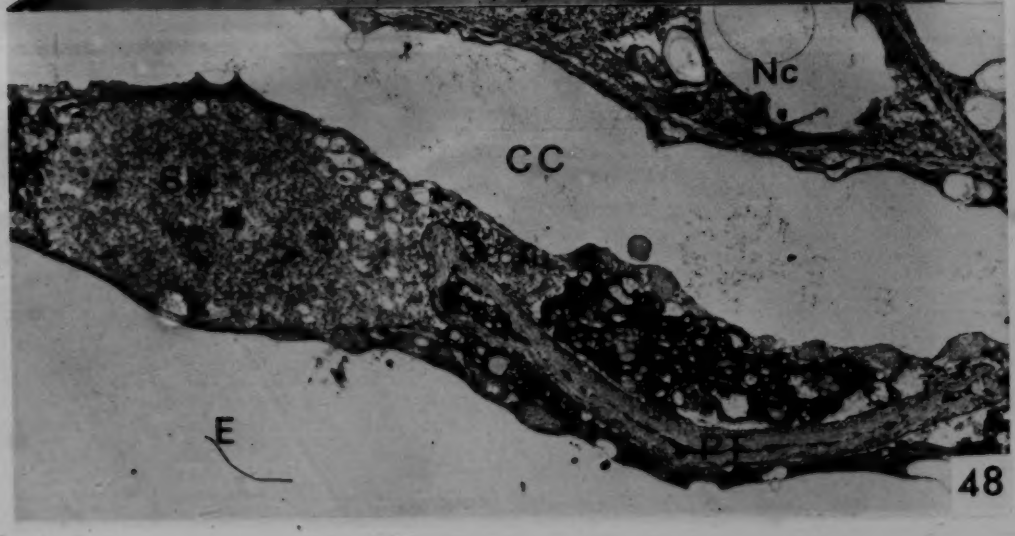

48

sperms are clearly cellular at this stage. The two sperms remain closely associated after their expulsion from the pollen tube and are separate cells, each surrounded by a single plasma membrane. At the electron microscopic level, the general cytology of sperm at this stage resembles that of sperm within the pollen grain and tube as described in a previous chapter. Possibly these two cells remain linked by plasmodesmata as in the pollen grain and growing tube (Fig. 27); however, this connection would presumably be disrupted near the time of gamete discharge or before gamete fusion.

The prefusion sperm cytoplasm is dominated by a nucleus with a prominent nucleolus, and contains a number of organelles which, by their ultrastructural appearance, seem to remain viable. Mitochondria are numerous within one cell, spherical to elongate, and approximately 0.2 um wide and up to 0.5 to 0.7 um long (Fig. 49). Plastids, up to 1.5 um long with dense stromata, are similar to those described within the pollen grain and growing pollen tube. The overall ground cytoplasm of sperms appears overall somewhat less electron dense than that of the surrounding egg and central cell (Fig. 49–51).

The two sperms are delimited by the sperm plasma membrane, but lack the surrounding inner vegetative cell plasma membrane observed throughout pollen grain maturation and as late as pollen tube penetration of the nucellar tissues. Following discharge, some parts of the sperm plasma membrane appear directly appressed to the plasma membranes of the egg and central cell. The loose, non-fibrillar cell wall observed at previous stages (see previous chapter) is apparently removed from the sperm surface with the removal of the vegetative cell membrane. The junction between the sperm and the egg and central cell varies from 0.02 um to 0.07 um (Fig. 50) depending on random variations and the presence of parts of the pollen cytoplasm lodged between the sperm cell and either of the female reproductive cells. At the perimeter of this junction with the sperm cells, microtubules within the egg and central cell may be observed oriented longitudinally with respect to the polarity of the embryo sac (Fig. 50). These microtubules frequently appear attached to the egg or central cell plasma membranes (as in Fig. 12, Cass and Karas, 1974), and may to some

Fig. 49: Electron micrograph of unfused sperm cell between the egg and central cell near the time of gamete delivery. Sperm cytoplasm contains the normal complement of organelles, including the nucleus (*SN*) and numerous mitochondria (*M* and unlabelled arrowheads). The sperm is delimited by a single membrane. Pollen tube (*PT*) visible to the right of the sperm cell. UA–PbCit staining. X 7900.

Fig. 50: Electron micrograph of junction between unfused sperm cell and central cell after gamete discharge showing the tightly appressed plasma membranes of the sperm (*S*) and central cell (*CC*). Microtubules located in female gametophyte (unlabelled arrowheads) may contribute to maintaining the conformation of sperm and female gametophyte cells during gamete delivery and fusion. UA–PbCit staining. X 24,950.

Fig. 51: Electron micrograph of unfused sperm, associated pollen cytoplasm, and pollen tube after gamete discharge. Degenerating discharged pollen cytoplasm, with rapidly disorganizing mitochondria indicated (*M*), is visible between the sperm cell and pollent tube (*PT*) The pollen tube aperture is located several micrometers from this site. *SN* sperm nucleus. UA–PbCit staining. X 22,150.

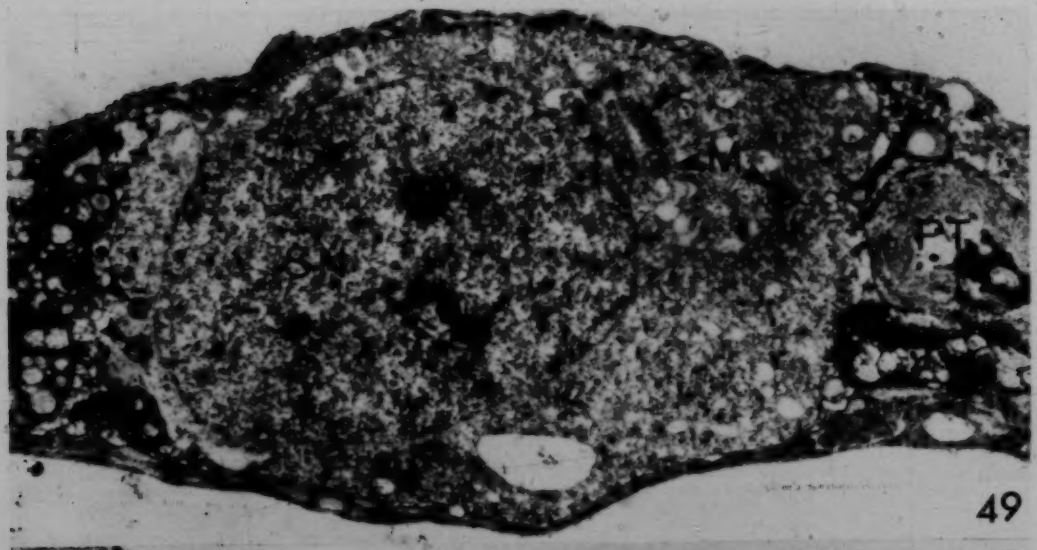

49

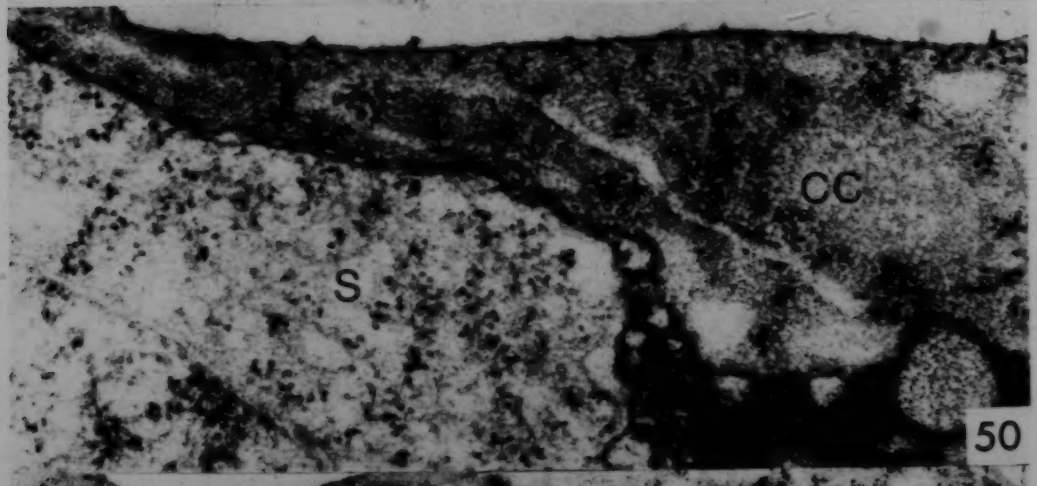

50

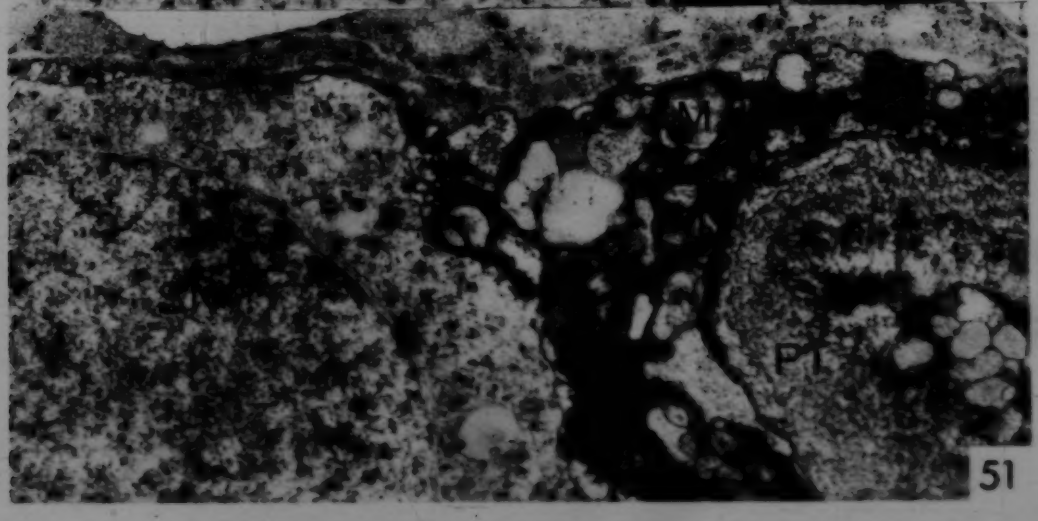

51

extent aid in determining the conformation of the egg-sperm-central cell relationship.

Male gametes within egg and central cell subsequent to gamete fusion

Sperm nuclei pass into the cytoplasms of egg and central cell soon after the arrival of male gametes within the embryo sac (see Table 6). As the location of the unfused sperm would indicate, the entry of sperm cells likely occurs near the site of their deposition, just beyond the tip of the pollen tube (Fig. 56). At this stage, the two sperm nuclei remain oriented in a linear fashion and the vegetative nucleus is located just beyond the distal sperm nucleus (Fig. 63-65). The sperm nuclei at this stage are typically separated from the egg and central cell nuclei by 25 and 17 um, respectively (Fig. 52), but this distance is quickly reduced during the ensuing 10 minutes (see Table 6). The sperm nucleus destined to fuse with that of the egg cell is shown in Figures 52, 53 and 57, while the sperm nucleus which will fuse with that of the central cell is seen in Figures 54-56.

Sperm nuclei appear approach the female nuclei by the most direct route, with subsequent nuclear fusion consistently occurring on the face of the egg or central cell nucleus nearest the site of gametic deposition and pollen tube discharge (Fig. 63-65). The events of subsequent nuclear fusion appear to be identical to those described in other angiosperm taxa (Jensen, 1964; Jensen and Fisher, 1970; Schulz and Jensen, 1977).

Sperm membranes following gamete fusion; modifications of egg-central cell wall

When sections are subjected to the PA-TCH-SP reaction, the plasma membrane of the egg and central cell (or certain components associated with it) are intensely stained. While endoplasmic reticulum and mitochondrial membranes are also stained somewhat by the reaction (with or without PA in OsO_4-fixed material), the only membranes stained as densely as the plasma membranes are those of the plastids and a membrane system of unknown origin located within five micrometers of the sperm nucleus in the central cell (Fig. 54, 55). This membrane system of unidentified origin is known to be absent prior to gamete

Fig. 52: Low magnification electron micrograph of an embryo sac soon after gamete fusion showing egg nucleus and sperm nucleus within the egg. Other sections of the same embryo sac are shown in Figs. 53–57. Sperm nucleus (SN_1) within the egg is flanked by plastids morphologically similar to those of the sperm cell (Fig. 53, 58). Electron-opaque material between the egg (*E*) and central cell (*CC*) represents the discharged, degenerate pollen cytoplasm. The central cell nucleus is located opposite the egg nucleus (*EN*) in other sections. The sperm nucleus which entered the central cell (SN_2) is located (in another plane of section) next to the pollen grain aperture, 5 to 7 um proximal to the sperm nucleus illustrated here. The vegetative nucleus is located (> 7 um away) in the distal degenerate pollen cytoplasm indicated by an arrowhead. UA–PbCit staining. X 1720.

Fig. 53: Electron micrograph of an unfused sperm nucleus in the egg flanked by two plastids of paternal origin. The sperm nucleus visible here is within micrometers of the site of gamete fusion, soon after gamete fusion. Two plastids (*Ps*) at the edge of the nucleus are morphologically similar to plastids known to originate in the male gamete (Fig. 58). Plastids flanking the unfused sperm nucleus have dense stromata, electron-lucent regions without starch grains, numerous plastoglobuli, poorly developed internal membrane systems, and occasionally (in uranium–lead stained preparations) paracrystalline bodies are visible. Discharged pollen cytoplasm and disrupted egg cell wall are evident between the egg and central cell. Small area of darkly staining membranes (arrowhead) is present near the edge of the unfused sperm nucleus. H_2O–TCH–SP reaction. X 17,550.

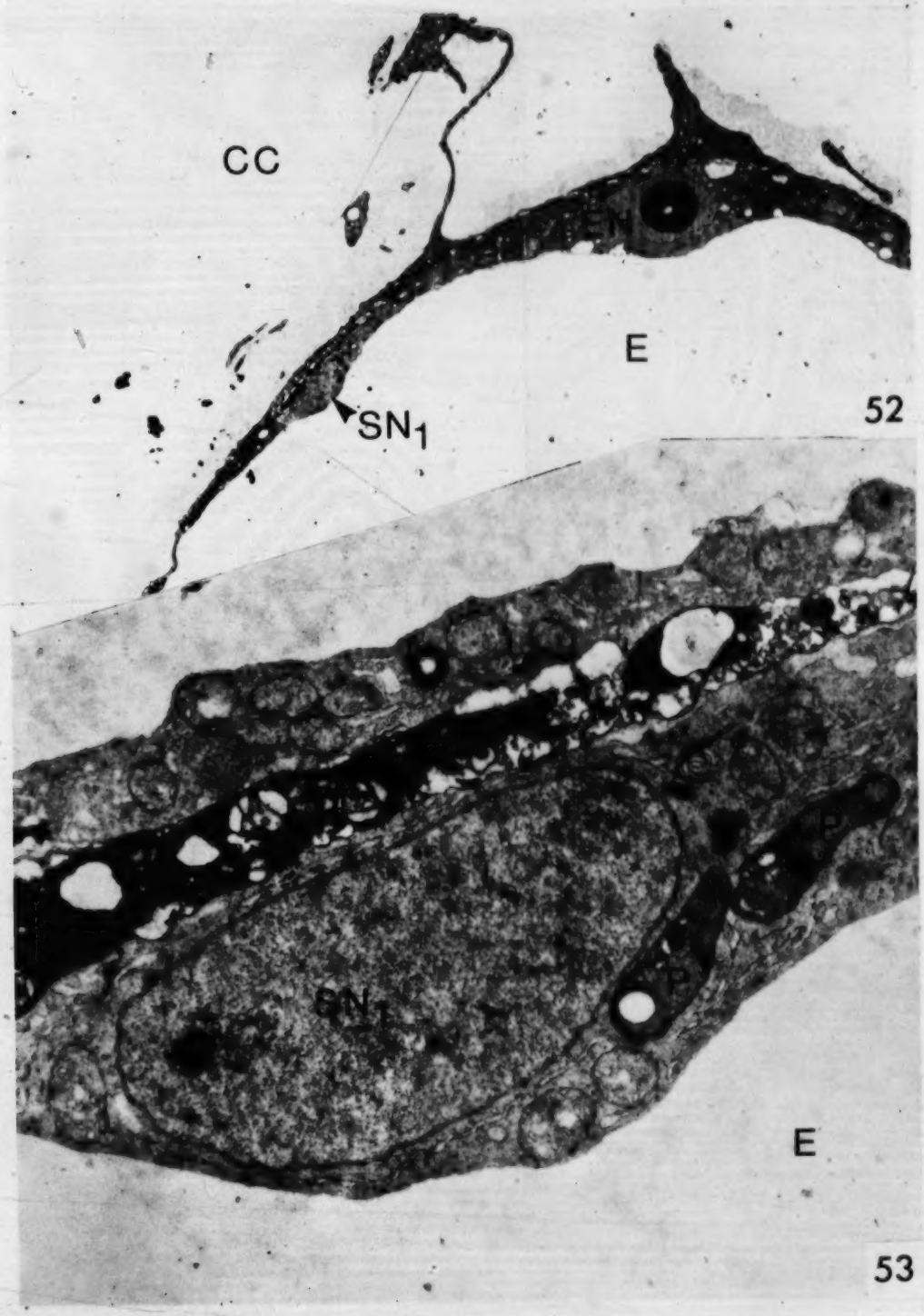
CC
E
SN1
52
SN1
P
P
E
53

Fig. 54: Electron micrograph of unfused sperm nucleus within the central cell soon after gametic fusion. This section was subjected to the TCH-SP reaction without prior PA oxidation. See serial section Fig. 55 for labels and TCH-SP reaction with PA oxidation. H_2O-TCH-SP reaction. X 37,400.

Fig. 55: Electron micrograph of unfused sperm nucleus within the central cell stained by the PA-TCH-SP reaction soon after gametic fusion. This section subjected to PA-TCH-SP reaction and photographically processed under the same conditions as the control (Fig. 54, without PA oxidation). Sperm nucleus (*SN*$_2$) located within the central cell (*CC*) is flanked by small mitochondia similar in size and morphology to those within the male gametes prior to fusion. The larger mitochondrion nearby probably represents one of the larger mitochondria of the central cell (*Mcc*). Note density of staining reaction of egg and central cell plasma membranes (unlabelled arrowheads) in TCH-SP reaction with and without prior PA oxidation. The same staining characteristics as the plasma membrane are also observed in a membrane system seen at the periphery of the sperm nucleus (unlabelled arrows) which appears to separate the two size classes of mitochondria (cf. Fig. 56). Plastids similar to those seen within the male gamete prior to fusion are visible (*Sp*) within the egg cell. PA-TCH-SP reaction. X 37,400.

Fig. 56: Electron micrograph of pollen tube aperture and unfused sperm nucleus within the central cell soon after gametic fusion. Pollen tube (*PT*) aperture indicated by unlabelled arrows. The secondary membrane system noted in Fig. 55 is also visible in this section (unlabelled arrowheads). (This section is serial to that shown in Fig. 55.) PA-TCH-SP reaction. X 11,000.

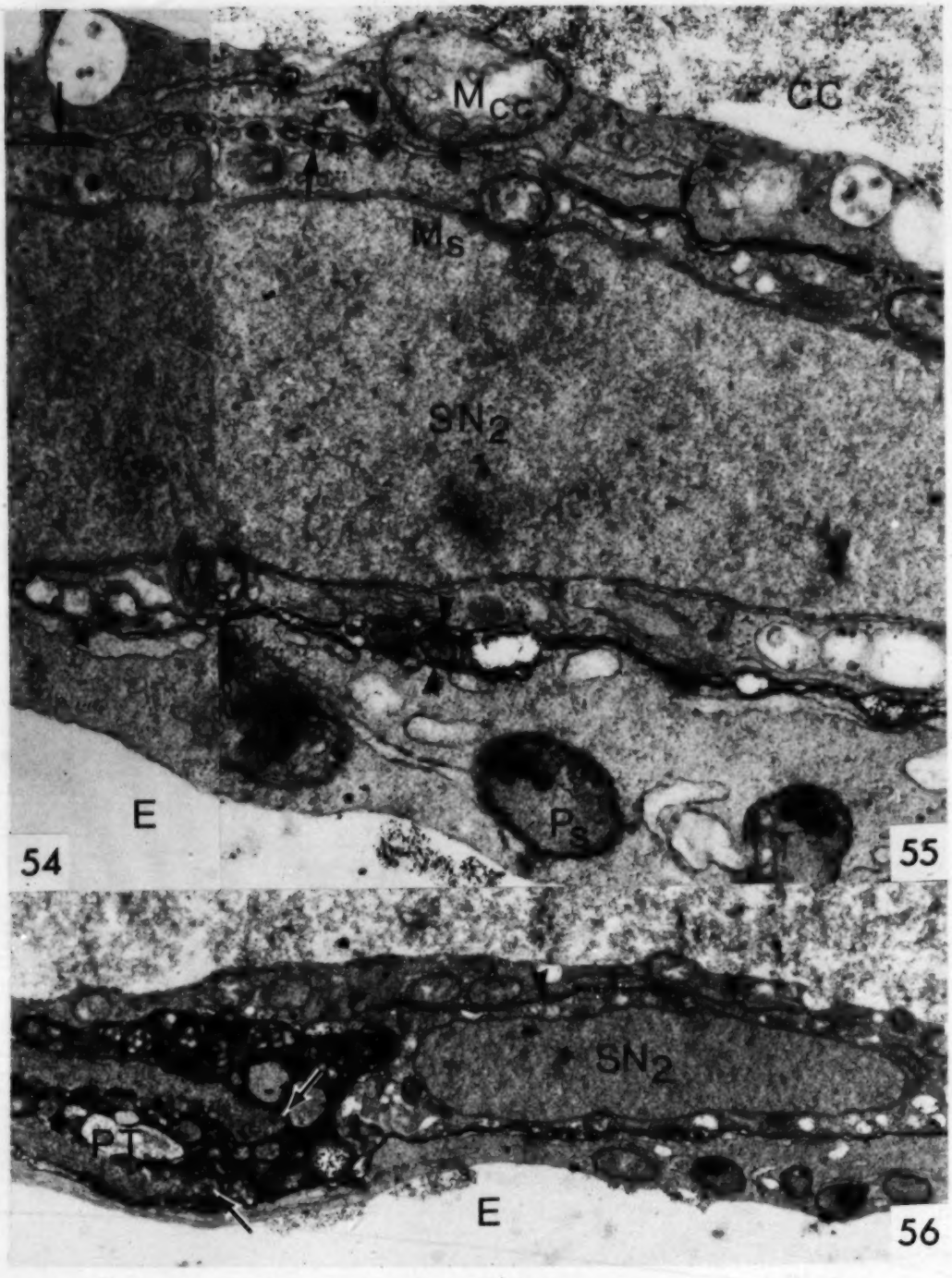
M_{cc}
CC
M_s
SN_2
E
P_s
54
55
SN_2
PT
E
56

fusion (Cass and Karas, 1974), but possesses essentially the same staining characteristics of PA-sensitivity as are observed in nearby plasma membranes (Fig. 54, 55). By the location of these membranes relative to the sperm nucleus, similarities in staining characteristics within plasma membranes, and the temporal relationship of these membranes with gamete fusion, it seems most reasonable that these membranes are of plasma membrane origin and that they are produced as a result of gamete fusion - possibly remnants of the sperm-central cell fusion membrane. Segments of this membrane system were found in all sections of the sperm nucleus examined, and appeared to be restricted to the narrow region surrounding this particular sperm nucleus (Fig. 54, 55, 56). At some locations along this membrane, vesicle patterns suggestive of vesiculation of the membrane are seen (upward arrow, Fig. 55), suggesting a process by which the presumed fusion membrane may become disorganized. Similar membranes were not observed near the other sperm nucleus, but a small membranous structure near a sperm nucleus within the egg (Fig. 53, arrowhead), may represent a remnant of a similar segment of sperm membrane in the egg cell. Evidence for such possible fusion membranes is temporally restricted to stages fixed very soon after gamete fusion, and are not evident during later migration of the sperm nucleus.

The egg cell wall at the upper lateral and chalazal end of the egg is quite different from that in the lower lateral and micropylar parts of the egg, as discussed previously in Chapter 5. In lower parts of the egg, the cell wall contains numerous longitudinally-aligned periodate-sensitive fibrils aligned parallel to the pollen tube, which may guide the pollen tube during its passage in the embryo sac. In the lateral egg wall, near the region of pollen tube discharge and above, the cell wall is homogenous, lacking in a fibrillar component, and as a result of pollen tube growth and discharge (Chapter 5) the egg cell wall is disrupted beyond the pollen tube aperture (Fig. 56, 66).

In the upper regions of the egg cell, from approximately the level of the pollen tube aperture to the summit of the egg, modified segments of egg cell wall are evident (Fig. 57, 60, 61) which appear to relate to the unequal

distribution of discharged pollen cytoplasm between the egg and central cell. These areas of modified cell wall were first reported during the development of the egg of *P. zeylanica* as electron-lucent regions with a constant thickness, which were associated with straight regions of the plasma membrane and stalked microtubules (Cass and Karas, 1974; see their Fig. 12). Similar segments are observed in the present study; however, after pollen tube discharge, these segments apparently become electron dense and granular (Fig. 57, 60, 61; arrowheads), and microtubules are more generally distributed in the embryo sac, occurring frequently near the region of gamete delivery (Fig. 50).

While the role of these modified regions of cell wall is not directly known, it appears that these regions influence the distribution of the degenerate pollen cytoplasm (arrowheads, Fig. 52, 66) and thus seem capable of influencing the position of larger objects introduced between the egg and central cell, including the sperms and vegetative nucleus. The presence of egg cell wall modifications between the pollen tube aperture and their location relative to the vegetative nucleus (Fig. 67) and the region of gamete fusion (Fig. 57, 60), suggests that egg cell wall modifications may effectively limit the movement of objects inserted between the egg and central cell - a role which may be important in stabilizing the position of sperm cells prior to gamete fusion.

Morphological evidence regarding male cytoplasmic transmission

Evidence favoring the transmission and incorporation of paternally-derived organelles in the female gametophyte was observed in both egg and central cell. Plastids which are uncharacteristically dense for those of the egg cell are noted at the periphery of the sperm nucleus within the egg cell soon after gamete fusion (Fig. 53, 57) and within adjacent egg cytoplasm in nearby sections (Fig. 55, 46 and 60). Compared to plastids within the unfertilized egg cell (seen in Fig. 59; also Cass and Karas, 1974, Fig. 3, 5, 6) and plastids of maternal-origin soon after gamete fusion (Fig. 61), sperm plastids possess a relatively dense stromata in uranium-lead stained material (Fig. 58), are somewhat narrower (approx. 1.2 um or less, instead of 1.5 um or more), and have a less highly developed internal membrane system (Fig. 58, 60). Content of plastoglobuli

Fig. 57: Electron micrograph of unfused sperm nucleus and associated cytoplasm in the egg soon after gamete fusion has occurred. Plastids (*Ps*) similar to those of known paternal origin seen in Fig 58 are seen flanking the sperm nucleus (*N*) within the egg cell, near probable site of gamete entry. The junction between the egg and central cell shows a number of periodically occurring wall modification (unlabelled arrowheads), also visible in Fig. 60, 61. These areas of parallel plasma membrane appear similar to those described by Cass and Karas, 1974 (see their Fig. 12), and may serve to limit the mobility of objects discharged within the egg cell wall, possibly including stabilizing the position of male gametes for cellular fusion. UA-PbCit staining. X 18,800.

Fig. 58: Electron micrograph of plastids in sperm cell within growing pollen tube approaching the ovule. These plastids are morphologically similar to plastids observed flanking the sperm nucleus in the egg soon after gamete fusion (cf. Fig. 53, 57). UA-PbCit staining. X 19,900.

Fig. 59: Electron micrograph of a typical plastid observed within a mature, unfertilized egg cell. Egg plastids (*Pe*) possess less dense stromata and better organized internal lamellae than sperm plastids prepared by the same methods (Fig. 58). *N* egg nucleus; *M* mitochondrion. UA-PbCit staining. X 13,900.

Fig. 60: Electron micrograph of plastids flanking the sperm nucleus stained by the TCH-SP reaction shortly after gamete fusion. These plastids are similar in morphology and staining characteristics to plastids of known paternal origin. Arrowheads indicate an area of modified egg cell wall apparently modified by the entry and discharge of the pollen tube, and subsequent gamete transmission. H_2O-TCH-SP reaction. X 31,600.

Fig. 61: Electron micrograph of plastids near the egg nucleus stained by the TCH-SP reaction shortly after gamete fusion. These plastids are similar in morphology and staining characteristics to plastids of known female gametophyte origin. Arrowheads indicate a modified region of egg cell wall near the summit of the egg cell. H_2O-TCH-SP reaction. X 14,900.

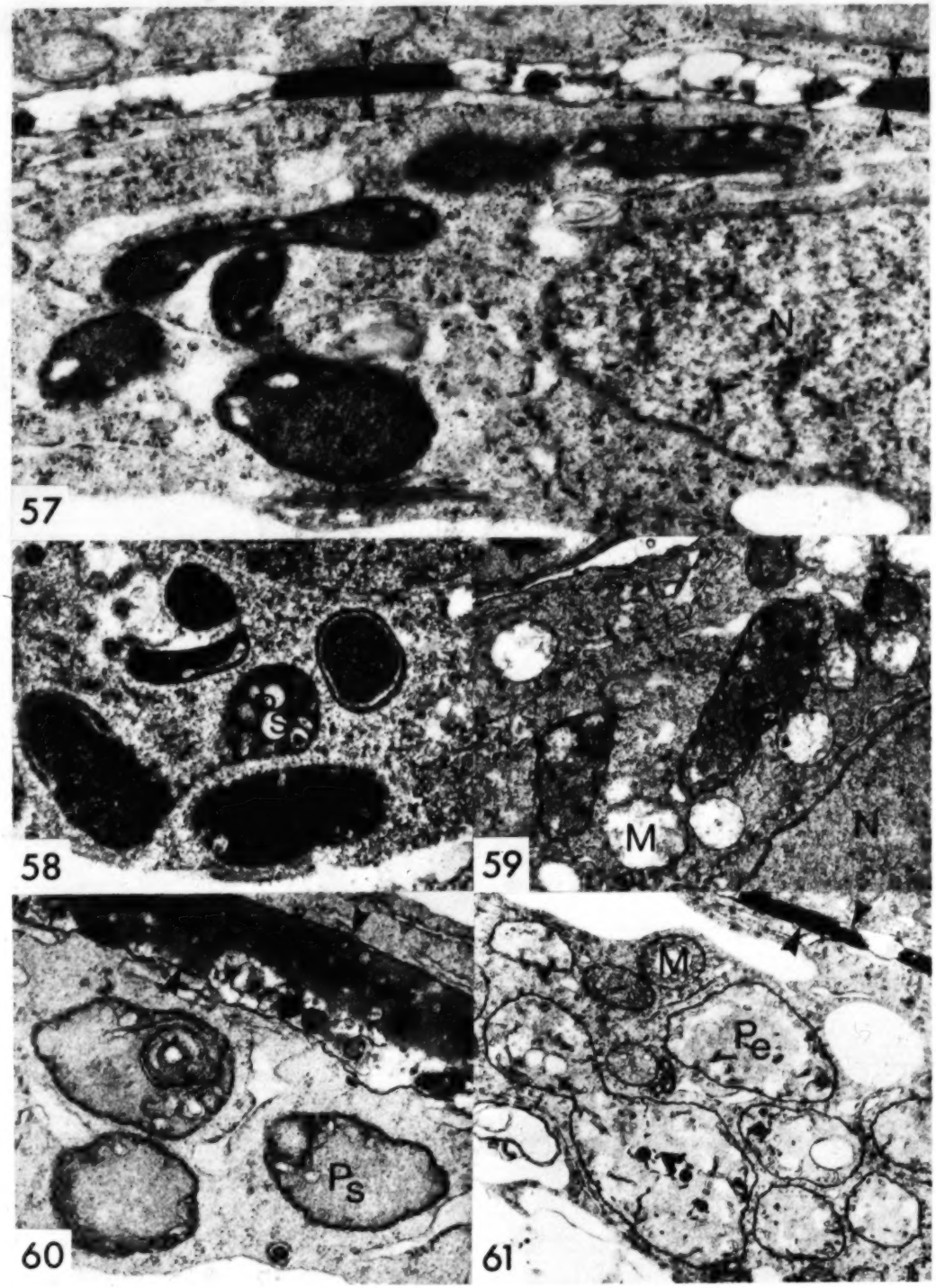
N
57
58
M
N
59
Ps
60
M
Pe
61

appears greater in these plastids, and occasionally there are paracrystalline arrays within the stromata (although such arrays also appear on occasion within plastids of known maternal origin). At this stage, the distribution of these atypical plastids within this embryo sac was restricted to within several micrometers of the sperm nucleus and did not extend elsewhere within the large egg cell (Fig. 52). Furthermore, the structure, morphology, and staining characteristics of these atypical plastids within two very different staining regimes, closely resembles plastids described within sperm cells of the same plant (see Chapter 3). The approximate number of plastids observed in the egg also agrees with the number observed in sperm cells (see Chapter 4; Appendix 1).

Statistical evidence of male cytoplasmic transmission

While the presence of dimorphic plastids in the sperm and female gametophyte permits differentiation of maternally and paternally-originating plastids on morphological grounds alone, differences in mitochondrial structure, although evident, are better dealt with in a statistical treatment. Size differences seemed apparent between mitochondria of male and female origin, and the regularity of mitochondrial shape (spherical to roundly ellipsoidal) suggested that selection of mitochondrial width, as a size parameter which is unbiased by section orientation, could prove useful in differentiating these organelles and identifying paternally-originating mitochondria within the female gametophyte.

Mitochondrial widths were measured in six different cell types: i) Sperm in pollen grains at anthesis; ii) Sperm in growing pollen tubes in the lower style, within 100 um of the ovule; iii) Vegetative cell in pollen grains at anthesis; iv) Vegetative cell in growing pollen tubes in the lower style; v) Mature, unfertilized central cell; vi) Mature, unfertilized egg. Average mitochondrial widths, standard deviation, comparison of the data with a normal distribution, and .95 confidence intervals are summarized in Table 7. Mitochondrial widths in the sperm cell average .29 um in pollen grains at anthesis (.95 confidence interval, .27 to .30 um) and in the sperm cells during late pollen tube growth, average .22 um (.95 confidence interval, .205 to .24 um). Mitochondrial width is greater in the pollen grains (ave. .45 um), pollen tubes (ave. .43 um), unfertilized egg (ave. .54 um), and

Table 7: Descriptive statistics comparing mitochondrial widths in six different cells of origin.

S.PG = Sperm cell within pollen grain at anthesis

PG = Vegetative cell within pollen grain at anthesis

E = Unfertilized egg, at receptivity

S.CC = Flanking sperm nucleus after gamete fusion

S.PT = Sperm cells within the pollen tube during active growth in the lower style

PT = Pollen tube, during active growth in the lower style

CC = Unfertilized central cell, at receptivity

S.UNFUSED = In unfused cytoplasmic bodies between egg and central cell

VARIABLE	N	MINIMUM	MAXIMUM	MEAN	STD DEV	SKEWNESS	KURTOSIS	.9500 CONFIDENCE INTERVAL
S.PG	31	.21500	.38700	.2864	.04226	.355	-.258	(.27095,.30195)
S.PT	16	.16500	.29100	.2237	.03420	.147	-.577	(.20553,.24197)
PG	26	.34100	.51700	.4527	.03980	-.626	.712	(.43669,.46885)
PT	52	.30000	.55400	.4334	.06231	-.071	-.558	(.41608,.45077)
E	36	.32200	.85800	.5362	.13174	.501	-.178	(.49167,.58083)
CC	37	.26900	.75300	.4894	.08793	.030	1.636	(.46009,.51872)
S.CC	41	.13200	.28800	.21422	.03690	-.149	-.730	(.20257,.22587)
S.UNFUSED	5	.18700	.28600	.24660	.03877	-.601	-.817	(.19847,.29473)

Table 8: Student's t comparison of population means and comparison of variance in mitochondrial widths in six different cell types.

S.PG = Sperm cell within pollen grain at anthesis

S.PT = Sperm cells within the pollen tube during active growth in the lower style

PG = Vegetative cell within pollen grain at anthesis

PT = Pollen tube, during active growth in the lower style

E = Unfertilized egg, at receptivity

CC = Unfertilized central cell, at receptivity

PAIRS	T-STATISTIC	DF	SIGNFICANCE	F-STATISTIC	DF	SIGNIFICANCE
S.PG						
S.PT	T= 5.124	45	.0000	F= 1.527	30, 15	.1946
PG	T=-15.196	55	.0000	F= 1.127	30, 25	.3831
PT	T=-11.622	81	.0000	F= 2.174	51, 30	.0000
E	T=-10.110	65	.0000	F= 9.720	35, 30	.0000
CC	T=-11.754	66	.0000	F= 4.330	36, 30	.0000
S.PT						
PG	T=-19.069	40	.0000	F= 1.35	25, 15	.2740
PT	T=-12.833	66	.0000	F= 3.32	51, 15	.0068
E	T= -9.303	50	.0000	F= 14.84	35, 15	.0000
CC	T=-11.657	51	.0000	F= 6.61	36, 15	.0002
PG						
PT	T= 1.440	76	.1538	F= 2.45	51, 25	.0086
E	T=-3.123	60	.0028	F= 10.96	35, 25	.0000
CC	T=-1.983	61	.0519	F= 4.88	36, 25	.0000
PT						
E	T=-4.900	86	.0000	F= 4.47	35, 51	.0000
CC	T=-3.518	87	.0007	F= 1.99	36, 51	.0118
E						
CC	T= 1.7915	71	.0775	F= 2.24	35, 36	.0090

central cell (ave. .49 um).

The .95 confidence intervals of mitochondrial width in sperm cells do not overlap with those of the pollen grain, tube, egg, or central cell. Cases in which there was a significant degree of overlap in these confidence intervals included the pollen grain and pollen tube mitochondria and those of the egg and central cell. A minor degree of overlap also occurred between .95 confidence intervals of mitochondrial width between the pollen grain and central cell (Table 7). It is interesting to note that .95 confidence intervals between sperm in the pollen grain and pollen tube do not overlap, probably a consequence of the elongation of sperm mitochondria noted as one of a number of developmental changes occurring during pollen tube growth.

Differences between population mean averages, as determined by Student's t-test (Table 8) indicate a statistically significant difference in mitochondrial width between the various mitochondrial widths which would permit their cell of origin to be determined within the female gametophyte. The Student's t test suggests that mitochondrial widths differ significantly between all classes of cells, with the exception of those in pollen grains and the central cell. Differences in population means were evident in comparing sperm mitochondria with all other classes presented thus far, but were slightly less significant when comparing sperm mitochondria in different developmental stages within the pollen grain and pollen tube.

These results strongly suggest that mitochondrial width differs within different cell types to the degree that it may be useful in identifying mitochondria of unknown origin within the embryo sac. Therefore, a seventh population (S.CC, Table 7) was constructed exclusively from mitochondria observed within one-half micrometer of the sperm nuclear envelope soon after gamete fusion (e.g., Fig. 54, 55) within the central cell. Descriptive statistics (Table 7) suggest that these are of paternal origin. The range of mitochondrial widths in this group, varying from .132 um to .288 um (ave. .21 um), overlaps closely with the range of mitochondrial widths observed in sperm cells within the growing pollen tube (.165 to .291 um, ave., .22 um).The .95 confidence intervals

corroborate this observation (Table 7). No such overlap in confidence intervals was observed between this group of sperm nucleus-associated organelles and any other group, including that of the unfertilized central cell in which this group was observed, nor was there significant overlap at the .99 confidence interval when this was tested (S.CC .99 confidence interval was .20 to .23 um; that of the unfertilized central cell, .45 to .53 um).

The Student's t-test (Table 9) was applied to this undetermined class of organelles to provide evidence that they differ significantly from mitochondrial widths in the unfertilized central cell and the pollen tube, the two most important cell sources to compare. The test proved significant at the $p < .0001$ level (Table 9), and this significance level also applies to mitochondrial widths in the unfertilized egg, pollen grain, and sperm within the pollen grain. Statistically insignificant differences were observed between the undetermined class of organelles and sperm cells within the pollen tube. Insignificant differences were observed in comparing this undetermined class of organelles with those found within cytoplasmic bodies found isolated between the egg and central cell (Table 9). The degree of variance differed insignificantly between the undetermined class and sperm cells, regardless of developmental condition, and with the inactive pollen grain (Table 9).

Presence and identification of unfused cytoplasmic bodies between the egg and central cell

Near the time of gamete fusion, a number of unfused membrane-bound, anucleate cytoplasmic bodies are frequently observed between the egg and central cell (Fig. 62, 63) and are restricted in distribution to within approximately 10-12 um beyond the aperture of the pollen tube, usually within micrometers of the vegetative nucleus. They are also observed up to a day after fertilization (Fig. 64). These bodies possess ribosomes, endoplasmic reticulum, and have a less electron-dense ground cytoplasm than either the egg or central cell; the latter feature is held in common with unfused sperm cells prior to gamete fusion (Fig. 49, 50, 51).

Table 9: Student's t comparison of population means and comparison of variance in mitochondrial widths in mitochondria flanking the sperm nucleus within the embryo sac and in unfused cytoplasmic bodies

S.PG = Sperm cell within pollen grain at anthesis

PG = Vegetative cell within pollen grain at anthesis

E = Unfertilized egg, at receptivity

S.CC = Flanking sperm nucleus after gamete fusion

S.PT = Sperm cells within the pollen tube during active growth in the lower style

PT = Pollen tube, during active growth in the lower style

CC = Unfertilized central cell, at receptivity

S.UNFUSED = In unfused cytoplasmic bodies between egg and central cell

	T-STATISTIC	DF	SIGNIFICANCE	F-STATISTIC	DF	SIGNIFICANCE
S.CC						
S.UNFUSED	T= -1.844	44	.0719	F= 1.104	4, 40	.3680
S.PG	T= -7.726	70	.0000	F= 1.312	30, 40	.2093
S.PT	T= -.894	55	.3754	F= 1.164	40, 15	.3891
PG	T=-25.014	65	.0000	F= 1.164	25, 40	.3274
PT	T=-19.926	91	.0000	F= 2.852	51, 40	.0004
E	T=-15.008	75	.0000	F= 12.749	35, 40	.0000
CC	T=-18.340	76	.0000	F= 5.679	36, 40	.0000
S,UNFUSED						
S.CC	T= 1.844	44	.0719	F= 1.104	4, 40	.3680
S.PG	T= -1.975	34	.0564	F= 1.188	30, 4	.4902
S.PT	T= 1.267	19	.2206	F= 1.285	4, 15	.3197
PG	T=-10.645	29	.0000	F= 1.054	25, 4	.5475
PT	T= -6.551	55	.0000	F= 2.584	51, 4	.1831
E	T= -4.839	39	.0000	F= 11.549	35, 4	.0140
CC	T= -6.044	40	.0000	F= 5.145	36, 4	.0603

Fig. 62: Electron micrograph of unfused segment of sperm cytoplasm soon after gamete fusion. An unfused single-membrane bound cytoplasmic body (unlabelled arrows) is seen appressed to the membranes of the egg (*E*) and central cell (*CC*). The size of mitochondria (*M*) inside this body, the lesser electron-density of the cytoplasm, and the proximity of this structure to the pollen tube aperture (several micrometers distal to this region) strongly suggest that this represents part of the sperm cell which has separated from the main cell body of the sperm prior to gamete fusion. H_2O-TCH-SP reaction. X 30,750.

Fig. 63: Electron micrograph of unfused cytoplasmic body after gamete fusion. Mitochondrion (*M*) is of the same dimensions as those within sperm cells of the growing pollen tube in the lower style. Single membrane delimiting this body (unlabelled arrow) tightly appressed to egg and central cell. UA-PbCit staining. X 39,800.

Fig. 64: Electron micrograph of unfused cytoplasmic body adjacent to an eight-celled embryo. This body, seen approximately one day after fertilization, is surrounded entirely by cell wall material of the endosperm (*En*) and suspensor (*S*). The cytoplasm of this body is membrane-bound and contains probable ER (unlabelled arrowhead), poorly-organized ground cytoplasm and a mitochondria (*M*) with dimensions similar to those of the endosperm and zygote. The location of the pollen tube aperture, seen at this location in adjacent sections, clearly indicates that the region of gamete fusion and the remains of the pollen tube (*PT*) are located in a region destined to become part of a characteristically massive suspensor reported elsewhere in the literature. UA-PbCit staining. X 28,600.

Fig. 65: Nomarski interference contrast micrograph of sperm and egg nuclei during fusion. Nearby sections of the same embryo sac are shown in Fig. 66, 67. Sperm nucleus (*SN*) and egg nucleus (*EN*) have formed nuclear bridges, trapping several cytoplasmic bodies within the fusion nucleus within the newly-formed zygote. ABB staining. X 1,700.

Fig. 66: Nomarski interference contrast micrograph of pollen tube aperture and wall modifications within the newly-formed zygote. The pollen tube aperture (unlabelled arrows) is unstained in this section stained for proteins. Just beyond the region of gamete fusion, a constriction of the intercellular space between primary endosperm and zygote is evident (unlabelled arrowheads), modifying distribution of the densely-stained discharged pollen cytoplasm. The region distal to this constriction contains the vegetative nucleus in another section (Fig. 67). ABB staining. X 1,700.

Fig. 67: Nomarski interference contrast micrograph of sperm and central cell nuclear fusion and vegetative nucleus. Fused polar nuclei (*PN*) within the incipient primary endosperm nucleus have formed nuclear bridges with the

sperm nucleus (*SN*), with several small cytoplasmic bodies visible between these two structures. Vegetative nucleus (*VN*) is visible between zygote and primary endosperm. A comparison of this figure with serial sections Fig. 65, 66 establishes that sperm nuclei fuse with their respective target nucleus at a point nearest the aperture of the pollen tube (see also Fig. 65). ABB staining. X 1,350.

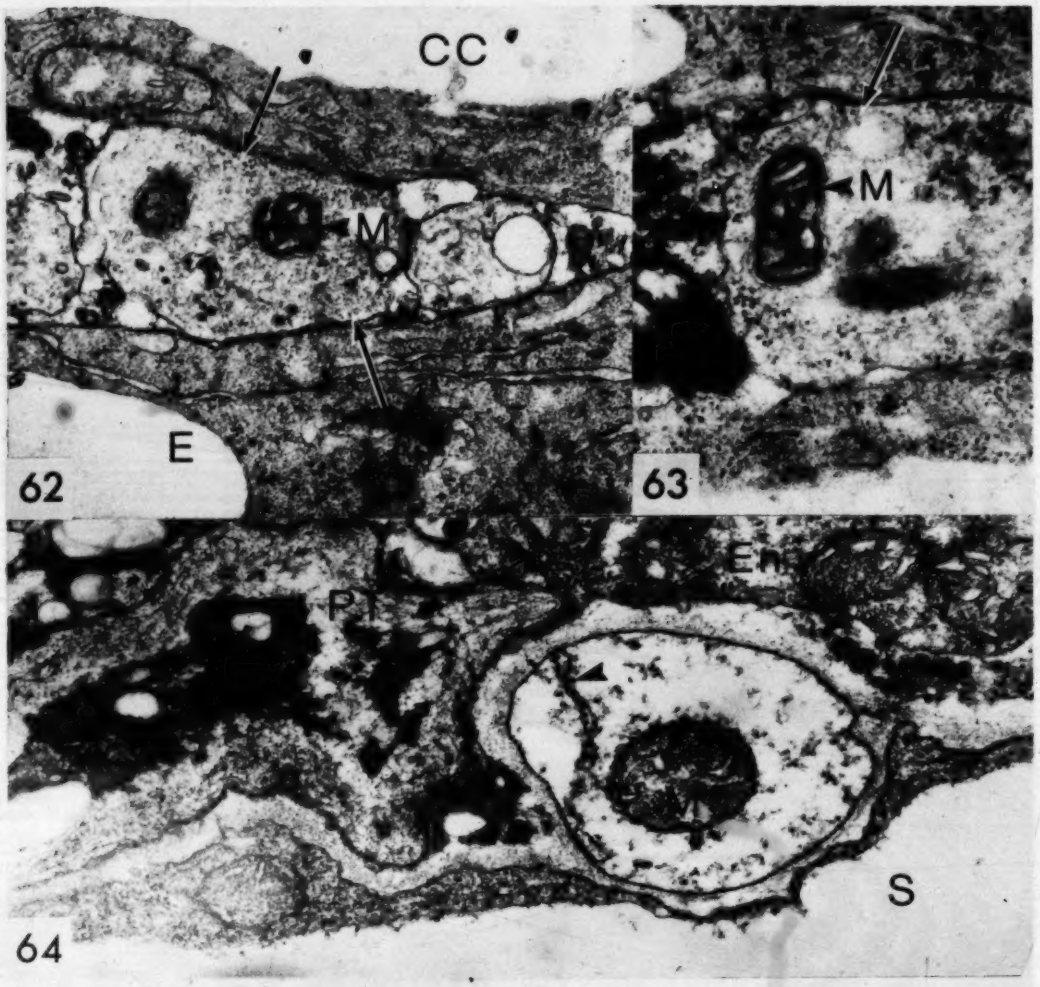
CC
M
E
62
M
63
P
En
S
64

SN
65

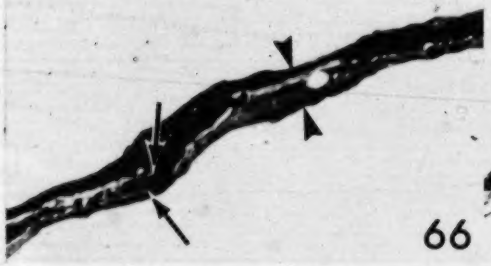
66

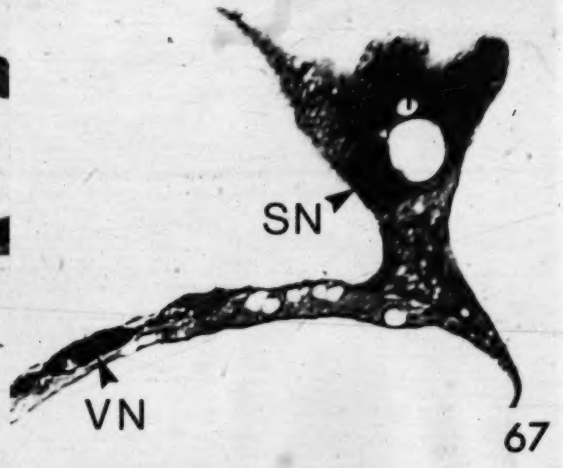
SN
VN
67

The mitochondria observed in these bodies range from 0.19 um to 0.29 um in width (mean average, 0.25 um) and appear similar in size and structure to those observed within the sperm cell in the pollen grain. The .95 confidence interval of the distribution overlaps with that of sperm mitochondria in the pollen grain, tube, and central cell, but did not overlap with that of mitochondria in the pollen grain or tube, egg, and central cell (Table 7), even when the confidence interval was raised to the .99 level. A Student's t-test (Table 9) comparison of the population means showed a very significant difference in mitochondrial widths within cytoplasmic bodies from those of the pollen (grain and tube) and female gametophyte. There were insignificant differences in comparing mitochondrial widths within cytoplasmic bodies with those of the sperm within the pollen grain, tube and central cell.

Statistical tests corroborate the identification of these cytoplasmic bodies as isolated segments of the sperm cell. Their location relative to the vegetative nucleus and the number of mitochondria observed within these bodies suggest more specifically that these segments originate in the sperm projection associated with the vegetative nucleus, which is possibly severed during expulsion of the vegetative nucleus and gametes from the pollen tube. The ratio of mitochondria observed flanking the sperm nucleus in the central cell relative to that in cytoplasmic bodies (roughly 8:1) is similar to actual counts of mitochondria in the main cell body and projection made in sperm within pollen grains at anthesis (range, approx. 1.4:1 to 4.9:1; average, 2.45:1). If one assumes that the projection becomes less elongated during pollen tube growth, as reported previously (Chapter 3), and that the probability of segmentation likely increases near the ends of the sperm projection, the 8:1 ratio observed may be an accurate estimate of the proportion of mitochondria in the main cell body transmitted into the female gametophyte versus those untransmitted during gamete fusion in cytoplasmic bodies between the egg and central cell.

C. Discussion

In unreduced angiosperms, the synergids appear to play an important role in receiving the pollen tube and physically mediating the transmission of sperm nuclei; the involvement of the synergid has thus figured prominently in the more recent embryological literature (Jensen, 1973; Mogensen, 1978; Folsom, 1980). In each of the over twenty plants examined to date, the synergid has proven to be the exclusive cell type to receive the pollen tube and its discharged contents during normal sexual reproduction. In all but one plant examined in the electron microscope to date (*Petunia*, van Went, 1970), morphological changes in one of the two synergids precede the arrival of the pollen tube. During normal function, this degenerated synergid alone receives the pollen tube and possesses the capability of transmitting the sperm into the egg and central cells. However important the synergid may be in these plants, a number of taxa in the subfamily Plumbaginoideae (family Plumbaginaceae) lack these apparently essential cells and contrary to the normal condition in angiosperms, possess an egg apparatus consisting of exclusively the egg cell. Functions universal to flowering plants will be expected to be present in these reduced megagametophytes, but the means by which synergid functions are transferred to other cells may provide insight into essential functions of the synergid.

In the past, the absence of synergids in taxa within the Plumbaginoideae has been used as evidence that the synergids are unnecessary for normal sexual reproduction (Maheshwari, 1950), on the presumption that normal sexual reproduction occurred in the Plumbaginoideae. The events of gametic transmission and nuclear fusion however, have not been recorded previously in any of the synergid-lacking taxa. In the only previous observation of events relating to the mechanism of fertilization in the Plumbaginoideae, Dahlgren (1916) identified and illustrated sperm nuclei in both egg and central cells of *Plumbagella micrantha*, but apparently did not observe nuclear fusion in the central cell. Dahlgren (1916, pg. 61) concluded: "So genannte Doppelbefruchtung findet wahrscheinlich statt." In *Plumbago zeylanica*, sperm nuclei have been observed within the egg and central cells, with subsequent nuclear fusion occurring to constitute the nuclear

complement of the zygote and endosperm. Events occurring during double fertilization in *Plumbago* appear essentially similar to those reported in other angiosperm taxa (Jensen, 1964; Schulz and Jensen, 1977).

Although cytoplasmic geneticists have long regarded that organelles of paternal origin accounted for certain patterns of non-Mendelian inheritance in angiosperms (Grun, 1976; Gillham, 1978), whether these organellar traits arise from hereditary characteristics transmitted by sperm organelles, by the pollen tube, or arise from some other genetic feature has remained a source of controversy among embryologists. The structure, condition, and ultrastructure of the sperm cytoplasm upon deposition in the female gametophyte is still largely unknown in flowering plants. Only three recent studies have reported observing sperms within the degenerate synergid (Cass and Jensen, 1970; Cocucci and diFulvio, 1969; Wilms, 1981), and in these cases, as in *Plumbago*, the sperms appear to remain cellular until transmission. Among the number of embryological accounts which have reported the non-transmission of sperm cytoplasm, only Jensen and Fisher have provided any evidence which would suggest that any sperm cytoplasm is shed prior to gamete fusion (Jensen and Fisher, 1968a, their Fig. 19, 20; Fisher and Jensen, 1969). In *Plumbago*, the presence of paternally originating plastids of probable sperm origin in the egg and statistically significant dissimilarity of mitochondria surrounding the newly transmitted sperm nucleus on a populational level with those of the pollen tube, central cell, and egg and the lack of such statistical dissimilarities between mitochondria surrounding the newly transmitted sperm nucleus and the sperm cell within growing pollen tubes indicate transmission of organelles originating within sperm cells. The numbers of plastids and mitochondria within cells of the female gametophyte soon after gamete fusion corroborate this interpretation (see Appendix 1). The mechanism of gamete fusion proposed in this work (in the following pages) and the degenerate condition of pollen tube cytoplasm make the possibility of transmission of vegetative cell (pollen) organelles highly unlikely. Further, there is no evidence that any mitochondria near the region of gamete fusion are large enough to have originated in the pollen tube rather than the sperm cell (Table 7; the maximum

mitochondrial width of any of the mitochondria measured within 0.5 um of sperm nucleus was .288 um; the minimum mitochondrial width in the pollen tube, .300 um; the .95 confidence intervals differ significantly).

Although there is yet no genetic evidence relating to the subsequent inheritance of heritable male cytoplasm into the later embryo and into future generations, detailed observations of sperm cell cytoplasmic organelles near stages surrounding gamete fusion permit an analysis of events during gamete fusion, including observations concerning the proportion of the sperm cytoplasm which may be transmitted into the female reproductive cells during this process. Several factors permitting this analysis include: i) the dimorphism between organelles in male and female cells; ii) that these two classes of organelles may be distinguished even after gamete fusion and fertilization; and iii) that sperm cytoplasmic organelles remain, at least for the time period covered in this study, similar to those reported previously in the growing pollen tube (Chapter 3). The most noteworthy alterations occurring in the pollen tube include loss of the inner and outer vegetative cell plasma membranes with consequent loss of soluble components of the sperm cell wall. As a result, the sperm plasma membrane is directly exposed to its surrounding environment, including egg and central cell plasma membranes and the rapidly degenerating pollen cytoplasm. Such a modification of male gamete-associated membranes with subsequent apposition of male and female cell membranes was also noted in spinach (Wilms, 1981), and strengthens the possibility that disruption of vegetative cell membranes is a general phenomenon in angiosperms which may be required before normal gametic fusion may occur. Similarly, in the female gametophyte the cell wall of the chalazal part of the egg is disrupted just beyond the tip of the pollen tube (Chapter 5). Schulz and Jensen (1968) also noted that portions of the egg cell wall were disrupted in *Capsella* and invoked a mechanism involving disruption of the wall during pollen tube discharge which is similar to that described in *P. zeylanica* (Chapter 5). A far more common situation in the unreduced egg apparatus is for the egg to lack a continuous wall prior to gamete deposition (Jensen, 1973). In *Plumbago*, upon the deposition of male gametes into the

embryo sac, each sperm become tightly appressed to both the egg and central cell plasma membranes. Since the intervening inner vegetative cell plasma membrane is lacking, and organized cell walls are either disrupted or absent, the only materials expected to be associated with the gametic and central cell surface would be those typically associated with the plasma membrane; thus the junction between each of the sperms and the egg and central cell constitutes essentially a direct membrane-to-membrane contact. Such a junction is visible in sperm cells deposited in the embryo sac observed prior to gamete fusion (Fig. 48-51). The membrane appositions and variable distance observed between apposed membranes, bear strong resemblance to membrane appositions reported during cellular interactions of fusing higher plant protoplasts (Fowke and Gamborg, 1980).

What is the sequence of events during gamete fusion? Based on the observations presented in this thesis, it appears that the process of gamete fusion in *Plumbago* begins with the delivery of two single membrane-bound male gametes between the plasma membranes of the egg and central cell. The geometrical location of the sperm cells between the egg and central cell results in the sperm cells becoming tightly appressed to the plasma membranes of both of the female reproductive cells (Fig. 68A). Gamete fusion would logically be expected to begin at a single location on each sperm plasma membrane, as shown in Fig. 68B (arrowhead near SN_2); however, subsequent instances of membrane fusion rapidly occur at multiple locations, as shown in Fig. 68B (arrowheads near SN_1 and Fig. 68C (arrowheads near SN_2). Fusion membranes disorganize by progressive vesiculation of remaining segments of membrane (Fig. 54, 55, 68C). Isolated membrane segments (like those in Fig. 54-56) are likely composed of elements of both the sperm and the female cell involved. Vesiculation of fusion membranes may be completed in less than five minutes following gamete fusion. In Fig. 68C only a small remnant of the fusion membrane may be visible near the sperm nucleus in the egg (arrowheads near SN_1). Even though sperm are surrounded, from their inception, by the inner vegetative cell plasma membrane and more distantly by the outer pollen plasma

Fig. 68: Reconstruction of gamete fusion in *P. zeylanica*.

Drawing 68A. Sperm cells (S_1 and S_2) located between the egg (*E*) and central cell soon after discharge from the pollen tube (*PT*). Plasma membranes of egg and central cell indicated by unlabelled arrowheads; heavy lines represent egg and central cell tonoplasts. Sperm nuclei are flanked by their cytoplasmic organelles, including mitochondria (*M*) and plastids (*P*). Vegetative nucleus (*VN*) is visible at the right of the figure between the egg and central cell, and is found within a layer of discharged, degenerating pollen cytoplasm (represented by gray shaded areas).

Drawing 68B. Gamete fusion is initiated by the fusion of the plasma membrane of the sperm and one ot the two flanking female cells (see arrowhead near S_2). Fusion is completed at more than one site, as seen in the egg (arrowheads near S_1), where a later stage of fusion is visible. Arrowheads in the egg indicate areas of fusion initiation and regions where the membrane is beginning to undergo progressive vesiculation.

Drawing 68C. A later stage of gamete fusion, where membranes of the sperm within the central cell are undergoing vesiculation (arrowheads near SN_2); little evidence of disorganizing membrane systems is seen within the egg cell (arrowhead near SN_1). Areas of sperm cytoplasm which are presumably sheared from the main body of the sperm cell near the time of gamete deposition, are evident near the vegetative nucleus (at unlabelled arrow). This drawing was traced from sections shown in Fig. 52, 53, 56, and is accurate in size, scale, and location of nuclei and organelles; drawings 1 and 2 are stages postulated from the data presented in this study. Approximately X 7,500.

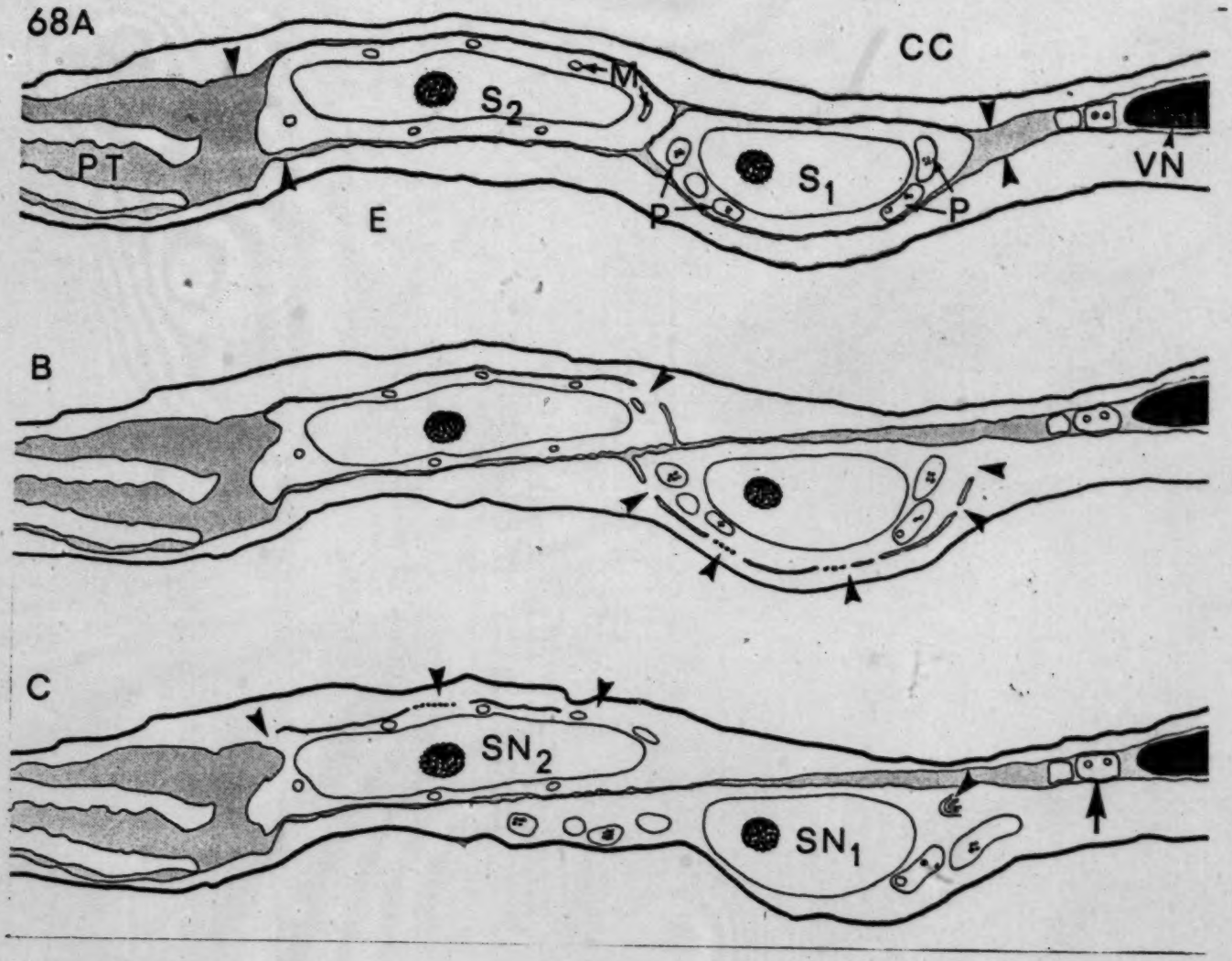
68A
CC
M
S_2
PT
E
P
S_1
P
VN
B
C
SN_2
SN_1

membrane. The loss of these two membrane systems may be necessary for male gametic transmission and is a feature in both of the ultrastructural studies in which sperm have been described soon after gamete delivery (Wilms, 1981; present study). Functionally, the presence of these additional membranes would be difficult to reconcile with the expected symmetry of plasma membrane fusion during transmission of the sperm. Further, membranes of the vegetative cell have no demonstrated capacity for genetically-programmed fusion with the female membranes, nor would they be expected to fuse with membranes of the sperm, as would be necessary for passage of sperm from the vegetative cell. Considering the outcome of the continuing presence of the vegetative cell membranes, the sperm would have to be transmitted through, or fuse with, two additional membranes. Such a pattern of membrane fusion is unparalleled in fertilization studies in other biological systems and seems unlikely in angiosperms. In angiosperms with an unreduced egg apparatus, the absence of the plasma membrane in the receiving synergid corroborates the concept that the number of membranes encountered during gamete fusion may be reduced to a minimal number.

The role of normal synergid degeneration in gametic transmission in normal flowering plants, if any, may necessarily include the disruption of the synergid plasma membrane and may also relate to the disorganization of membrane and cell wall layers surrounding the sperm. In *Plumbago*, the presence of a degenerating cell is not observed, but a specific, localized region of pollen cytoplasm degeneration is noted between the egg and central cell (see Chapter 5, Fig. 42, 43). The rapidity of pollen degeneration is a characteristic of sexual reproduction which *Plumbago* shares with the other angiosperms studied to date (Jensen, 1973). Even though the presence of unfused sperm within the persistent synergid is abnormal within angiosperms, their occurrence has been used as evidence that synergid degeneration may be related to the transmission of sperm nuclei into the egg and central cell (Mogensen, 1978). A specific mechanism by which synergid degeneration effects gametic transmission, however, has not been reported.

In the few accounts where the course of synergid degeneration is reported in entirety, it appears that the penetrated synergid lacks a cell membrane and wall, especially at the chalazal end of the degenerated synergid. In cotton (Jensen and Fisher, 1968a; Fisher and Jensen, 1969), a plasma membrane is lacking in the chalazal end of the degenerate synergid in chemically-prepared materials. The degenerate synergid undergoes a variable degree of degradation prior to penetration and is believed to guide sperms to the chalazal end part of the synergid in part by differences in the cytoplasmic consistency of the synergid and the location and direction of the subterminal pollen tube aperture (Fisher and Jensen, 1969). Although freeze-substituted preparations of unpenetrated synergids did not display conspicuous features of synergid degeneration after pollination (as did the chemically-prepared tissue), it was observed that material from the penetrated synergid was often forced from that cell regardless of preparative technique used (Fisher and Jensen, 1969). The only electron micrograph of a newly-transmitted sperm nucleus in their study was located in the egg near some discharged pollen cytoplasm between the egg and persistent synergid (Fisher and Jensen, 1969; their Fig. 8); they did not discount the possibility of this region serving as a possible site for nuclear transmission.

In spinach, electron micrographs clearly show some of the discharged pollen cytoplasm and vegetative nucleus overarching the egg (Wilms, 1981; his Fig. 18). According to Wilms, a single instance of a binucleate sperm cell was noted, "within the penetrated synergid", but the location of this sperm in the chalazal end of the synergid, where the synergid plasma membrane and cell wall are lacking, makes this account difficult to evaluate. Van Went's work on *Petunia* (van Went, 1970), showed that the integrity of the synergid was disrupted after pollen tube penetration and that the discharged tube cytoplasm was often observed between the central cell, persistent synergid, and egg. In *Linum*, the products of synergid degeneration are frequently observed between the persistent synergid, egg, and central cell, even before the arrival of the pollen tube (Vazart, 1969). Vazart further suggests that the region occupied by these degradation products (rather than the synergid proper) constitutes the site of male gamete

deposition and transmission. Several additional studies note the breakdown of the degenerated synergid plasma membrane and the consequent loss of cellular integrity (including, Cocucci and Jensen, 1969b; Maze and Lin, 1975; Mogensen, 1972; Mogensen and Suthar, 1979). Events reported during synergid degeneration may also be induced in cultured ovules by adding IAA and gibberellic acid to the medium (Jensen, Schulz, and Ashton, 1977); synergid degeneration occurring in these cultured ovules is essentially identical to that which occurs *in vivo*.

Clearly, in these plants the synergid is not intact following the arrival and discharge of the pollen tube into the embryo sac and the presence of material forced into intercellular spaces between surrounding gametophytic cells and the ultimate position of the vegetative nucleus (Fisher and Jensen, 1969; Cass and Jensen, 1970; Wilms, 1981) suggests an unexpected degree of similarity with the *Plumbago* system.

The absence in penetrated synergids of a delimiting plasma membrane and cell wall suggests that the pollen tube arrives in a region which shares boundaries with the egg and central cell, which in this regard is similar to the penetration region in *P. zeylanica*. Such a geometric organization of the egg apparatus would permit simultaneous membrane contact between sperm cell membranes and the plasma membranes of the egg and central cell, a prerequisite for gamete fusion; further, such simultaneous contact is a logical prerequisite for possible gametic recognition. The likelihood of simultaneous membrane contact between the sperm and both the egg and central cell may be further increased by shrinkage in the degenerate synergid, which is a common occurrence in penetrated synergids (Jensen and Fisher, 1968a; Schulz and Jensen, 1968; van Went, 1970; Mogensen, 1972; Wilms, 1981) or the occurrence of invaginated egg or central cell membranes into the synergid, as reported in degenerated synergids of barley (Cass, 1981).

The idea that synergid shrinkage may increase the possibility of contact between sperm and the female reproductive cells is further supported by examining the relative volumes of synergids, before and after fertilization, and comparing this to the volume of a sperm cell in a given taxon. Using data

provided by Jensen and Fisher (1968a) on freeze-dried paraffin sections of synergids, the degenerated synergid shrank from an original volume at anthesis of about 3500 um^3 to a post-degeneration volume of 820 um^3 within one day after pollination (several hours after fertilization). According to Jensen and Fisher, some of the synergid shrinkage occurs before pollen tube arrival, but the completion of vacuolar collapse appears intimately associated with the entrance and discharge of the pollen tube. The reported size of the mature sperm cells of cotton, 8 X 14 um (Jensen and Fisher, 1968b), would yield a sperm volume of approximately 230 um^3 each (see Appendix One for calculation techniques), which could occupy between one-fourth and one-sixth of the volume of the degenerating synergid upon gamete deposition into that synergid. This would seem to be such a large proportion of the volume of the degenerating synergid that the occurrence of simultaneous membrane contacts between the sperms and more than one of the female reproductive cells may be favored. Since membrane contacts between the sperms and the other synergids are unlikely because of the typical presence of a well-defined cell wall between the two synergids, these contacts would likely occur between the sperm and the egg and/or central cell. An obvious implication of the large size of the sperm cells relative to the degerating synergid and the organization of the normal egg apparatus is that the presence of sperm-egg and sperm-central cell junctions without an intervening cell wall is possible and perhaps favored near the time of pollen tube receipt, particularly near the chalazal end of the degenerated synergid.

If the position of the vegetative nucleus is assumed to indicate typical patterns for the movement of sizeable objects within the penetrated female gametophyte (Fisher and Jensen, 1969), the consistent location of the vegetative nucleus in chalazal parts of the penetrated synergid in angiosperms studied to date (Fisher and Jensen, 1969; Cass and Jensen, 1970; Cocucci and diFulvio, 1969; van Went, 1970; or slightly exceeding the pre-penetration boundries of the synergid, Wilms, 1981) may suggest similar movement patterns may be true for discharged sperm cells within the embryo sac. Simultaneous membrane contact between sperm plasma membranes and those of both the egg and

central cell constitutes a minimal requirement for a possible system of gamete recognition at the membrane level in which each sperm has an individual, specific target cell even prior to gametic deposition within the embryo sac. The possibility of this occurrence in angiosperms is a matter of conjecture; however, the presence of individually identifiable sperm cells in *Plumbago* makes this plant an important subject for future research that will attempt to identify whether gametic transmission of sperm plastids, which are predominantly present in only a single sperm cell (Chapter 4), are preferentially transmitted into either the egg or central cell, or whether such transmission is random. Preliminary data indicates the presence of a significant number of paternally-originating plastids only in the egg and zygote in three cases carefully examined to date (Fig. 53, 57, 60) and strongly supports this possibility. If such sperm cell-specific fusions occur between sperm and the egg and central cell in *Plumbago*, one is faced with questions concerning the generality of such a cell in other more typical angiosperms. While the morphological characteristics that make the synergidless egg apparatus unique may be features subject to rapid evolutionary processes, as the general occurrence of synergid disruption during embryo sac function may suggest; events at the cellular level, particularly those relating to gamete function, may be expected to remain subject to less rapid evolutionary change. The possibility that sperm in normal embryo sacs may also undergo simultaneous membrane contact between the egg and central cell, supports the likelihood that cell-specific recognition events regulated at the membrane level are not restricted to the genus *Plumbago* alone and may occur during double fertilization in other angiosperms. It is thus possible that any specific membrane changes occurring in the egg or central cell of *Plumbago* as a result of prior gamete fusion may render that cell unavailable for fusion with a second sperm cell, preventing polyspermy, but that a second gamete recognition event may be needed to determine the fate of the remaining, unfused sperm.

The majority of angiosperms studied to date have revealed sperm cells which are identical in ultrastructural organization, but if the same type of sperm cell polarity and association with the vegetative nucleus occurs in other plants as

has been seen in *Plumbago*, differences in sperm cytoplasmic structure in other flowering plants may simply be more subtle. The possibility that differentiation of sperm cells is a relatively advanced evolutionary characteristic must also be considered, and if valid, would suggest that plants in which the sperm are not individually recognized would likely represent the ancestral condition in flowering plants. In these ancestral plants, it would be expected that gamete fusion occurs by a mechanism similar to that described by Jensen (1973), in which gamete fusion with either the egg or central cell causes that cell to become incapable of further fusion events, and therefore, that the remaining sperm is transmitted to the opposite female cell.

VII. Summary and Conclusions

In summary, *Plumbago zeylanica* L. possesses one of the most highly reduced female gametophytes in angiosperms, consisting of five cells – only two of which directly participate in fertilization. The absence of synergids, characteristic of this subfamily, is indicative of a transference of synergid functions to the egg which is expressed in the structure of the egg. The egg, located at the far micropylar end of the gametophyte, has numerous cell wall ingrowths and mitochondria reflective of a higher physiological activity than that displayed to date in angiosperm eggs within unreduced embryo sacs. Unlike typical angiosperms, the pollen tube of *Plumbago* grows through egg cell wall ingrowths, terminates growth, and discharges its contents, two male gametes, a vegetative nucleus and some pollen cytoplasm, directly between the egg and central cell. Since one complicating factor in elucidating the fate of the sperm cytoplasm has been the presence of the synergid cytoplasm, a thorough study of the ultrastructure of the male and female gametophyte of *P. zeylanica* was undertaken to contribute to an understanding of the structural basis for genetic transmission of plastids and mitochondria in flowering plants.

The mature male gametophyte consists of three cells, including two sperm cells with a normal complement of organelles and a vegetative cell with a polymorphic, lobed nucleus. Within indentations of the vegetative nucleus is associated a long, slender cellular projection of one of the two sperm cells, which is the structural basis for the association of sperms and vegetative nucleus throughout pollen tube growth. The second sperm is connected to the first by a cell wall with plasmodesmata, and the internal pollen plasma membrane. The content of organelles within each cell is somewhat variable; however, the majority of plastids are consistently found in the second sperm cell, whereas the opposite is true of mitochondria. Serial reconstruction of 22 paired sperm cells reveals that plastid content in the second sperm may vary from 8 to 46, mitochondria, from 22 to 52; the other sperm cell contains 0 to 2 plastids (usually none), and from 154 to 319 mitochondria. Several possible microbodies were noted, but in most cases were found in the second sperm cell. The basis

of this asymmetric distribution of heritable organelles (and possibly microbodies also) appears to originate in the generative cell. The polarity of this distribution, i.e., the predominance of mitochondria in the sperm associated with the vegetative nucleus and plastids in the other sperm, was consistent in each of the more than 50 pollen grains examined in this study.

During pollen tube growth, this association continues, but becomes looser and the sperm cell wall decreases in thickness. The pollen tube enters the ovule through the micropyle, displaces several nucellar cells, penetrates the egg's filiform apparatus, and completes growth between the egg and central cell, at a region of strong curvature of the egg cell wall, 70 to 80 um deep within the embryo sac. There, a terminal aperture forms and the pollen tube contents, including two sperms, the vegetative nucleus, and a limited amount of pollen cytoplasm, are released. Near or during pollen tube discharge, the egg cell wall becomes disrupted, the outer and inner vegetative cell membranes are lost, the sperm cell wall apparently dissipates, and the sperm plasma membrane becomes tightly appressed to the plasma membranes of the egg and central cell. Gamete fusion is initiated, in each sperm cell, at a single location in the plasma membrane, but is completed at several locations as evidenced by the presence (and thus non-incorporation) of fusion membranes within female cells. Remnant fusion membranes undergo rapid vesiculation following gamete fusion and are quickly disorganized. Initially, the organelles of each sperm cell are clearly evident following gamete fusion in the egg and central cell, associated with the periphery of the sperm nuclei. These organelles may be distinguished by morphology and location within the embryo sac. Nuclear fusion occurs on the closest side of the egg and central cell with respect to the pollen tube aperture, and is similar to the process described in other angiosperm taxa. Unfused cytoplasmic bodies, lacking nuclei but possessing mitochondria and other organelles, are probable remnants of the sperm cell projection disrupted during gamete discharge, and remain between the egg and central cell, presumably degenerating with time. The vegetative nucleus degenerates rapidly between the egg and central cell near the summit of the egg.

In terms of its structure and function, the egg of *Plumbago* represents an egg apparatus which has been reduced to a single cell. Similar to a synergid in terms of its structural organization and physiological state (as reflected by its ultrastructure), the egg of *Plumbago* determines in its outer surface the characteristics of gamete delivery, possessing constricted regions within its junction with the central cell that may determine the behavior and distribution of cells and nuclei introduced into this region, and mediates the passage of the sperm nucleus into its cytoplasm. Unlike a synergid, the egg does not undergo internal degeneration, although degeneration of the pollen cytoplasmic contents occurs at the egg's exterior; the egg does not directly receive the pollen tube; and it functions directly as a gamete. Subsequent research concerning the significance of asymmetric distribution of plastids and mitochondria may reveal a mechanism for conservation of paternal plastids in the embryo, the occurrence of genetic transmission of organellar heredity into the offspring, and additional capabilities of the egg of *P. zeylanica* with respect to gametic recognition.

Literature Cited

Baker, H. G. 1948. Dimorphism and monomorphism in the Plumbaginaceae. I. A survey of the family. Ann. Bot., n.s. 12: 207-219.

Baur, E. 1909. Das Wesen und die Erblichkeitsverhaltnisse der "varietates albomarginatae hort" von *Pelargonium zonale*. Z. Vererbungs. 1: 330-351.

Boyes, J. W. 1939a. Embryo sac development in *Plumbagella*. Proc. Nat. Acad. Sci. (Wash.) 25: 141-145.

Boyes, J. W. 1939b. Development of the embryo sac of *Plumbagella micrantha*. Amer. J. Bot. 26: 539-547.

Boyes, J. W. 1959. Demonstration of embryo sac development in *Plumbagella micrantha*. Proc. Congr. Internat. Bot. 9th 2: 43-44.

Boyes, J. W., and E. Battaglia. 1951. The tetrasporic embryo sacs of *Plumbago coccinea, P. scandens,* and *Ceratostigma willmottianum*. Bot. Gaz. 112: 485-489.

Burgess, J. 1970. Cell shape and mitotic spindle formation in the generative cell of *Endymion non-scriptus*. Planta 95: 72-85.

Cass, D. D. 1972. Occurrence and development of a filiform apparatus in the egg of *Plumbago capensis*. Amer. J. Bot. 59: 279-283.

Cass, D. D. 1973. An ultrastructural and Nomarski-interference study of the sperms of barley. Can. J. Bot. 51: 601-605.

Cass, D. D. 1981. Structural relationships among central cell and egg apparatus cells of barley as related to transfer of male gametes. Acta Bot. Soc. Pol. 50:

Cass, D. D., and W. A. Jensen. 1970. Fertilization in barley. Amer. J. Bot. 57: 62-70.

Cass, D. D., and I. Karas. 1974. Ultrastructural organization of the egg of *Plumbago zeylanica*. Protoplasma 81: 49-62.

Cass, D. D., and I. Karas. 1975. Development of sperm cells in barley. Can. J. Bot. 53: 1051-1062.

Cheng, Z., H. Shiyi, X. Liyun, L. Xiuru, and S. Jiaheng. 1980. Ultrastructure of sperm cell in mature pollen grain of wheat. Sci. Sinica 23: 371-379.

Clauhs, R. P., and P. Grun. 1977. Changes in plastid and mitochondrion content during maturation of generative cells of *Solanum* (Solanaceae). Amer. J. Bot. 64: 377-383.

Cocucci, A. E., and T. E. diFulvio. 1969. Sobre la naturaleza nuclear de los "cuerpos X". Kurtziana 5: 317-323.

Cocucci, A. E., and W. A. Jensen. 1969a. Orchid embryology: Pollen tetrads of *Epidendrum scutella* in the anther and on the stigma. Planta 84: 215-229.

Cocucci, A. E., and W. A. Jensen. 1969b. Orchid embryology: The mature megagametophyte of *Epidendrum scutella*. Kurtziana 5: 23-38.

Correns, C. 1909. Vererbungsversuche mit blass (gelb) grunen und buntblattrigen Sippen bei *Mirabilis jalapa, Urtica pilulifera* und *Lunaria annua*. Z. Vererbungs. 1: 291-329.

D'Amato, F. 1940a. Apomissia in *Statice oleafolia* var. *confusa*. N. G. Bot. Ital. 47: 504.

D'Amato, F. 1940b. Contributo all'embriologia della Plumbaginaceae. N. G. Bot. Ital. 47: 349-382.

D'Amato, F. 1943. Nuovo contributo alla embriologia della Plumbaginaceae. N. G. Bot. Ital. 50: 79-99.

D'Amato, F. 1949. Triploidia e apomissia in *Statice oleafolia* var. *confusa*. Caryologia 2: 71-84.

Dahlgren, K. V. O. 1915. Der Embryosack von *Plumbagella*, ein neuer Typen unter den Angiospermen. Arkiv. f. Bot. 14: 1-10.

Dahlgren, K. V. O. 1916. Zytologische und embryologische Studien uber die Reihen Primulales und Plumbaginales. Kgl. Svenska Vetenskapsakademiens Handlingar. 56: 1-80.

Dahlgren, K. V. O. 1937. Die Entwicklung des Embryosackes bei *Plumbago zeylanica*. Bot. Notiser 487-497.

Davis, G. 1966. Systematic embryology of the angiosperms. John Wiley & Sons, New York.

Dexheimer, J. 1965. Sur les structures cytoplasmiques dans les grains de pollen de *Lobelia erinus*. C. R. Acad. Sci. (Paris) 260: 6963-6965.

Diers, L. 1963. Elektronmikroskopische Beobachtungen an der generative Zelle von *Oenothera hookeri*. Z. Naturforsch. 18: 562-566.

Dulberger, R. 1975. Intermorph structural differences between stigmatic papillae and pollen grains in relation to incompatibility in Plumbaginaceae. Proc. Roy. Soc. Lond. B. 188: 257-274.

Erdtman, G. 1970. Uber Pollendimorphy in Plumbaginaceae. Unter besonderer Berucksichtigung von *Dyerophytum indicum*. Svensk. Bot. Tidskrift. 64: 184-188.

Fagerlind, F. 1938a. Embryosack von *Plumbagella* und *Plumbago*. Ark. Bot. 29B: 1-8.

Fagerlind, F. 1938b. Wo kommen Tetrasporische durch drei Teilungsschritte vollentwickelte Embryosacke unter den Angiospermen vor? Bot. Notiser 461-498.

Fagerlind, F. 1939. Drei Beispiele des *Fritillaria*-Typus. Svensk. bot. Tidskr. 33: 188-204.

Finn, W. W. 1925. Male cells in angiosperms. Bot. Gaz. 98: 1-25.

Finn, W. W. 1935. Einige Bemerkungen uber den mannlichen Gametophyten der Angiospermen. Ber. Deut. Bot. Ges. 53: 679-686.

Fisher, D. B. 1968. Protein staining of ribboned epon sections for light microscopy. Histochemie 16: 92-96.

Fisher, D. B., and W. A. Jensen. 1969. Cotton embryogenesis: The identification, as nuclei, of the X-bodies in the degenerated synergid. Planta 84: 122-133.

Folsom, M. W. 1980. An ultrastructure study of the embryo sac of soybean *Glycine max* (L.) Merr. M. S. Thesis, Auburn University, Auburn, Alabama.

Fowke, L. C., and O. L. Gamborg. 1980. Applications of protoplasts to the study of plant cells. Intl. Rev. Pl. Cytol. 68: 9-51.

Frederick, S. E., and E. H. Newcomb. 1969. Cytochemical localization of catalase in leaf microbodies (peroxisomes). J. Cell Biol. 43: 343-353.

Galey, F. R., and S. E. G. Nilsson. 1966. A new method for transferring sections from the liquid surface of the trough through staining solutions to the supporting film of a grid. J. Ultrastruct. Res. 14: 405-410.

Gillham, N. W. 1978. Organelle heredity. Raven Press, New York.

Grun, P. 1976. Cytoplasmic genetics and evolution. Columbia University Press, New York.

Hagemann, R. 1976. Plastid distribution and plastid competition in higher plants and the induction of plastom mutations by nitroso-urea compounds. In: Genetics and biogenesis of chloroplasts and mitochondria (Bucher, T., Neupert, W., Sebald, W., Werner, S., Eds.), pp. 331-338. North Holland Publ. Co., Amsterdam.

Haupt, A. W. 1934. Ovule and embryo sac of *Plumbago capensis*. Bot. Gaz. 95: 649-659.

Hoefert, L. L. 1969. Fine structure of sperm cells in pollen grains of *Beta*. Protoplasma 68: 237-240.

Hoefert, L. L. 1971. Pollen grain and sperm cell ultrastructure in *Beta*. In: Pollen: development and physiology (Heslop-Harrison, J., Ed.), pp. 68-69. Appleton-Century-Crofts, New York.

Jensen, W. A. 1962. Botanical histochemistry. W. H. Freeman & Co., San Francisco.

Jensen, W. A. 1964. Observations on the fusion of nuclei in plants. J. Cell Biol. 23: 669-672.

Jensen, W. A. 1973. Fertilization in flowering plants. BioScience 23: 21-27.

Jensen, W. A., and D. B. Fisher. 1967. Cotton embryogenesis: Double fertilization. Phytomorph. 17: 261-269.

Jensen, W. A., and D. B. Fisher. 1968a. Cotton embryogenesis: The entrance and discharge of the pollen tube in the embryo sac. Planta 78: 158-183.

Jensen, W. A., and D. B. Fisher. 1968b. Cotton embryogenesis: The sperm. Protoplasma 65: 277-286.

Jensen, W. A., and D. B. Fisher. 1970. Cotton embryogenesis: The pollen tube in the stigma and style. Protoplasma 69: 215-235.

Jensen, W. A., P. Schulz, and M. E. Ashton. 1977. An ultrastructural study of early endosperm development and synergid changes in unfertilized cotton ovules. Planta 133: 179–189.

Johansen, D. A. 1940. Plant microtechnique. McGraw-Hill, New York.

Karas, I., and D. D. Cass. 1976. Ultrastructural aspects of sperm cell formation in rye: Evidence for cell plate involvement in generative cell division. Phytomorph. 26: 36–45.

Karnovsky, M. J. 1965. A formaldehyde–glutaraldehyde fixative of high osmolality for use in electron microscopy. J. Cell Biol. 27: 137A.

Knoth, R. 1975. Struktur und Funktion der genetischen Information in den Plastiden. XIV. Die Auswirkungen der Plastommutationen en: *alba-1* von *Antirrhinum majus* und en: *gilva-1* von *Pelargonium zonale* auf die Feinstruktur der Plastiden. Biol. Zentralbl. 94: 681–694.

Lombardo, G., and F. M. Gerola. 1968. Cytoplasmic inheritance and ultrastructure of the male generative cell of higher plants. Planta 82: 105–110.

Maheshwari, P. 1949. The male gametophyte in angiosperms. Bot. Rev. 15: 1–75.

Maheshwari, P. 1950. Introduction to the embryology of angiosperms. McGraw-Hill, New York.

Mathur, K. 1940. A note on the development of the embryo sac of *Vogelia indica*. Curr. Sci. 9: 180–182.

Mathur, K., and R. Khan. 1941. The development of the embryo sac in *Vogelia indica* Lamk. Proc. Indian Acad. Sci. Sect. B. 13: 360–368.

Maze, J., and S-C. Lin. 1975. A study of the mature megagametophyte of *Stipa elmeri*. Can. J. Bot. 53: 2958–2977.

Meyer, B., and W. Stubbe. 1974. Das Zahlenverhaltnis von mutterlichen und vaterlichen Plastiden in den Zygoten von *Oenothera erythrosepala* Borbas (syn. *Oe. lamarckiana*). Ber. Deutsch. Bot. Ges. 87: 29–38.

Mogensen, H. L. 1971. A modified method for re-embedding thick epoxy sections for ultratomy. J. Ariz. Acad. Sci. 6: 249–250.

Mogensen, H. L. 1972. Fine structure and composition of the egg apparatus before and after fertilization in *Quercus gambelii*: The functional ovule. Amer. J. Bot. 59: 931–941.

Mogensen, H. L. 1978. Pollen tube-synergid interactions in *Proboscidea louisianica* (Martineaceae). Amer. J. Bot. 65: 953-964.

Mogensen, H. L., and H. K. Suthar. 1979. Ultrastructure of the egg apparatus of *Nicotiana tabacum* (Solanaceae) before and after fertilization. Bot. Gaz. 140: 168-179.

Nawashin, S. G. 1909. Uber das selbstandige Bewegungsvermogen der Spermakerne bei enigen Angiospermen. Oester. Bot. Zeitschr. 59: 457-467.

Nawashin, S. G., and W. W. Finn. 1913. Zur Entwicklungsgeschichte der Chlazogamen. *Juglans regia* und *J. nigra*. Acad. Imp. Sci. St. Petersbourg VIII 31: 1-59. Amsterdam.

Russell, S. D. 1980. Participation of male cytoplasm during gamete fusion in an angiosperm, *Plumbago zeylanica*. Science 210: 200-201.

Russell, S. D., and D. D. Cass. 1981a. Ultrastructure of the sperms of *Plumbago zeylanica*. I. Cytology and association with the vegetative nucleus. Protoplasma 107: 85-107.

Russell, S. D., and D. D. Cass. 1981b. Ultrastructure of fertilization in *Plumbago zeylanica*. Acta Soc. Bot. Pol. 50:

Sanger, J. M., and W. T. Jackson. 1971. Fine structure study of pollen development in *Haemanthus katherinae* Baker. II. Microtubules and elongation of the generative cells. J. Cell Sci. 8: 303-315.

Schulz, R., and W. A. Jensen. 1968. *Capsella* embryogenesis: The synergids before and after fertilization. Amer. J. Bot. 55: 541-552.

Schulz, P., and W. A. Jensen. 1977. Cotton embryogenesis: The early development of the free nuclear endosperm. Amer. J. Bot. 64: 384-394.

Spurr, A. R. 1969. A new low viscosity epoxy resin embedding medium for electron microscopy. J. Ultrastruct. Res. 26: 31-43.

Stebbins, G. L. 1974. Flowering plants: Evolution above the species level. Edward Arnold, London.

Strasburger, E. 1884. Neure Untersuchungen uber den Befruchtungsvorgang bei den Phanerogamen als Grundlage fur eine Theorie der Zeugung. Jena.

Takhtajan, A. 1980. Outline of the classification of flowering plants (Magnoliophyta). Bot. Rev. 46: 1-225.

Thiery, J. P. 1967. Mise en evidence des polysaccharides sur coupes fines en microscopie electronique. J. Microscopie 6: 987-1018.

Toyama, S. 1980. Electron microscopic studies on the morphogenesis of plastids. X. Ultrastructural changes of chloroplasts in morning glory leaves exposed to ethylene. Amer. J. Bot. 67: 625-635.

van der Pluijm, J. E. 1964. An electron microscopic investigation of the filiform apparatus in the embryo sac of *Torenia fournieri*. *In:* H. F. Linskens (ed.), Pollen physiology and fertilization, pp. 8-16. North-Holland Publ. Co.,

van Went, J. L. 1970. The ultrastructure of the fertilized embryo sac of *Petunia*. Acta Bot. Neerl. 19: 468-480.

Vazart, J. 1969. Organisation et ultrastructure du sac embryonnaire du Lin (*Linum usitatissimum* L.). Rev. Cytol. Biol. Veg. 32: 227-240.

Veillet-Bartoszewska, M. 1958. Embryogenie des Plumbagacees. Developpment de l'embryon chez *Plumbago europea*. C. R. Acad. Sci. Paris 247: 2178-2181.

Venable, J. H., and R. Coggeshall. 1965. A simplified lead citrate stain for use in electron microscopy. J. Cell Biol. 25: 407.

Ward, H. M. 1880. A contribution to our knowledge of the embryo sac in angiosperms. J. Linn. Soc. Bot. Lond. 17: 519-546.

Wilms, H. J. 1981. Pollen tube penetration and fertilization in spinach. Acta Bot. Neerl. 30: 101-122.

Wylie, R. B. 1923. The sperms of *Vallisneria spirilis*. Bot. Gaz. 75: 191-202.

Wylie, R. B. 1941. Some aspects of fertilization in *Vallisneria*. Am. J. Bot. 28: 169-174.

Ya-E, M. 1941. Development of the embryo sac in *Statice japonica*. Sci. Reports Tohoku Imp. Univ. Biol. 16: 279-303.

Appendix 1. Morphometry of Sperm Cells

Introduction

Before an understanding of the importance of male cytoplasmic transmission is possible, there must emerge a clear idea of how many organelles are transferred to the female reproductive cells during gamete fusion, in an attempt to determine whether it appears to be a significant number in comparison with the organelles originally present in the egg and central cell. In Chapter 4, the absolute quantity of mitochondria, plastids, and microbodies in each sperm cell was determined by serial ultrathin sectioning over 50 pollen grains simultaneously. After more than 320 serial sections were taken and mounted, it was possible to count the number of organelles in 11 pairs of sperm cells (22 sperms); the total number of organelles represented an actual count, rather than an estimate. However, it is evident that not all sperm organelles are transmitted during gamete fusion, as some mitochondria of sperm origin appear to remain untransmitted in the female reproductive cells, found in membrane-bound cytoplasmic bodies between the egg and central cell (Chapter 6).

Reconstructing the site of gamete fusion in the female gametophyte by serial ultrathin sections would be the most accurate technique of determining how many organelles of sperm origin enter the egg and central cell, but identification of certain organelles, particularly mitochondria, would be difficult under the best of circumstances. Distinguishing sperm mitochondria from those of maternal origin on the basis of populational differences in mitochondrial width would be impossible if too much time had elapsed since gamete fusion; the circumstances under which one could observe paternal organelles near the sperm nuclei are likely to be transient.

A more practical alternative to this procedure would be constructing a mathematical model of sperm morphology with the capability of predicting how many male organelles are actually present in female cytoplasm based on the number observed in selected sections. In brief, this technique (explained in greater detail on following pages) would be based on: 1) determining the frequency of mitochondria or plastids in a given volume of sperm cytoplasm; 2)

calculating the frequency of organelles in selected sections of newly transmitted sperm nuclei with associated paternal organelles; 3) calculating the total number of organelles based on their expected density in sperm cytoplasm. The validity of this technique can then be examined for accuracy by using a selected section of a given sperm cell from Chapter 4 (for which an absolute organelle count is available), and comparing the predicted total number of organelles in the sperm cell with the actual number of organelles determined by serial reconstruction.

A Cellular Mathematical Model

The following model assumes that spindle shaped sperm cells may be represented by two cones joined at their bases and that the height and width of the union of these two cones is the same as that of sperm cells. The nucleus is represented by a sphere of the same dimensions and approximate volume as the sperm nucleus.

Mathematical equations

Given two cones united at their bases, the equations relating to its volume are as follows:

$$\text{Total sperm volume} = 2/3 * \langle Pi \rangle * (rS)^2 * hS$$

$$= 1/3 * \langle Pi \rangle * (rS)^2 * lS$$

Where:

hS = height of one cone
lS = length of model
rS = radius of cone base

The volume of the sperm nucleus, represented as a sphere is calculated as follows:

$$\text{Nuclear volume} = 4/3 * \langle Pi \rangle * (rN)^3$$

Where:

rN = sphere radius

The volume of the sperm cytoplasm may be represented by subtracting nuclear volume from the total sperm volume.

The volume of the median longitudinal section is then calculated as the volume of a rhomboid of the same length and width as the sperm cell and has a thickness identical to section thickness. Volume of the rhomboid may be calculated as follows:

$$\text{Volume of sperm in section} = 1/2 * W * L * ST$$

Where:

W = width of rhomboid
L = length of rhomboid
ST = section thickness

The nuclear volume within the section is then represented as a disc of thickness identical to section thickness.

$$\text{Volume of nucleus in section} = 2/3 * \langle Pi \rangle * rN^2 * ST$$

Where:

rN = nuclear radius

The volume of the sperm cytoplasm in the median longitudinal section may then be determined by subtracting the volume of the sectioned nucleus from the total volume of the sectioned sperm. The volume of the sperm projection associated with the vegetative nucleus is represented by a cylinder of length and width similar to that of the sperm cell and may be calculated as follows:

$$\text{Volume of cylinder} = 1/3 * \langle Pi \rangle * (rS)^2 * IS$$

Organellar frequency per volume may be determined using the number of organelles in a median longitudinal section of the sperm cell. Organellar frequency is calculated as follows:

$$\text{Organellar frequency} = \frac{(\#\ \text{Organelles}) * ST\ /\ Do}{\text{Sectional volume of sperm cytoplasm}}$$

Where:

Do = organelle average diameter

The organellar content of the sperm cell may then be calculated using the following formulae:

Main sperm cell body:

$$\text{Organellar content} = \frac{\text{(Organellar frequency)} * \text{Total volume}}{\text{Sectional volume of sperm cytoplasm}}$$

Sperm cell projection:

Organellar content = Organellar frequency * Cylinder volume

Then total organellar content may be calculated as:

Organellar content (sperm body) + Organellar content (sperm projection)

Sample data and analysis.
Assume:

lS = Sperm length = 8 um
dS = Sperm diameter = 4 um
rS = Sperm radius = 2 um
dN = Nuclear diameter = 3.5 um
rN = Nuclear radius = 1.775 um
lSP = Sperm projection length = 30 um
dSP = Sperm projection diameter = 2.1 um
rSP = Sperm projection radius = 1.05 um

Each of these represents values which occur in sperm cells, and which are close to the average values given in Chapter 3. Next, assume the following values for data from a given median longitudinal section of a sperm cell.

#M = Number of mitochondria visible = 28
wM = Mitochondrial width = .2864 um
ST = Section thickness = 60 nm

These values are taken from electron micrographs of sections which have a silver to gold interference reflection color during sectioning, and were therefore assumed to be approximately 60 nm in thickness. The diameter of the mitochondria is based on mitochondrial width in sperm cells observed within pollen grains at anthesis (Table 7). The resulting calculations are as follows:

Organellar frequency = 10.61 mitochondria / um^2
Organelles in sperm body = 174.29 mitochondria
Organelles in sperm projection = 80.93 mitochondria
Organelles in whole sperm cell = 255.22 mitochondria

Documentation for the program on the facing page:

Program keys:

A	B	C	D	E
START PROGRAM	CHANGE Sperm Length (um)	CHANGE Sperm Nuclear Diameter (um)	CHANGE # of Organelles per Section (#)	SPERM PROJ Length Width (um)
a	b	c	d	e
INITIALIZE PROGRAM	CHANGE Sperm Width (um)	CHANGE Section Thickness (nm)	CHANGE Organelle Diameter (um)	PRINT ALL REGISTERS

Memory structure:

Register 1: Sperm length = lS
Register 2: Sperm radius = rS = 1/2 * dS
Register 3: Sperm nucleus radius = rN = 1/2 * dN
Register 4: Section thickness = ST
Register 5: # of organelles in section = #O
Register 6: Organelle diameter = dO
Register 7: Total sperm volume
Register 8: Nuclear volume
Register 9: Sperm cytoplasmic volume
Register A: Volume of sperm in section
Register B: Volume of nucleus in section
Register C: Volume of sperm cytoplasm in section
Register D: Frequency of organelle
Register E: Organellar content in entire sperm cell
Register 0': Sperm projection length
Register 1': Sperm projection width
Register 2': Volume of sperm projection
Register 3': Organellar content in sperm projection

Table 10: A program (designed for a progammable Hewlett Packard calculator) to calculate the number of organelles or other subcellular objects within a spindle shaped sperm cell based on organelle number in a median longitudinal section.

1	*LBLa	45	GTOe	89	GTOe	133	ENTI	177	GTOe
2	R/S	46	R/S	90	GTO2	134	RCL1	178	R/S
3	STO1	47	STO6	91	*LBLD	135	X	179	STO1
4	X<Ø?	48	X<Ø?	92	STO5	136	RCL4	180	X<Ø?
5	GTOe	49	GTOe	93	X<Ø?	137	X	181	GTOe
6	R/S	50	GTOA	94	GTOe	138	STOA	182	ENTI
7	ENTI	51	*LBLB	95	GTO3	139	2	183	2
8	2	52	STO1	96	*LBLd	140	ENTI	184	÷
9	÷	53	X<Ø?	97	STO6	141	3	185	X^2
10	STO2	54	GTOe	98	X<Ø?	142	÷	186	2
11	X<Ø?	55	GTOA	99	GTOe	143	RCL3	187	X
12	GTOe	56	*LBLb	100	GTO3	144	X^2	188	3
13	R/S	57	ENTI	101	*LBLA	145	X	189	÷
14	ENTI	58	2	102	1	146	Pi	190	Pi
15	2	59	÷	103	ENTI	147	X	191	X
16	÷	60	X<Ø?	104	3	148	RCL4	192	RCLØ
17	STO3	61	GTOe	105	÷	149	X	193	X
18	X<Ø?	62	GTOA	106	Pi	150	STOB	194	STO2
19	GTOe	63	*LBLC	107	X	151	CHS	195	P=S
20	R/S	64	ENTI	108	RCL2	152	RCLA	196	RCL9
21	ENTI	65	2	109	X^2	153	+	197	1/X
22	1	66	÷	110	X	154	STOC	198	X
23	Ø	67	STO3	111	RCL1	155	*LBL3	199	RCLD
24	Ø	68	X<Ø?	112	X	156	RCL5	200	X
25	Ø	69	GTOe	113	STO7	157	ENTI	201	P=S
26	÷	70	GTO1	114	*LBL1	158	RCLC	202	STO3
27	STO4	71	*LBLc	115	4	159	÷	203	P=S
28	1/X	72	ENTI	116	ENTI	160	RCL4	204	PSE
29	RCL2	73	1	117	3	161	X	205	RCLE
30	X	74	Ø	118	÷	162	RCL6	206	+
31	5	75	Ø	119	Pi	163	÷	207	R/S
32	–	76	Ø	120	X	164	STOD	208	GTOa
33	X<Ø?	77	÷	121	RCL3	165	PSE	209	*LBLe
34	GTOe	78	STO4	122	X^2	166	RCL9	210	9
35	RCL4	79	1/X	123	X	167	X	211	9
36	ENTI	80	RCL2	124	RCL3	168	RCLC	212	9
37	1	81	X	125	X	169	÷	213	9
38	–	82	5	126	STO8	170	STOE	214	.
39	X>Ø?	83	X<Ø?	127	RCL7	171	R/S	215	9
40	GTOe	84	GTOe	128	–	172	GTOA	216	9
41	RCL4	85	ENTI	129	CHS	173	*LBLE	217	R/S
42	R/S	86	1	130	STO9	174	P=S	218	PREG
43	STO5	87	–	131	*LBL2	175	STOØ	219	RTN
44	X<Ø?	88	X>Ø?	132	RCL2	176	X<Ø?		

These data alone do not show the validity of the technique; however, the fact that these represent data that is not far from the average values for length and width of the sperm cell body and projection suggests that this approximation is reasonable. The number of calculated organelles in the mathematical model compares favorably with the average figures for mitochondria in serially reconstructed sperm cells (*cf.* Table 3).

The structure and simplicity of the mathematical model lends itself readily to use of pocket calculators and is easily programmable. Table 10 illustrates a program generated for a Hewlett Packard calculator. Instructions for use of the program are given on the facing page. The data given in this section were designed to give data on organelle numbers that was similar to those seen in actual data from Chapter 4. In order to get these figures, only the two most questionable parameters were altered, namely sperm nuclear diameter and the thickness of the sperm projection. In my opinion, the sperm nuclear diameter was appropriate because an ellipsoidal model based on real nuclear dimensions (3 um X 6 um) gives a volume of 28.33 um^3; the model's spheroidal volume was calculated as 23.47 um^3. (The behaviour of either nuclear model is very sensitive to the radius or semi-axes calculated, as these values are either cubed or squared, respectively, to determine the volume.) The diameter of the sperm projection varied from 0.5 to 2.5-3.0 um depending on location relative to the sperm cell body. The fact that the diameter of the sperm projection had to be exaggerated somewhat beyond the expected average projection diameter most probably relates to problems in identifying location at which the sperm projection begins relative to the sperm body. Mitochondria near the sperm cell body tended to be included in the organelle counts of the sperm cell body rather than in those of the sperm cell projection; thus, the original data may have had a systematic source of error.